NAA-SR-11142
COPY

PIQUA NUCLEAR POWER FACILITY REACTOR OPERATIONS ANALYSIS PROGRAM SEMIANNUAL PROGRESS REPORT NO. 5

July 1 – December 31, 1964

AEC Research and Development Report

ATOMICS INTERNATIONAL
A DIVISION OF NORTH AMERICAN AVIATION, INC.

Price $4.00
Available from the Office of Technical Services
Department of Commerce
Washington 25, D. C.

NAA-SR-11142
PROGRESS REPORTS
109 PAGES

PIQUA NUCLEAR POWER FACILITY
REACTOR OPERATIONS ANALYSIS PROGRAM
SEMIANNUAL PROGRESS REPORT NO. 5

July 1 – December 31, 1964

ATOMICS INTERNATIONAL
A DIVISION OF NORTH AMERICAN AVIATION, INC.

CONTRACT: AT(11-1)-GEN-8
ISSUED: JUNE 15, 1965

DISTRIBUTION

This report has been distributed according to the category "Progress Reports" as given in "Standard Distribution Lists for Unclassified Scientific and Technical Reports" TID-4500 (40th Ed.), March 1, 1965. A total of 750 copies was printed.

CONTENTS

		Page
I.	Review of Operations	1
II.	Nuclear Analysis	9
	B. Core Power, Temperature, and Heat Flux Distribution	12
	1. Power Distribution Code	12
	2. Outlet Thermocouple Discrepancy	13
	3. Review of Hot-Channel Calculations	14
	4. Review of Burnout Heat Flux Calculation	17
	C. Relative Power Studies	19
	D. Instrumented Fuel Element Temperatures	23
	E. Nuclear Parameters of Core 1-B at Startup	25
	F. December Fuel Rearrangement	26
	1. Consideration Prior to the December Shutdown	26
	2. Element Operating Histories	27
	3. Removal of the Element from F-13	28
	G. Considerations Following Fuel Rearrangement	28
	1. Equivalent Core Exposure Remaining	28
	2. Consideration of the E-12 Element	29
III.	Systems and Components Analysis	31
	A. Main Heat Transfer System Analysis	31
	1. Computer Program	31
	2. Main Coolant Pump Performance	31
	3. Pressurizing Pump Performance	34
	4. Steam Generator Performance	35
	B. Flow Rate and Pressure Drop for Main Heat Transfer and Degasification Systems	39
	1. Main Heat Transfer System Filters	39
	2. Degasification System Filters	42
	C. Coolant Distillation System	43
	D. Decay Heat System	47
	E. Waste-Fired Boiler Operation	48

CONTENTS

		Page
	F. Aqueous Waste and Waste-Gas System	49
	1. Aqueous Waste System	49
	2. Waste Gas System	51
	G. Plant Radiation Levels	52
	1. Plant Radiation Levels	52
	2. Waste Gas	54
	3. Aqueous Waste	54
	H. Failed Element Location System	54
	I. Flux at Charpy Impact Specimens and Neutron Window	57
	J. Coolant Decomposition Rate	58
IV.	Examination of Incore Filters	61
	A. Introduction	61
	B. Summary of Results	61
	C. Conclusions	62
	D. Filter Sample Selection and Preparation	65
	1. Sample Selection	65
	2. Sample Preparation	65
	E. Examination Procedures and Results	65
	1. Visual Appearance	65
	2. Spectrographic Analysis	72
	3. X-Ray Diffraction	73
	4. Manual Examination	74
	5. Tensile Strength	74
	6. X-Ray Fluorescence	75
V.	Coolant Chemistry and Analysis	77
	A. Review of Coolant Quality	77
	B. PHA Analysis of Coolant	80
	C. PHA Analysis of Gaseous Fission Products	83
	D. Evaluation of Air Inleakage to Coolant	84

CONTENTS

		Page
	E. Evaluation of Filter Efficiency	91
	F. Coolant Particle Analysis	93
	G. Analysis of Raw Coolant	97
VI.	Effect of Oxygen on Irradiated PNPF Coolant	99
	A. Introduction	99
	B. Oxygen Uptake By Irradiated Coolant	99
	1. Experiments in Which Air was Bubbled Through PNPF Coolant	100
	2. Experiments Where Air Was Exposed to Coolant in a Closed System	102
	C. Total Oxygen in Irradiated Coolant	106
	D. Conclusions	108
	1. Oxidation by Bubbling Air Through Hot PNPF Coolant	108
	2. Oxidation of PNPF Coolant in Fixed Volume Experiments	108
	3. Total Oxygen Determination	109

TABLES

		Page
I.	Operations Statistics Summary	2
II.	Uncertainties in Heat Transfer Calculations	16
III.	Burnout Heat Fluxes from Various Correlations	18
IV.	Nomenclature for Figures 8 and 9	20
V.	Main Coolant Pump P-1A and P-1B Performance	32
VI.	Typical Pressurizing Pump Performance	35
VII.	Fels Survey Data for Shuffled Fuel	55
VIII.	Failed Element Location System Survey Activity	56
IX.	Chemical Analysis of New Fibers	73
X.	Effect of Sampling Variations on MST Data	79
XI.	Gaseous Fission Product Activities During Core 1-A and Core 1-B Operation	84
XII.	Ar^{41} Values in PNPF Coolant Before and After Air Leak	87
XIII.	Estimated Equivalent Moles of Oxygen Activated in the PNPF Reactor Based on Ar^{41} Activity and Offgas Flow	90
XIV.	Isotope Removal Efficiencies by Filtration and Degassification	92
XV.	Gamma Emitters in Upper Guide Grid, In-Core Filters, and H-1 Heater Particles	95
XVI.	Ash and Emission Spectroscopy Data for H-1 Heater, Upper Guide Grid, and In-Core Filter Particles	96
XVII.	Raw Coolant Data for Core 1-B	98
XVIII.	Oxidation of a PNPF Coolant Sample by Bubbling an Air-Helium Mixture Through Coolant at 236°C	100
XIX.	Effect of Flow Rate and Temperature on Oxidation of PNPF Coolant by Bubbling an Air-Helium Mixture Through Liquid Coolant	101
XX.	Oxidation of Irradiated PNPF Coolant	102
XXI.	Oxidation of PNPF Coolant Sample at 160°C by Exposing Quiescent Coolant to an Atmosphere of Oxygen in a Closed System	103
XXII.	Oxidation of PNPF Coolant Samples at 300°C by Exposing Quiescent Coolant to an Atmosphere of Oxygen in a Closed System	104

FIGURES

		Page
1.	PNPF Operations January - December 1964	3
2.	Average Daily Power (Gross Mwe)	4
3.	Reactivity History for August	9
4.	Reactivity History for September	10
5.	Reactivity History for October	10
6.	Reactivity History for November	11
7.	Reactivity History for December	11
8.	Griffith Correlation for the Prediction of Critical Heat Flux	19
9.	Griffith Correlation for the Prediction of Critical Heat Flux (Diphenyl Data Deleted)	21
10.	Relative Power Behavior of Fuel Elements in Core Positions E-10, -12, F-13, and G-14	22
11.	Instrumented Fuel Element Normalized Cladding-Surface Temperatures	24
12.	IFE Thermocouple Locations and Identifications	25
13.	Main- and Pressurizing-Pump Performance	33
14.	Steam Generator Heat Transfer Performance	37
15.	Flow and Pressure Drop for MHTS Degassification System	40
16.	Relation of HB Content, Distillation Column Feed Rate, and Thermal Power	44
17.	Distillation Column Sketch	45
18.	HB Content vs Distillation Time Following Shutdown	46
19.	Plant Radiation Levels	53
20.	Charpy Specimen Locations in Core	57
21.	Charpy Impact Specimen and Assembly	58
22.	Reactor Vessel Filter Assembly Installation	63
23.	Glass Fiber Cartridges	66
24.	Glass Fiber Yarns	67
25.	Transverse Section of New Glass Fibers	68
26.	Longitudinal Section of New Glass Fibers	68
27.	Transverse Section of Used Glass Fibers	69
28.	Longitudinal Section of Used Glass Fibers	69

FIGURES

		Page
29.	Electron Micrograph of Incore Filter Fiber After Solvent Extraction	70
30.	Electron Micrograph of Unused Glass Spool Filter Fiber	71
31.	Coolant Analysis History for Core 1-B	77
32.	Specific Activities of Radioisotopes in Core 1-B Coolant	81
33.	Ar^{41} Activity and MST Carbonyl and Water Values for Core 1-A	86
34.	Ar^{41} Activity and MST Carbonyl and Water Values for Core 1-B	87
35.	Radioactivity on Bypass Filters	93

I. REVIEW OF OPERATIONS

The Piqua Nuclear Power Facility (PNPF) achieved criticality in June, 1963; fuel loading was completed in July, 1963; and initial power operation took place early in November of the same year. After first achieving full power January 27, 1964, the reactor operated steadily until the first scheduled shutdown on May 21, 1964 for the removal of the first evaluation element for Hot-Cell examination, maintenance, and a required containment building leak test.

Power operation resumed August 11, and, but for a week shutdown in October for repair of a superheater tube leak, it continued until December 7 when the Technical Specifications limit for pressure drop across the in-vessel filters was reached. During the shutdown, 15 filters were replaced and the element in core position F-13 was removed for examination. The element had shown a steadily increasing outlet temperature following the October shutdown. Ten days after startup, the ΔP limit was again reached; this time one of the two main pumps was shutdown to reduce flow and, therefore, the filter pressure differential. The reactor operated in this mode through the end of the year.

Pertinent operating statistics of the PNPF for the report period, both monthly and cumulative, are given in Table I. Figure 1 demonstrates the cumulative electrical energy generation history for the year, while Figure 2 illustrates the average daily generation (gross).

Significant occurrences at the PNPF during this report period are presented in chronological order.

a) Refueling was completed during the first week in July with the addition of one fuel element and the shuffling of several others. Checkout of the control rods was completed satisfactorily.

b) During the second week in July, the reactor was operated for a short period of time at zero power to determine the new critical position, shutdown margin, and control rod worths with the new core configuration. Operation of the waste-fired boiler on HB was initiated.

TABLE I

OPERATIONS STATISTICS SUMMARY

Operations Parameters	Oct. 30, 1963 to June 30, 1964	July	August	September	October	November	December	To Date (December 31, 1964)
Thermal Power Generation (Mwht)	77,734	0	9,625	18,098	12,666	17,017	13,369	148,509
Cumulative Thermal Power Generation (Mwht)	77,734	77,734	87,359	105,457	118,123	135,140	148,509	148,509
Availability (%)	94.2		88.3	100.0	73.7	100.0	73.8	91.8
Capacity Factor (%)	39.4		28.4	55.2	37.4	51.9	39.5	35.7

Note: Cumulative thermal power generation is calculated from October 30, 1963; the capacity factor and availability are calculated as of January 27, 1964. Availability is defined as the ratio of the number of hours steam was produced or available during a given period, to the number of hours in the same period, less the number of hours for planned shutdown. Capacity factor is the ratio of the gross energy produced during a period of time to the gross rated production capability for the same period of time.

c) During the second and third weeks in July all of the in-core filter elements were replaced, the reactor vessel head was installed, the main heat transfer system was filled with coolant, and circulation of the coolant was initiated.

d) The isothermal temperature coefficient test for both ascending and descending temperatures was started during the third week in July and completed on July 27. The maximum temperature attained during this testing was 570°F.

e) On July 27, the reactor vessel was opened to permit repair of a control rod jumper which had caused an electrical short in one of the two hold coils in control rod No. 4. The control rod jumper head was replaced.

f) On July 28, leaks were discovered in the decay heat removal condenser tube bundle (X-6). The entire tube bundle was replaced, the installation of the new bundle being completed 1-1/2 weeks later.

g) During preparations for reactor startup on July 30, pressure in the purification system increased sharply. Other indications such as

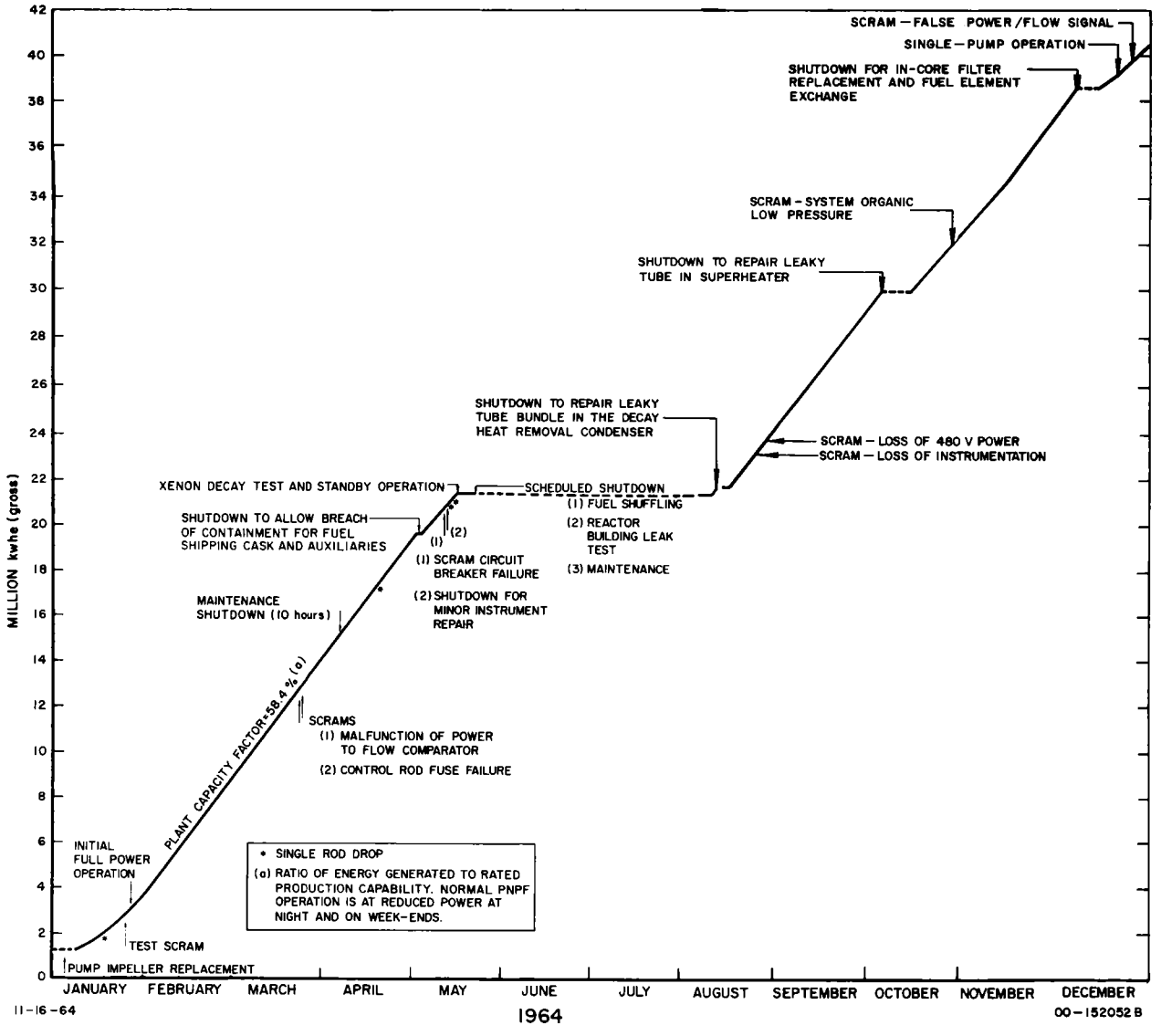

Figure 1. PNPF Operations

degasifier pressure increase and main heat transfer system pressure increase resulted in the conclusion that a leak had occurred in the main boiler or superheater. The main loop was isolated, the pumps were stopped, and the system was drained to permit investigation and correction of the problem. On August 1, it was determined that the leakage was definitely in one of the superheater tubes; the leak was repaired by plugging both ends of the failed tube. All tubes were checked individually with no further leaks discovered.

The reactor was made critical on August 10 and power operation resumed on August 11. At 1201 (EST) on August 12, the responsibility of the Piqua

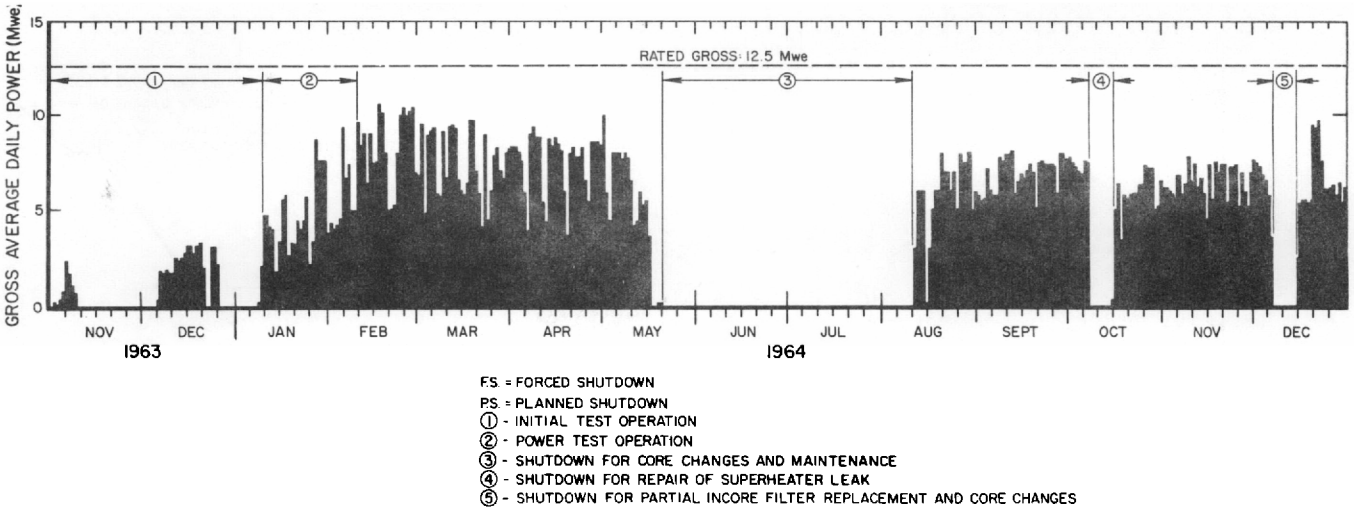

Figure 2. Average Daily Power

Nuclear Power Facility was transferred from Atomics International to the City of Piqua. During August, the PNPF generated steam for about 445 hours producing 9,624,840 kwh of thermal energy. Power levels ranged from 0 to 34.9 Mwt, the maximum occurring on August 28, and the average for the month being 20.6 Mwt. Plant availability for August was 88.3% and the capacity factor was 28.4%.

During the month, one brief shutdown and two scrams occurred. On August 14, the reactor was shutdown to allow another repair of a leaky tube bundle in the decay heat removal condenser. The first scram (August 24) was due to loss of instrument air, the second to an operational error which resulted in opening of the main 480 volt breaker (August 29).

Operational occurrences of significance during August follow.

a) Power coefficient measurements were made at intervals up to 30 Mwt.

b) Operation of the purification system was continuous except for two brief down times, each during a shutdown period.

c) The waste-fired boiler operated intermittently.

d) Pressurizing pump P-3A was shutdown twice during the month. The first time, an unidentified piece of magnetic metal was found in the impeller. The second time, August 29, when the seal temperature rose, the pump was disassembled; the shaft was found to be bent and

its bearing surface damaged. The shaft was repaired, P-3A assembled, and put into service on September 3.

During September, the PNPF was operated in both load-following and base-load modes for 720 hr at power levels ranging from 13 to 35 Mwt (the average for the month was 25.1 Mwt) producing 18,097,700 kwh of thermal energy. Plant availability for September was 100% and the capacity factor was 55.2%. Events of major importance occurring in September follow.

a) The noise-free motor-alternator was taken out of service early in September because of a faulty pillow block bearing. After replacement of the bearing and successful operability check-out, the unit was not returned to service because the immediate need for noise-free power was not evident. The plant continued to operate on raw power throughout September.

b) Both bottoms transfer pumps (P-21A and P-21B) in the purification system malfunctioned frequently. Due to shutdowns for repairing, intermittent operation of the purification system continued throughout the month.

c) Control valve CV-211A, in the decay heat removal system, failed in the closed (fail safe) position. This failure, by diverting the flow through the decay heat condenser, demonstrated that the capacity of the newly-installed X-6 decay heat condenser was more than adequate.

d) The waste-fired boiler was operated intermittently during September with the major problems occurring in the flue gas dust collection system.

The PNPF generated steam for 548.4 hours during October, producing 12,666,490 kwh of thermal energy at power levels ranging from 0 to 32.7 Mwt. The October capacity factor was 37.4% and the plant availability, 73.7%. These low values, compared to September, were due to the October 7-15 shutdown for repair of a superheater tube leak. During the shutdown, the noise-free motor alternator was returned to service.

Other significant occurrences during October follow.

a) The waste-fired boiler operated through most of the month with the exception of a 3-day shutdown period to correct leaks between the

water side and the fire box, and short shutdown times to dump soot from F-6 or to replace loaded filters.

b) The purification system remained in operation throughout most of the month with system repairs being the cause of the few hours shutdown time. A 12-hr shutdown resulted from a partially plugged vacuum line. It was believed that this came about because of the turning off of part of the steam tracing of the line to obtain temperature measurements on the waste gas stream.

c) Steam generation was interrupted twice (October 15 and 18) due to low water level in the evaporator, a result of the boiler feedwater control valves being closed.

d) Main heat transfer pump P-1A was shutdown on October 28 due to a leaking seal. Reactor power was reduced and pump P-1B carried the plant at reduced power until P-1A was repaired and returned to service October 30.

e) On October 30, the reactor scrammed when the organic system pressure was reduced rapidly while filling P-1A and the associated piping. Power operation was resumed within four hours.

f) The in-core filter pressure differential increased during the month to 7.4 psi.

With a plant availability for November of 100%, PNPF produced 17,016,930 kwh of thermal energy. Power levels ranged from 8.1 to 33.8 Mwt with an average of 23.6 Mwt or a capacity factor of 51.9%.

Events of significance occurring during November follow.

a) A state inspection of the waste-fired boiler was made. The results of the inspection were very satisfactory; no problems were discovered and the certification was renewed.

b) The buildup of in-vessel filter pressure drop that was noted in October continued throughout the month increasing from 7.4 to 9.4 psi. A December shutdown was indicated by the extrapolated pressure drop data.

c) Problems involving a loose demister and the release of Raschig ring packing (which caused partial plugging) were experienced in operation of the purification system. After these problems were corrected, satisfactory operation of the system followed.

d) Considerable effort was expended to clear up the partial plugging of the charcoal-filled tanks of the first bank of the waste gas delay tanks, but no entirely satisfactory solution was found.

e) The maximum power level was limited by conventional plant maintenance work during the first half of the month and the Technical Specifications maximum local heat flux limitation during the last half.

f) A 3 to 5°F difference still existed between the mixed mean temperatures and the reactor outlet temperature (TRC-300) measured by thermocouples located in the 14-in. reactor outlet lines.

g) Trouble-free operation of the control rods and control rod position indicators was realized.

h) Small leaks in the spent fuel storage pool developed again, as treatment of the walls with chemical grout did not provide a permanent solution.

Due to the one-week shutdown early in December, a comparatively small total of 13, 369, 440 kwh of thermal energy was produced (plant availability of 73. 8%) for an accumulated total of 148, 509, 200 kwh. The plant capacity factor for the month was 39. 5%.

The reactor shutdown December 7 when the in-vessel filter ΔP reached the Technical Specifications limit of 10 psi. During the shutdown, the media in 15 of the in-vessel filters were replaced, and the element in position F-13 was removed for Hot-Cell examination. This element had shown a steadily increasing outlet temperature for about 2 months; the indicated relative power rose from a constant value of 1. 65 to a final 2. 20. Power operation resumed one week later on December 14. On December 25, the filter ΔP again approached the Specifications upper limit. At this time, one main pump (P-1A) was shutdown to reduce flow and thereby decrease the filter pressure drop. With only one main pump operating, reactor power was limited to 27. 3 Mwt.

Operation continued through the end of the report period with one scram occurring on the 28th while repair work was being done on power-to-flow trip units.

Events of interest that occurred during the month follow.

a) The purification system was erratic in its operation and was shutdown on the 14th to permit revision of suction piping for P-1A and P-1B and for replacement of pump discharge pressure relief valves. The system returned to operation December 18.

b) In investigating the problem of outlet temperature measurement, it was concluded that there was a 4°F loss between the containment vessel penetration and instrument TRC-300 on which the reactor outlet temperature is recorded; the loss was not isolated.

c) During the report period, the waste-fired boiler was beset by several difficulties and operated satisfactorily for only seven days; yet, sufficient burning was accomplished to gain considerable HB storage space.

d) Degasifier tank pressure was difficult to maintain because of malfunctioning of the control valve and pressure transmitter. In addition, control of low flow rates constituted a problem. By using the bypass around the valve, satisfactory control was maintained.

e) Above normal argon activity levels detected in the waste gas system after the December 14 startup returned to normal after the point of air inleakage in the vicinity of the degasifier tank was found and temporarily sealed.

f) An increase in the back pressure of the waste gas delay train was evident at the end of the month.

A. REACTIVITY HISTORY

Measured values of excess reactivity (8.0% ΔK), shutdown margin (4.0% ΔK), and control rod and position indicator calibration data for Core I-B were received from PNPF and entered in the reactivity history program before the August 11 startup. The reactivity difference results and reactor power history for the August-December operating period are presented in Figures 3 through 7. No reason for the constant 75 to 80¢ displacement of the difference from zero has yet been established, but it is believed to arise from inaccuracy in control rod worth for Core I-B.

In August, several abrupt changes in reactivity difference, each coinciding with a period of control rod manipulation, were noted. September, rod-interchange tests verified the discrepancy in rod calibrations. Subsequent

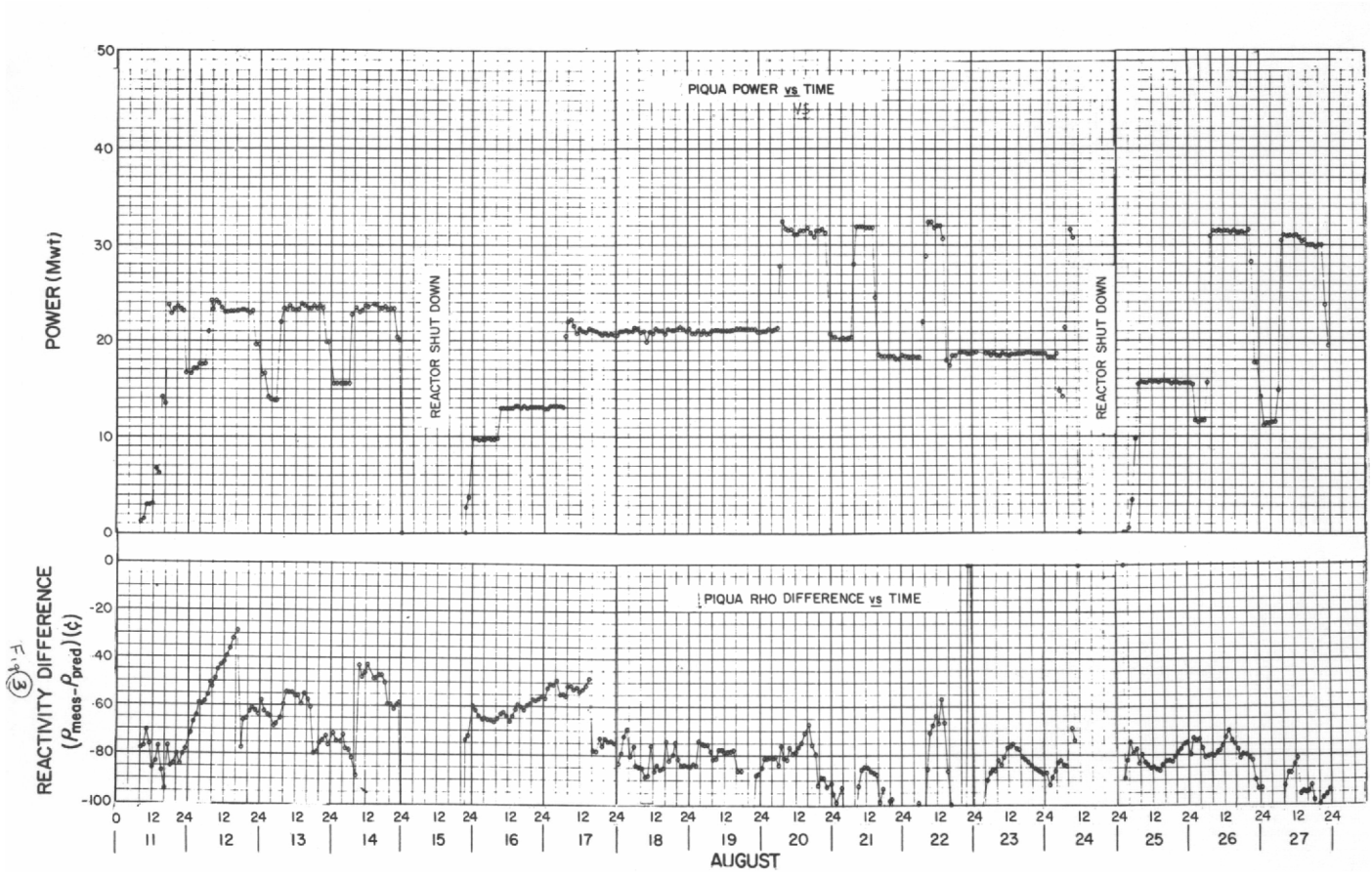

Figure 3. Reactivity History for August

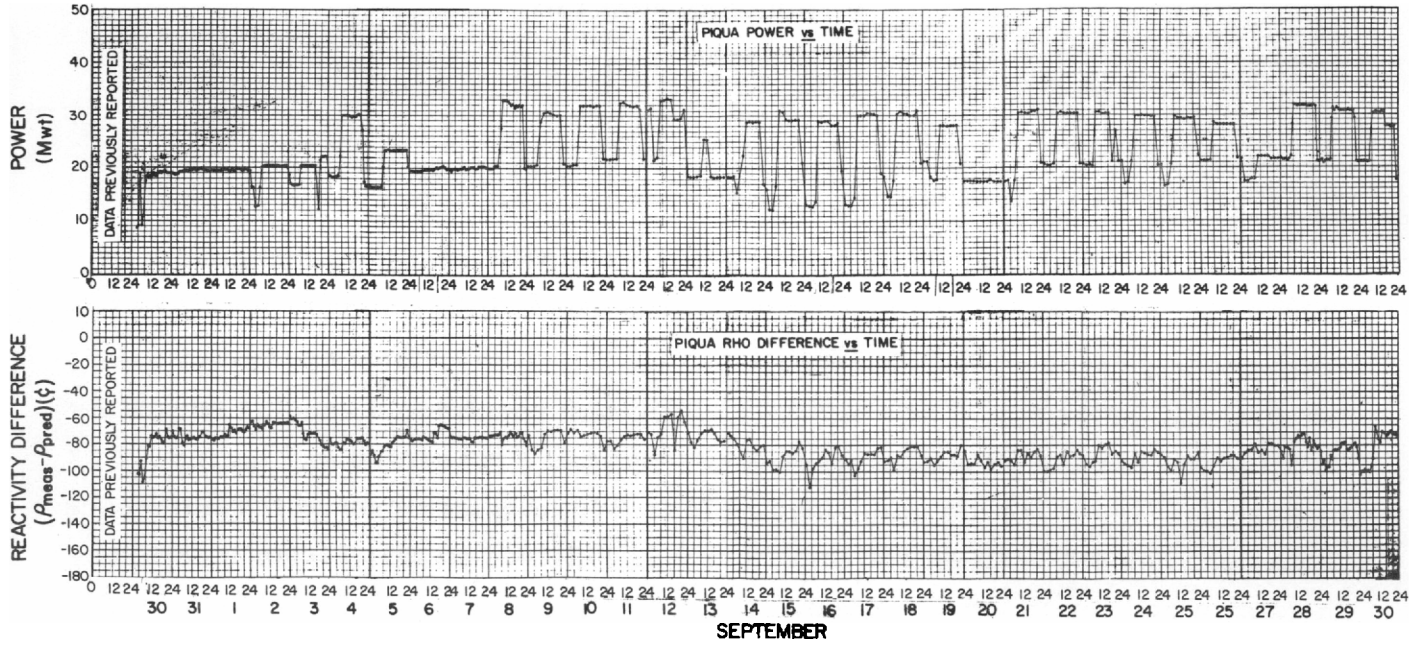

Figure 4. Reactivity History for September

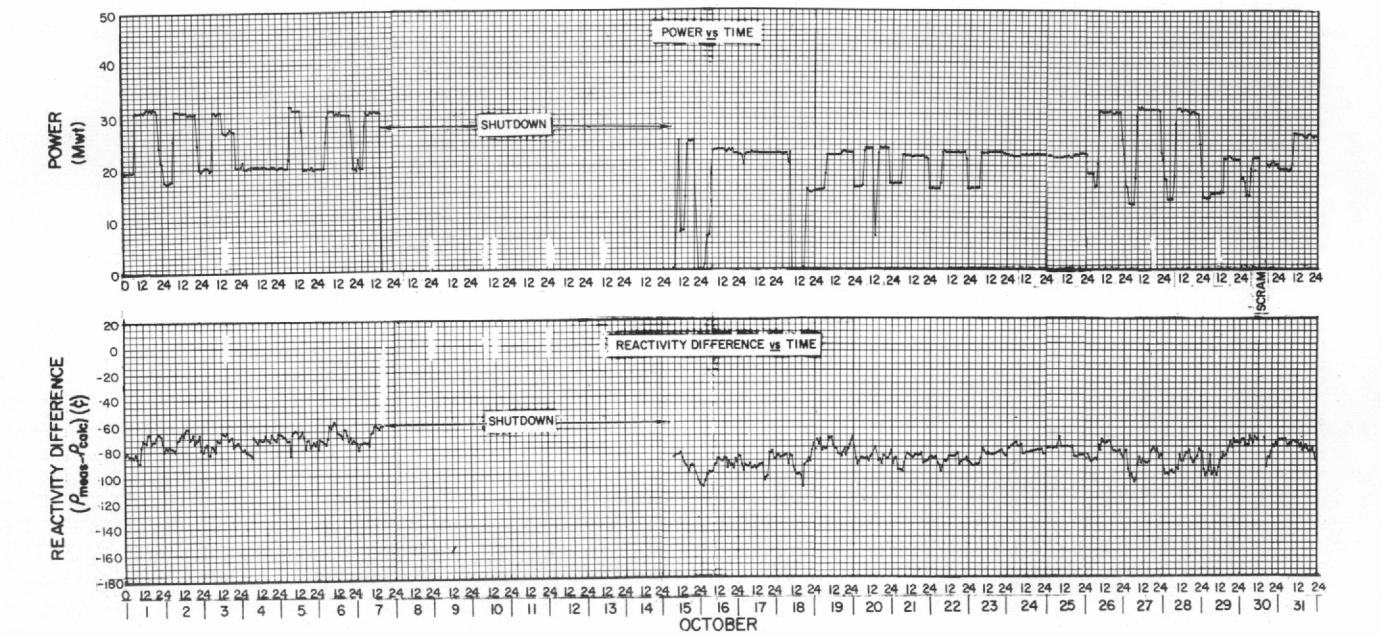

Figure 5. Reactivity History for October

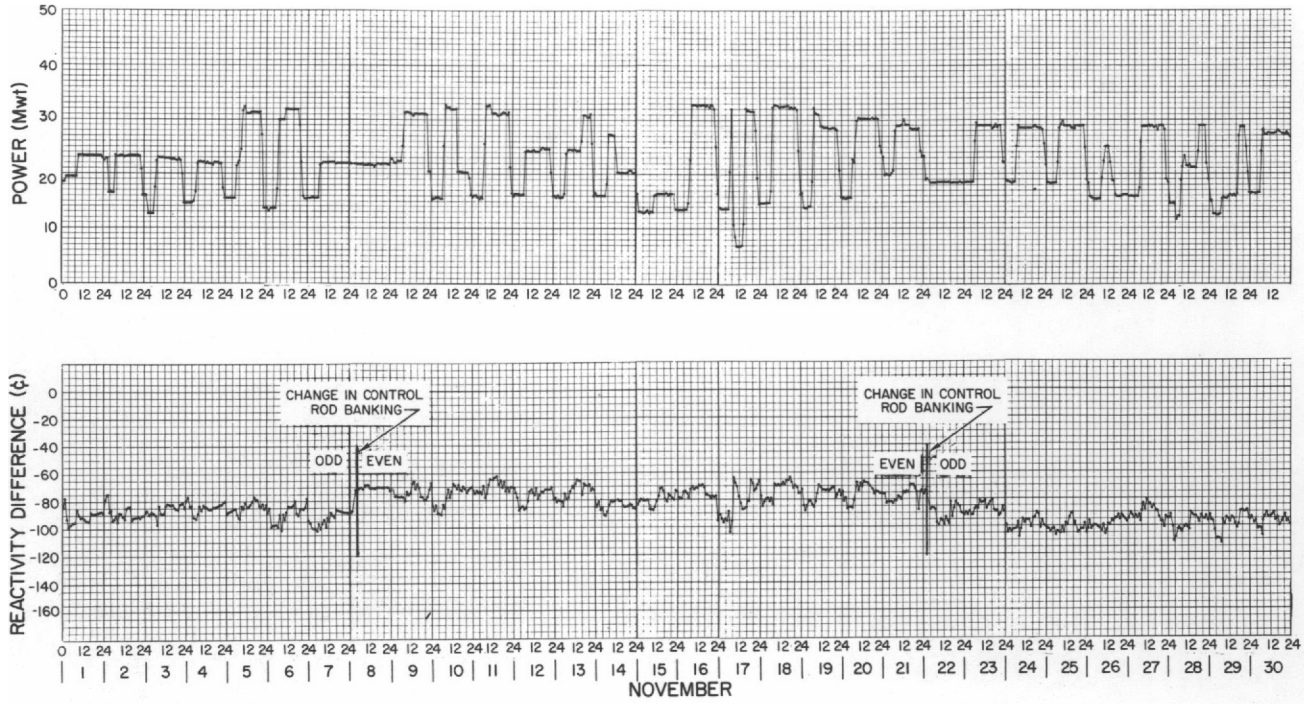

Figure 6. Reactivity History for November

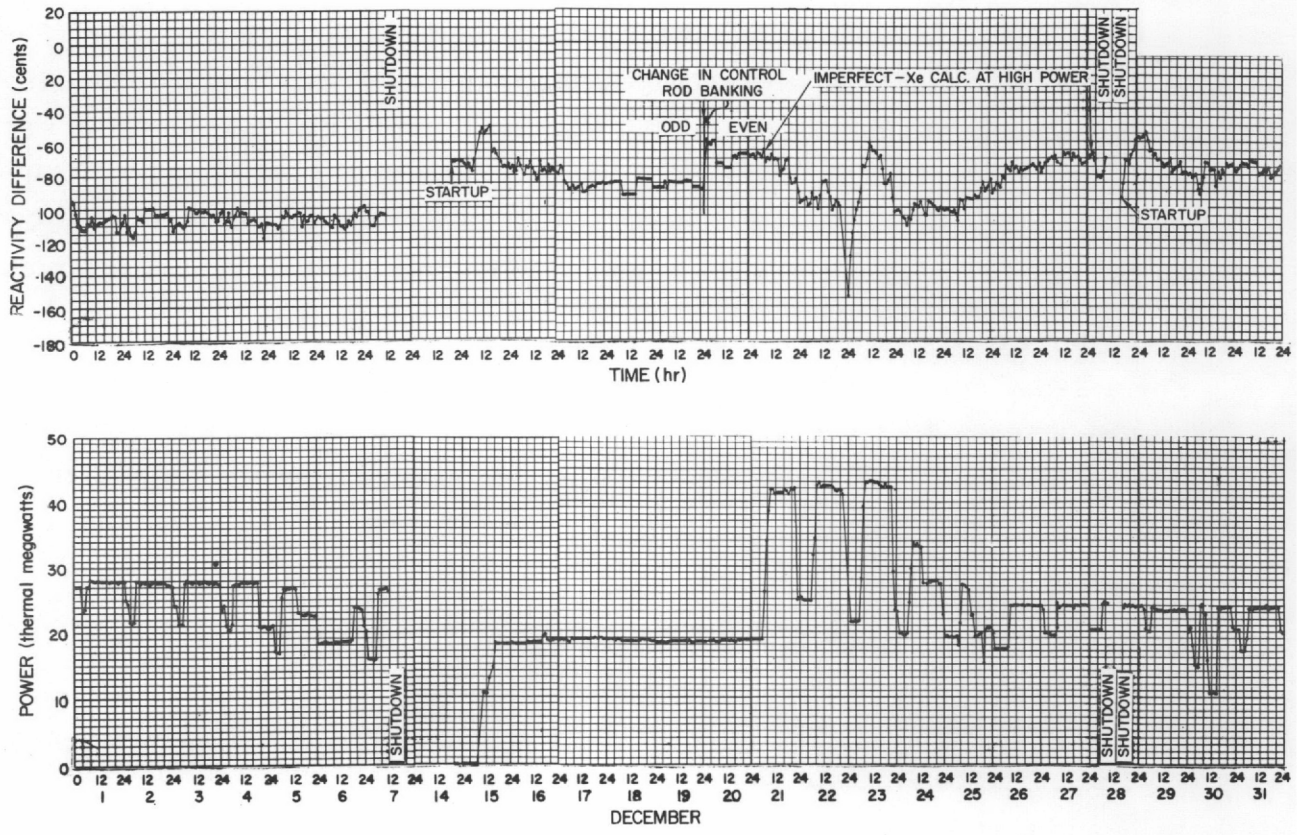

Figure 7. Reactivity History for December

calibration data incorporated in the reactivity history program resulted in a reduction of the magnitude of these changes from the range of 19 to 48¢ to a range of 8 to 15¢ . Although this represents considerable improvement, such disturbances still occur and further investigation may be required to completely explain and eliminate them.

The behavior of the core during most of the October-December period was essentially normal. Normally, the reactivity difference overshoots during power startup because of the inaccuracy of the xenon calculation during a transient period; this situation is seen a number of times in Figures 5, 6, 7. The level change of 20¢ before and after the October shutdown is attributed to the change in control rod banking from the even to the odd rods and the slight differences in the respective position indicators. During the last week of November and first week of December, the reactivity difference was 10¢ more negative than the previously established level for operation with the odd control rod bank. No reason for this indicated change has been established, but two possible causes are (a) inaccuracy in power level determination arising from inexact flow or ΔT measurement, and (b) slippage of one of the outer ring control rods. The wide variation of difference values during the December 21-27 period is a result of high power operation with an accompanying magnification of the inaccuracy due to the approximate Xe constants. In addition, during reactor operator examinations on December 23, the reactor was at zero power between two normal data reporting intervals. This transient condition was not factored into the code calculation and is believed to be the cause of variation in reactivity difference for the day.

For a 3-day period in November, uneven banking of the three inner ring rods was in effect. Rod 4 was about 13% withdrawn while rods 2 and 6 were about 29% withdrawn. The lack of any detectable change in reactivity difference behavior implies that the control rod worth determination is not adversly affected by an inbalance in rod banking.

B. CORE POWER, TEMPERATURE, AND HEAT FLUX DISTRIBUTION

1. Power Distribution Code

The core power distribution program has been expanded to provide the following additional information:

1) Contour map and tabulation of the percent change in relative power of the fuel elements from one computer run to the next,

2) Contour map and tabulation of cumulative fuel element exposure, and

3) Punched card output of the relative power of each fuel element, for use in normalization of the count rates in the FELS (Failed Element Location System) program and for computer plotting of data for long term studies.

2. Outlet Thermocouple Discrepancy

On September 1, a complete set of thermocouple measurements was made using a potentiometer in place of the normal recorders. The data obtained indicated that at 21.0 Mwt, the mixed mean outlet thermocouple used for direct comparison with 54 individual element outlet thermocouples recording on TdR-383 was 3°F higher than the reactor outlet thermocouple printed out on TR-300. The latter had previously been used as the average outlet temperature reference for seven special fuel elements in the core.

The fact that the mixed mean outlet temperature measured in the primary vessel was higher than a comparable temperature (reactor outlet) obtained outside, suggested the possibility of a gamma heating influence on thermocouple junctions in close proximity to the reactor core. However, isothermal calibration data obtained during the October shutdown demonstrated that the same discrepancy existed at zero power. It was concluded from this result, that the effect of gamma heating on the element outlet thermocouples is negligible.

In late November, measurement of the actual coolant temperature at the position of the reactor outlet thermocouple showed it to be in agreement with the mixed mean value. The cause of the loss of 3-5°F between the thermocouple and the recorder has not yet been ascertained. With a correction for the discrepancy, the relative powers of the 54 elements connected to TdR-383 would increase slightly over previous results, while the seven other elements would decrease slightly.

3. Review of Hot-Channel Calculations

A comprehensive review of the hot-channel uncertainties and their application has been completed and a report (NAA-SR-TDR 10720) has been drafted. A brief summary of the analysis follows.

The approach taken was to consider the uncertainties that may affect any of the factors used in calculating the fuel cladding surface temperature or heat flux. The equations used for calculating the axial maxima of these two quantities are:

$$T_s^{\text{peak axial}} = T_{in} + \left[\left(\frac{q}{\bar{q}}\right)_z \frac{WC_p \Delta T_{e\ell}}{A_{HT}\, h} + \phi_z \Delta T_{e\ell}\right]^{\max} \quad \ldots(1)$$

and

$$\left(\frac{Q}{A}\right)^{\text{peak axial}} = \left(\frac{q}{\bar{q}}\right)_z^{\max} \frac{WC_p \Delta T_{e\ell}}{A_{HT}} \quad \ldots(2)$$

where:

T_{in} = channel inlet temperature

W = channel flow rate

C_p = specific heat of coolant

A_{HT} = fuel element heat transfer area

h = film heat transfer coefficient

$\Delta T_{e\ell}$ = coolant channel temperature rise

$(q/\bar{q})_z$ = axial relative power at elevation z

ϕ_z = coolant enthalpy fraction at elevation z

and the superscript max denotes the axial maximum value of the quantity to which it is applied.

It is important to note that the temperature and heat flux obtained from Equations (1) and (2) are averages of the local variations around the circumference of the element at a particular axial location. Since there is a gradient of neutron flux through each element, the highest circumferential value of cladding surface temperature and heat flux will normally occur at the point where the neutron flux is a maximum. To calculate this, temperature and heat flux

Equations (1) and (2) are modified by applying calculated values of the circumferential peaking factor $(q/\bar{q})_{el}$ as follows:

$$T_s^{\substack{\text{nominal}\\\text{channel}\\\text{max}}} = T_{in} + \left(\frac{q}{\bar{q}}\right)_z \left(\frac{q}{\bar{q}}\right)_{e\ell} \frac{WC_p \Delta T_{e\ell}}{A_{HT}\, h} + \left\{ 1 + 0.67 \left[\left(\frac{q}{\bar{q}}\right)_{e\ell} - 1\right] \left(1 - 0.3\, \phi_{\frac{3\ell}{4}} - 0.21\, \phi_{\frac{\ell}{2}} - 0.147\, \phi_{\frac{\ell}{4}}\right) \right\} \phi_z \Delta T_{e\ell} \quad \ldots(3)$$

$$\left(\frac{Q}{A}\right)^{\substack{\text{nominal}\\\text{channel}\\\text{max}}} = \left(\frac{q}{\bar{q}}\right)_{e\ell} \left(\frac{q}{\bar{q}}\right)_z \frac{WC_p \Delta T_{e\ell}}{A_{HT}} \quad \ldots(4)$$

where:

$\phi_{\frac{3\ell}{4}}$, $\phi_{\frac{\ell}{2}}$, and $\phi_{\frac{\ell}{4}}$ are the enthalpy fractions at points 3/4, 1/2, and 1/4 of the way from the top to the bottom of the element, respectively. The additional factors, 0.67 and $(1-0.3\phi_{\frac{3\ell}{4}} - 0.21\, \phi_{\frac{\ell}{2}} - 0.147\, \phi_{\frac{\ell}{4}})$ in Equation (3) arise from consideration of the spiraling fin configuration and coolant mixing between element subsections, respectively.

If all of the factors in Equations (3) and (4) were known precisely and not affected by any uncertainty which does not appear explicitly in (3) and (4), then values calculated from these equations would be the maximum values for any particular element. Since many uncertainties do exist, higher values of temperature and heat flux are to be expected. Further, since the probabilities for occurrence of these uncertainties are not defined, it is reasonable to adopt a statistical approach to take them into account.

The uncertainties which were considered to have a significant effect on the calculations are summarized in Table II and are briefly defined as follows.

1) Estimated uncertainty in axial neutron flux distribution in an element
2) Estimated uncertainty in circumferential neutron flux distribution around an element

TABLE II

UNCERTAINTIES IN HEAT TRANSFER CALCULATIONS

i	Thermo-Physical Quantity	Uncertainty Factors $\equiv \left\{\frac{\text{Hot-Channel Value}}{\text{Nominal Value}}\right\} - 1$		
		$U_\theta \equiv$ Film Drop Factor	$U_{\Delta T} \equiv$ Coolant Temperature Rise Factor	$U_\phi \equiv$ Heat Flux Factor
1	Axial neutron flux distribution	0.10	0.05	0.10
2	Local or circumferential peaking in an element	0.10	0.67 (0.10) K*	0.10
3	Heat transfer coefficient	0.10	-	-
4	Coolant flow rate	0.02	-	0.10
5	Fuel thickness	0.03	0.03 K	0.03
6	Mechanical tolerances on individual flow channels	0.10	0.30 K	0.06
7	Measured temperature rise in element	$\frac{2.0}{\Delta T_{e\ell}}$	$\frac{2.0}{\Delta T_{e\ell}}$	$\frac{2.0}{\Delta T_{e\ell}}$

*$K \equiv (1 - 0.3\phi_{3\ell/4} - 0.21\phi_{\ell/2} - 0.147\phi_{\ell/4})$

3) Uncertainty in heat transfer coefficient arising from inaccuracies in, and extrapolation of, the experimental data used to arrive at a correlation for the coefficient

4) Allowance for flow variation in an element based on results from flow tests of 20 elements

5) Allowance for variation of fuel meat thickness within prescribed tolerances

6) Allowance for effect on heat transfer area and flow arising from variations within mechanical tolerance limits

7) Estimated uncertainty present in measurement of temperature rise in any element.

Each of the factors is applied to the film drop, temperature rise, or heat flux as appropriate to obtain the deviation of the influenced quantity. Assuming no correlation between the deviations caused by the seven thermo-physical quantities, the formulation for the hot channel maximum cladding surface temperature and heat flux can be written as

$$T_s^{\text{hot channel}}_{\text{max}} = T_s^{\text{nominal channel}}_{\text{max}} + \sqrt{\sum_i \left[d_{\theta_i} + d_{\Delta T_i}\right]^2} \qquad \ldots(5)$$

and

$$\left(\frac{Q}{A}\right)^{\text{hot channel}}_{\text{max}} = \left(\frac{Q}{A}\right)^{\text{nominal}}_{\text{channel max}} \left(1 + \sqrt{\sum_i U_{\phi_i}^2}\right) \qquad \ldots(6)$$

where

$$d_{\theta_i} = U_{\theta_i}\left[\left(\frac{q}{\bar{q}}\right)_{e\ell}\left(\frac{q}{\bar{q}}\right)_z \frac{WC_p \Delta T_{e\ell}}{A_{HT} h}\right]$$

and

$$d_{\Delta T_i} = U_{\Delta T_i}\left[1 + 0.65\left(\left(\frac{q}{\bar{q}}\right)_{e\ell} - 1\right)\left(1 - 0.3\,\phi_{\frac{3\ell}{4}}\right)\right]\phi_z \Delta T_{e\ell} \quad .$$

4. Review of Burnout Heat Flux Calculation

A survey has been made of the various correlations which can be used for the prediction of the critical heat flux for PNPF. Using the latest available physical properties for the Santowax OMP coolant, all correlations indicate a significantly higher burnout heat flux than the 432,000 Btu/ft^2-hr limit implied from the given value of maximum allowable heat flux and minimum steady state burnout safety factor in the technical specifications for the 61 element core. This limit was based specifically on the Griffith correlation, but present calculations using current physical data give a much higher value. The values calculated from the various correlations are presented in Table III, together with the respective reference sources.

Technical specifications for the PNPF also indicate that for the sake of conservativeness the lower limit of the Griffith correlation which is reproduced in Figure 8*, was used to obtain the critical heat flux. However, diphenyl data

*Nomenclature used in Figures 8 and 9 is defined in Table IV

TABLE III

BURNOUT HEAT FLUXES FROM VARIOUS CORRELATIONS

Correlation	Fluid	Predicted $(Q/A)_c$ (Btu/ft^2-hr)
Griffith* (lower)	Santowax R&OM	754,000
Griffith* (upper)	Santowax R&OM	1,820,000
Core & Sato†	Santowax OMP	980,000
Core & Sato†	Santowax R	1,320,000
Robinson & Lurie†	Santowax R + 27 w/o HB	2,080,000

*P. Griffith, "The Correlation of Nucleate Boiling Burnout Data," ASME Paper 57-HT-21, 1957

†NAA-SR-MEMO 7343, "Organic Reactor Heat Transfer Manual," J. D. Gylfe, et. al., December, 1962

is inappropriate since the reactor coolant is Santowax OMP which contains less than 1.0% diphenyl. In Figure 9 the diphenyl data points have been removed from the graph. It is clear from Figure 5 that in the region of normal operation ($P/P_c \approx 0.2$) the upper limit of the Griffith correlation is a much better fit of the Santowax OMP data than the lower limit. Using the upper limit to compute the burnout heat flux, the resulting value is ~2.4 times higher than the value obtained from the lower limit as can be seen from Table III.

Applying the Technical Specification minimum steady-state burnout safety factor of 3.4 to the critical heat flux obtained from the upper limit of the Griffith correlation results in a maximum allowable heat flux of 535,000 Btu/ft^2-hr. Even if the lower limit is applied, the revised critical heat flux of Table III yields a maximum allowable value of 222,000 Btu/ft^2-hr.

From the foregoing discussion, it would appear that the limitation of 127,000 Btu/ft^2-hr is unduly restrictive and it was recommended that it either should be changed to reflect the more recent information or should be eliminated entirely.

Effective December 4, the limitation on peak steady-state heat flux was eliminated from the Technical Specifications. With this deletion, the remaining

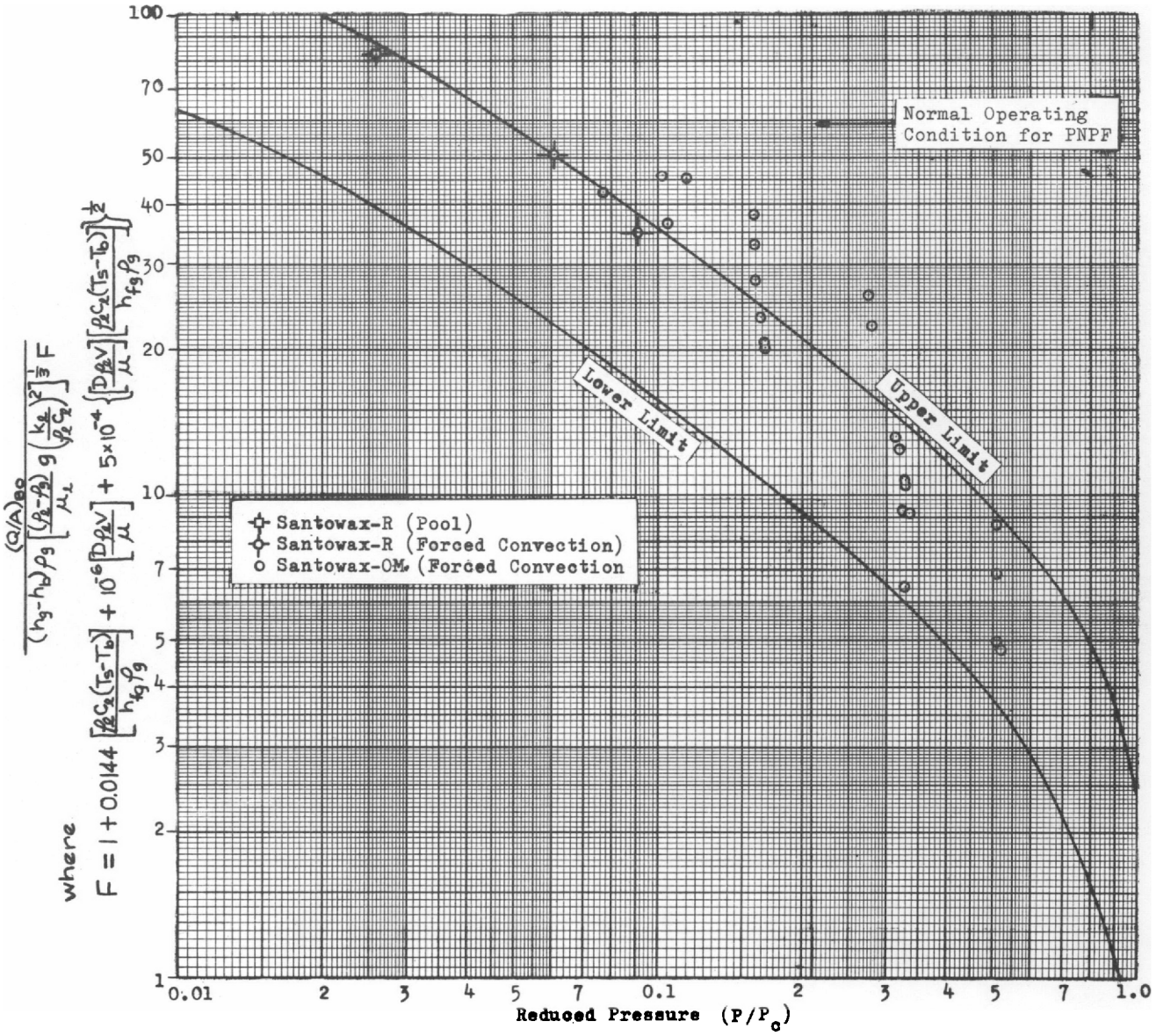

Figure 8. Griffith Correlation for the Prediction of Critical Heat Flux

limitation of 750°F on steady-state peak cladding temperature became the governing factor with regard to reactor operation.

C. RELATIVE POWER STUDIES

During October, a rise in the calculated relative power of the element in core position F-13 from 1.65 to 1.79 was noted. The accuracy of this result was questionable at the time due to loose connections in the thermocouple circuitry, but the thermocouple situation was remedied and the increase was seen to continue through November to the December 7 shutdown. Figure 10 shows

TABLE IV

NOMENCLATURE FOR FIGURES 8 AND 9

C_l	=	liquid specific heat at saturation temperature
D	=	channel equivalent diameter
F	=	correction factor (see Figure)
g	=	gravitational constant
h_b	=	liquid enthalpy at bulk temperature
h_g	=	saturated vapor enthalpy
h_{fg}	=	latent heat of vaporization
k_l	=	liquid thermal conductivity at saturation temperature
P	=	operating pressure
P_C	=	critical pressure
$(Q/A)_{BO}$	=	burnout heat flux
T_b	=	bulk coolant temperature
T_s	=	saturation temperature
V	=	coolant velocity
ρ_l	=	coolant density at saturation temperature
ρ_g	=	vapor density
μ_l	=	coolant viscosity at saturation temperature

the relative power behavior of the elements in core locations E-10, E-12, F-13, and G-14 since November 10. The constancy in relative power of the element in E-10 is representative of the majority of elements in the core. From the figure, the following information can be gathered.

1) The indicated relative power of the F-13 element continued to increase to a value of 2.25 (obtained from a least squares fit of the data) before the December 7 shutdown. At full power with a core ΔT of 46°F, a change in relative power from 1.65 to 2.25 reflects an outlet temperature of 25°F. Behavior of the replacement element in F-13 after the December 14 startup appears normal at a relative power of 1.41. A higher relative power (1.65) had been predicted based on the relative powers of the other inner-ring elements. It is felt that the element placed in F-13 could be receiving a larger share of the flow than the

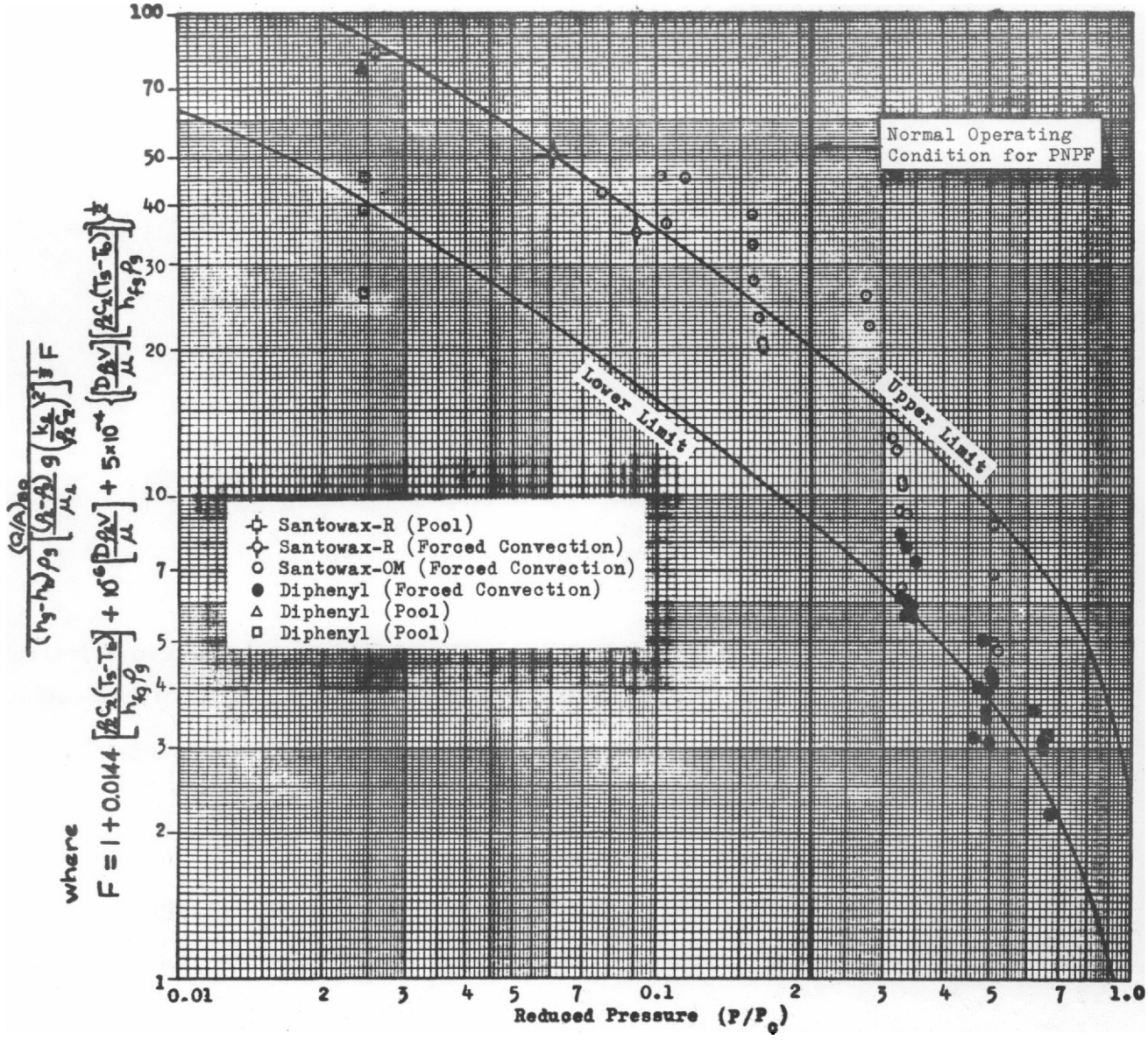

Figure 9. Griffith Correlation for the Prediction of Critical Heat Flux (Diphenyl Data Deleted)

other inner-ring elements, because of their greater burnup and attendant dimensional changes. At the peak burnup of the inner-ring elements (2000 to 2500 Mwd/MTU) a lineal dimensional change of slightly over 1% would be expected. A 10% decrease in the flow area would not be inconsistent with this dimensional change. The change in indicated relative power that would accompany this flow restriction would have occurred at a very slow rate, starting at the commencement

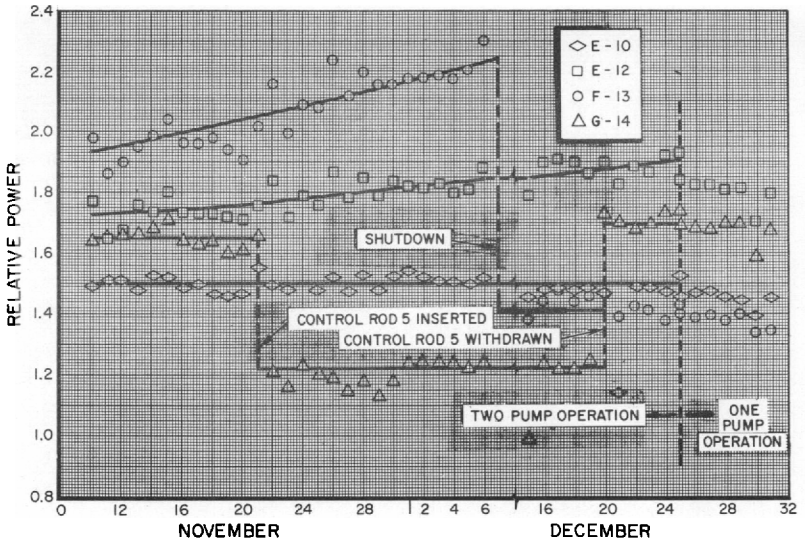

Figure 10. Relative Power Behavior of Fuel Elements in Core Positions E-10, -12, F-13, and G-14

of reactor operation. Although no such increase was noted in relative power calculations, three effects that could have masked this rise are:

a) A change in power distribution on replacement of the special dummy elements,

b) Periodic changes in control rod banking, and

c) Changes or modifications of temperature instrumentation.

2) The indicated relative power of the element in core location E-12 increased at a linear rate of about 0.006 $\frac{\text{units of relative power}}{\text{day of operation}}$ starting about November 12 at a relative power of 1.72 and ending with the start of single pump operation on December 25 at a relative power of 1.92. Sufficient data for single pump operation had not been accumulated to establish relative power behavior, but results from the first few days indicated that the element relative power had dropped to a lower, constant value of about 1.83. A cause for this effect is being sought.

3) When the odd-numbered bank of control rods was fully withdrawn on December 20, the relative power of the G-14 element (location of control rod 5) rose from 1.22 to 1.70. This change is similar to the

behavior of all control rod elements; the G-14 element is shown because it has the second highest relative power. Although the relative power after December 19 is slightly higher than previous values with Rod 5 completely withdrawn, the data are not sufficient to allow a conclusion to be drawn.

D. INSTRUMENTED FUEL ELEMENT TEMPERATURES

Normalized cladding temperatures for the instrumented fuel elements (D-13, D-15 and E-12) August-December operating period are shown in Figure 11. No change in established behavior is present in the results, and hence no malfunction or loss of heat transfer capability is apparent in these elements.

A detailed examination of the normalized cladding temperatures has revealed that some measured values are not easily reconciled with expected values at the thermocouple locations as shown in Figure 12. In particular, the following cases are apparent:

1) The lower thermocouple on the inner cylinder of the element at core location D-13 indicates a temperature which is essentially the same as the coolant inlet temperature. Shorting of this thermocouple has been suspected for some time.

2) The upper thermocouple on the inner cylinder of the element at core location E-12 indicates a temperature ~30F° higher than that at a similar position on the same cylinder 16 in. lower in the element. Since the latter location is expected to be the higher temperature region, there is a possibility that two thermocouple locations in this element are being misinterpreted.

In addition to these observations, it is of interest to note that the maximum cladding temperature of element E-12 does not show a rising characteristic as does the relative power during the interval preceding single-pump operation on December 25. However, the present technique of utilizing the IFE temperature information (normalization to full power) may not be sufficiently sensitive to emphasize small trends. Additional methods will be investigated to permit more sensitive utilization of the IFE temperatures as a diagnostic tool.

A

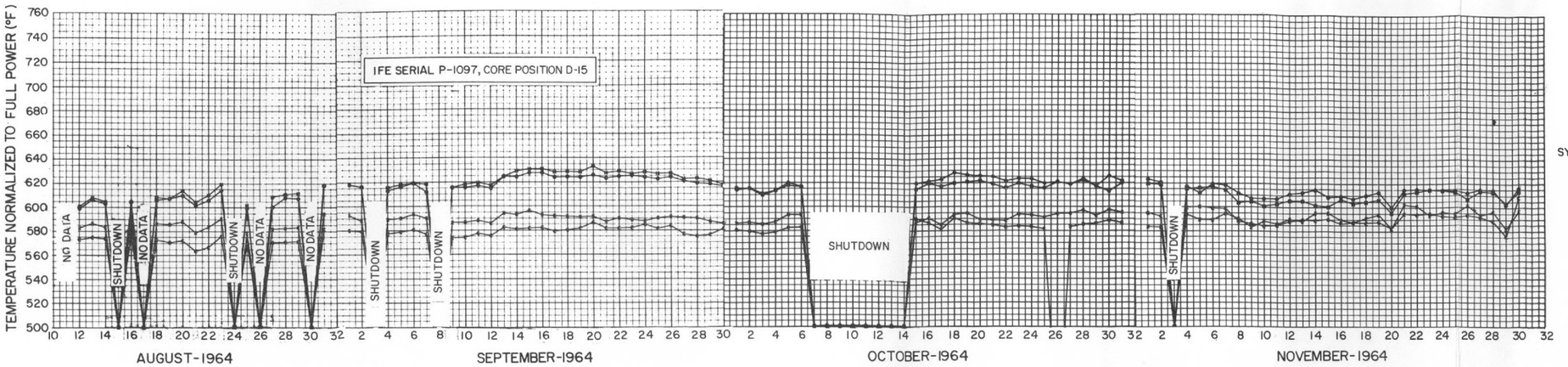

SYMBOL	T/C	INCHES FROM BOTTOM OF ACTIVE CORE	T/C LOCATION
C	120	28.375	INNER CYLINDER
H	120	12.125	INNER CYLINDER
O	122	12.125	OUTER CYLINDER
X	125	12.125	OUTER CYLINDER

B

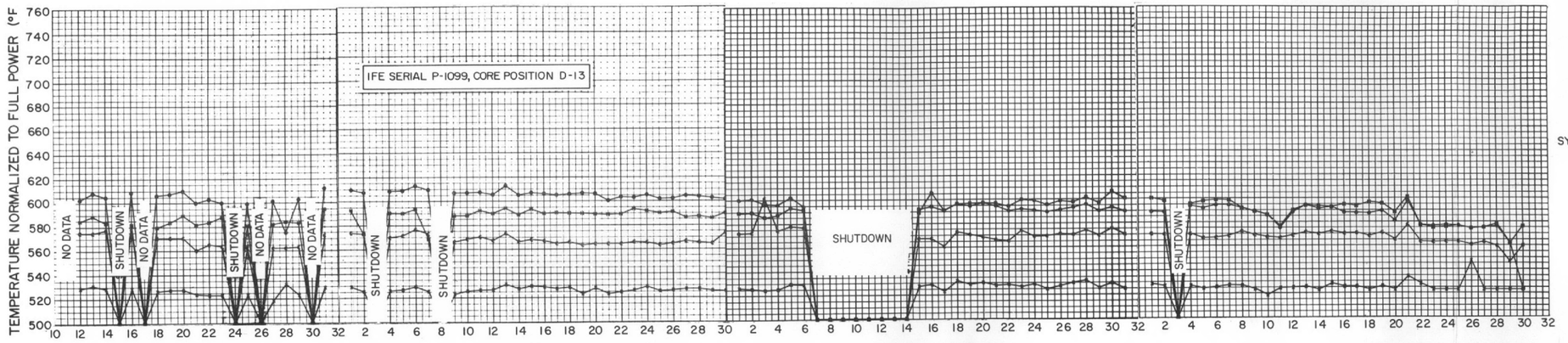

SYMBOL	T/C	INCHES FROM BOTTOM OF ACTIVE CORE	T/C LOCATION
C	117	28.375	INNER CYLINDER
H	118	12.125	INNER CYLINDER
O	119	12.125	OUTER CYLINDER
X	125	12.125	OUTER CYLINDER

C

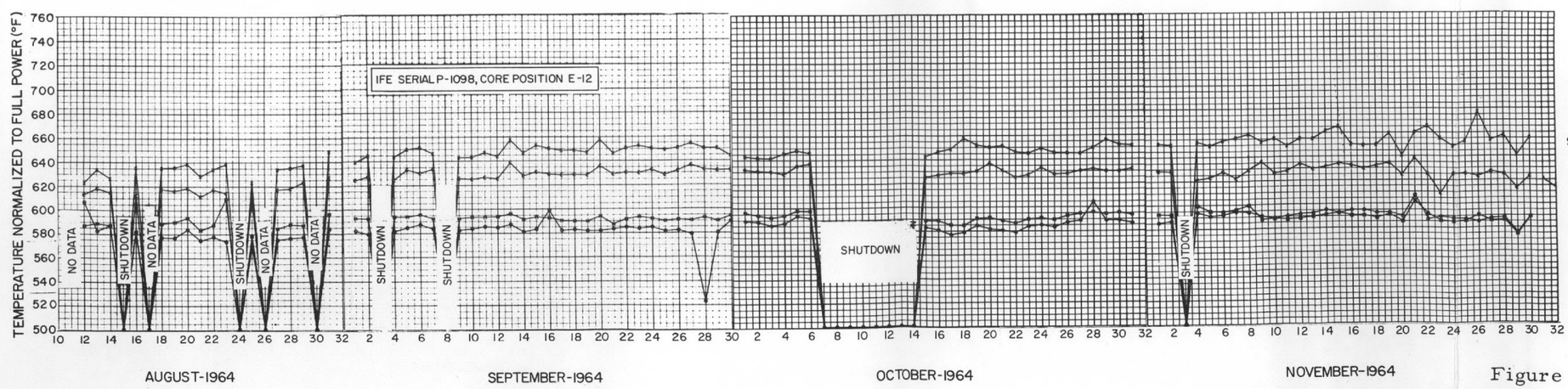

SYMBOL	T/C	INCHES FROM BOTTOM OF ACTIVE CORE	T/C LOCATION
C	114	28.137	INNER CYLINDER
H	120	12.125	INNER CYLINDER
O	116	12.125	OUTER CYLINDER
X	123	12.125	OUTER CYLINDER

Figure 11. Instrumented Fuel Element Normalized Cladding-Surface Temperatures

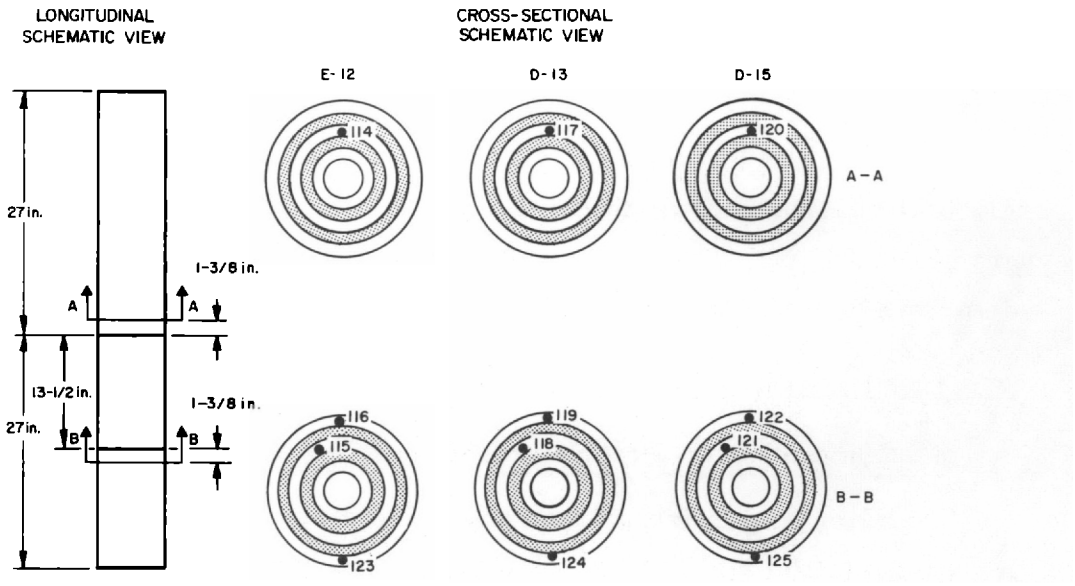

Figure 12. IFE Thermocouple Locations and Identifications

E. NUCLEAR PARAMETERS OF CORE 1-B AT STARTUP

Estimates of excess reactivity, total control rod worth, and shutdown margin were made for Core 1-B at 350°F prior to the August 11 startup. The figures were calculated with Core 1-A initial values of 7.06, 10.54, and 4.32% Δk being used as starting points for these three nuclear parameters (respectively). Assumptions made for the analysis were as follows:

1) A reactivity loss due to burnup of 0.88% Δk (an average core burnup of 664 Mwd/MTU and a reactivity loss rate due to burnup of 1.328% Δk/1000 Mwd/MTU were used),

2) An equilibrium samarium worth of 0.63% Δk,

3) An increase in ρ_{ex} due to replacement of two dummy elements with fuel (2.7% Δk). This value was determined experimentally at the time of insertion of the dummy elements into the 44 core loading.

4) An increase in worth of the 17 peripheral elements whose worth was determined after the dummy element insertion, attributed to the replacement of the dummy elements with fuel, 0.36% Δk,

5) A loss of ρ_{ex} due to the removal of elements from D-3 and H-19 (0.13% Δk)

6) An increase in total control rod worth of 1.32% Δk associated with the replacement.

The resultant values for Core 1-B were 8.52% Δk excess reactivity, 11.86% Δk total control rod worth (in the shutdown configuration), and a shutdown margin of 4.18% Δk. The difference between this last figure and the experimentally determined 4.0% Δk is less than the ±0.2%Δk limit set for startup.

F. DECEMBER FUEL REARRANGEMENT

1. Consideration Prior to the December Shutdown

In making a decision on the second element to be removed from the core for examination and at what date the removal should take place, a number of considerations were evaluated:

a) the fuel management program requirement for removal of an element with an average burnup of ~1700 Mwd/MTU;

b) the steady increase in outlet temperature of the element in F-13;

c) the increase in pressure differential across the in-vessel filter.

With regard to the third point, it was conceivable that there would be a switch to one-pump, reduced flow operation when the filter ΔP had risen to the to the Technical Specifications 10 psi limit. This could have resulted in a degradation of the condition in fuel channel F-13 where the increasing outlet temperature was considered to reflect a continuing flow restriction. From this standpoint, the one-pump operation was not considered desirable.

Although the plan for fuel examinations called for removal of an evaluation or premeasured element, there appeared little doubt that F-13 would be the element removed rather than the evaluation element in H-9. The cause of the steady increase in calculated relative power of F-13 had to be ascertained. In addition, this element would provide almost the same information as a premeasured element with respect to:

a) the extent of surface film formation,

b) abnormal deposits on the fuel element inlet screen,

c) the condition of the aluminum nickel uranium bond, and

d) swelling of the fuel alloy material.

Precise fuel cylinder dimensional and density changes would not be obtained; however, changes greater than the tolerance ranges would be meaningful. Thus, the information gained from selection of the element was considered to outweigh that loss due to lack of precise preirradiation dimensional data.

2. Element Operating Histories

The operating histories and required cooling times of the two elements considered are presented below.

a) Fuel Element in Core Position H-9

With average values of reactor power and element relative power, the operating history of H-9 was assumed to consist of 105 days at 600 Kwt, a shutdown period of 87 days, and a second operating interval of 112 days at an average power of 530 Kwt. The average and peak burnups for the element, as of December 7, were estimated as 1685 and 2530 Mwd/MTU, respectively. A cooling time of 6.5 days would be required to reduce the element decay heat in the shipping cask to less than the AEC requirement of 1.2 Kwt.

b) Fuel Element in Core Position F-13

Two cases were considered in establishing an operating history for F-13. Case (1) assumed that the calculated relative powers provide a true indication of element power over its operating interval. Case (2) assumed that the true relative power remained unchanged despite the observed increase starting in August 1964; burnup and cooling times were calculated based on the initial level of relative power. This latter treatment was used for estimating actual burnup levels, but the more conservative data, Case (1), were utilized for establishing cooling time requirements.

For Case (1) the operating history consisted of 105 days at 550 kwt, a shutdown interval of 87 days, and the second operating interval of 112 days at 690 kwt. During this last period, the element relative power was assumed to rise from its initial value of 1.65 to a final value of 2.25 with a time-weighted average of 1.80. For Case (2), the relative power over the second operating interval was assumed to remain constant at 1.65 (average element power of 630 kwt).

The estimated average and peak burnups on December 7 were 1825 and 2740 Mwd/MTU, respectively. A cooling period of 11.5 days was calculated to reduce the element decay heat to less than 1.2 kwt.

3. Removal of the Element from F-13

Due to the three considerations noted, the reactor was shutdown December 7. On December 12, the element was removed from the core and placed in an HB-40 filled thimble where it remained cooling until December 24. It was then loaded into the shipping cask and sent to the Santa Susana Hot-Cell for post-irradiation examination. At the time of shipment, the decay heat was estimated at 1.0 kwt and the fission product content at 2.1×10^5 curies. For Case (1) relative powers, the peak heat flux and cladding temperature for the interval were calculated as $103,000 \frac{BTU}{hr\text{-}ft^2}$ and 690°F, respectively.

The fuel element movement accompanying the removal of element P-1091 from F-13 was simple in execution. The element previously in location E-16 (P-1022) was moved to F-13 and was, in turn, replaced with a fresh element (P-1053).

Three recommended tests were performed following the shutdown, in an effort to explain the behavior of the F-13 element:

1) An isothermal test was conducted at 460°F during which the outlet temperatures of all but a few of the channels were recorded. The F-13 temperature recorded on TdR-393 was in line with the other elements' temperatures; i.e., the outlet thermocouple appeared to be functioning properly.

2) The orifice of the element in F-13 was checked and was found to have been properly adjusted at 30 turns open (completely open).

3) An examination of the F-13 filter revealed that it was completely intact and free of any obstructions.

G. CONSIDERATIONS FOLLOWING FUEL REARRANGEMENT

1. Equivalent Core Exposure Remaining

As of December 7, the second bank of inner ring control rods was withdrawn 30% at the average operating power level of ≈20 Mwt. The reactivity

associated with the remaining 70% of the bank (2.50% Δk) could be available for core burnup. As an estimate of what actually would be available, this figure was modified by two considerations: (1) 0.49% Δk was allowed for the increase in xenon concentration for full power operation, and (2) no withdrawal of the remaining three inner ring rods above 80% was permitted. The combination of these two points plus a small gain in excess reactivity due to the fuel shuffle itself results in ≈6600 Mwd of exposure remaining for the rest of the cycle (a burnup rate of 3.88×10^{-2} cents/Mwd was used). Under a normal full power load cycle (average power of 35 Mwt), this is equivalent to six months operation.

2. Consideration of the E-12 Element

Although the data for single-pump operation have shown a constant relative power value of 1.83 (see Section C) for the element in E-12 (P-1098), full-flow results are considered sufficient to warrant a movement of the element.

It was recommended for several reasons that the element be moved to a position of lower relative power (D-5) rather than be removed completely from the core. First, the apparent rate of rise (or flow restriction) is considerably less for E-12 than it was for F-13. Also, the additional information obtained on this phenomenon could avoid unnecessary removal of future elements which exhibit a similar behavior. Finally, as an IFE, the E-12 element represents an analytical tool; the presence of the special cladding thermocouples affords a further check on variation of cladding temperature. The relative power characteristics which should result from this exchange are as follows:

Element No.	Core Position		Relative Power	
	Original	Final	Original	Final
P-1098	E-12	D-5	1.92	0.9
P-1062	D-5	E-12	0.7	1.4

With the new arrangement, the peak cladding temperature in P-1098 is estimated as 625°F. At the same rate of increase of outlet temperature seen in November and December during full flow conditions, the P-1098 cladding temperature should not exceed the 750°F limit before the scheduled shutdown for removal of the third evaluation element. The actual rate of rise is expected to be lower with the element in the lower power position.

A. MAIN HEAT TRANSFER SYSTEM ANALYSIS

1. Computer Program

The Main Heat Transfer System (MHTS) digital computer program, employed for routine calculation of performance parameters for the main coolant pumps, pressurizing pumps, and steam generator, was expanded to calculate reactor thermal power, from total organic flow, total temperature drop (TdR-305) across the boiler-superheater combination, and from the sum of the separate boiler and superheater heat duties. This procedure should point out any errors in temperature readings around the steam generating equipment.

An additional modification to the code was made to enable automatic plotting of the performance parameters vs time, on a monthly basis. With this routine the percent deviation between measured and predicted performance parameters for the main pumps, pressurizing pumps, and steam generator is plotted vs time. The percent deviation is defined as follows:

$$\% \text{ Deviation} = \frac{\text{Measured Value - Predicted Value}}{\text{Predicted Value}} \times 100\%.$$

Thus, a positive deviation indicates better-than-expected performance, and a negative deviation indicates poorer-than-expected performance.

2. Main Coolant Pump Performance

Following repair of the superheater tube leak on August 6, the main organic coolant pumps, P-1A and P-1B, were returned to service. Pump performance data taken shortly after the startup showed excellent agreement with data taken prior to the shutdown as well as with previous pump test data.

Parallel operation of P-1A and P-1B continued until October 29 when the seal temperature on P-1A increased to 400°F. Seal leakage was confirmed subsequently by temperature rise in the seal drain line, indicating terphenyl flow through the line. The pump was shutdown and isolated from the system. Disassembly and inspection showed that the U-cup in the mechanical seal had been

damaged. The damage is ascribed to high (>400°F) seal temperatures experienced as the result of a check-valve failure in the shield-cooling water system, with subsequent temporary low cooling-water flow to the seal. Typical pump performance parameters (head and efficiency) calculated for parallel pump operation, and for P-1B operating singly, are summarized in Table V. The agreement between predicted and measured results during this period is indicative of overall satisfactory pump performance.

TABLE V

MAIN COOLANT PUMP P-1A AND P-1B PERFORMANCE

Date	Flow (gpm)	Meas. Head (ft)	Mfr. Pred. Head (ft)	Head Deviation (%)	Meas. Efficiency (%)	Mfr. Pred. Efficiency (%)	Efficiency Deviation (%)
10/1	14,025	139.4	145.9	-4.5	79.2	75.7	+4.7
10/5	13,950	139.3	146.7	-5.0	78.2	75.7	+3.2
10/7	13,950	139.2	146.8	-5.1	77.5	75.8	+2.3
10/16	14,175	141.9	144.9	-2.0	80.5	75.6	+6.5
10/19	14,175	141.8	144.8	-2.0	80.6	75.6	+6.6
10/22	14,175	143.1	144.8	-1.2	81.3	75.6	+7.6
10/26	14,100	142.3	145.1	-1.9	81.2	75.6	+7.3
10/28	14,100	143.5	144.9	-1.0	82.0	75.6	+8.4
10/29	8,850*	93.8	86.1	+9.0	66.3	69.5	-2.9

*P-1B only in service. P-1A down for seal replacement.

In early November, it was noted that the deviation between the measured and predicted efficiency and pump head showed an increased positive deviation from previous results. Due to the increased in-vessel filter drop, the pump suction pressure had decreased. Since the reactor inlet pressure is controlled by the degasification and pressurization system, the main pump ΔP has increased. Although the main loop flow had decreased slightly (as governed by the pump head capacity curve), it is not possible to see this flow decrease accurately on

the main loop flowmeter; therefore, the higher pump ΔP (at about the same measured system flow) resulted in the large positive deviation between measured and predicted pump efficiency and the consistent positive deviation between measured and predicted pump head.

This increase in % deviation is seen in the top two graphs of Figure 13 which is typical of the graphical data display produced by the MHTS computer

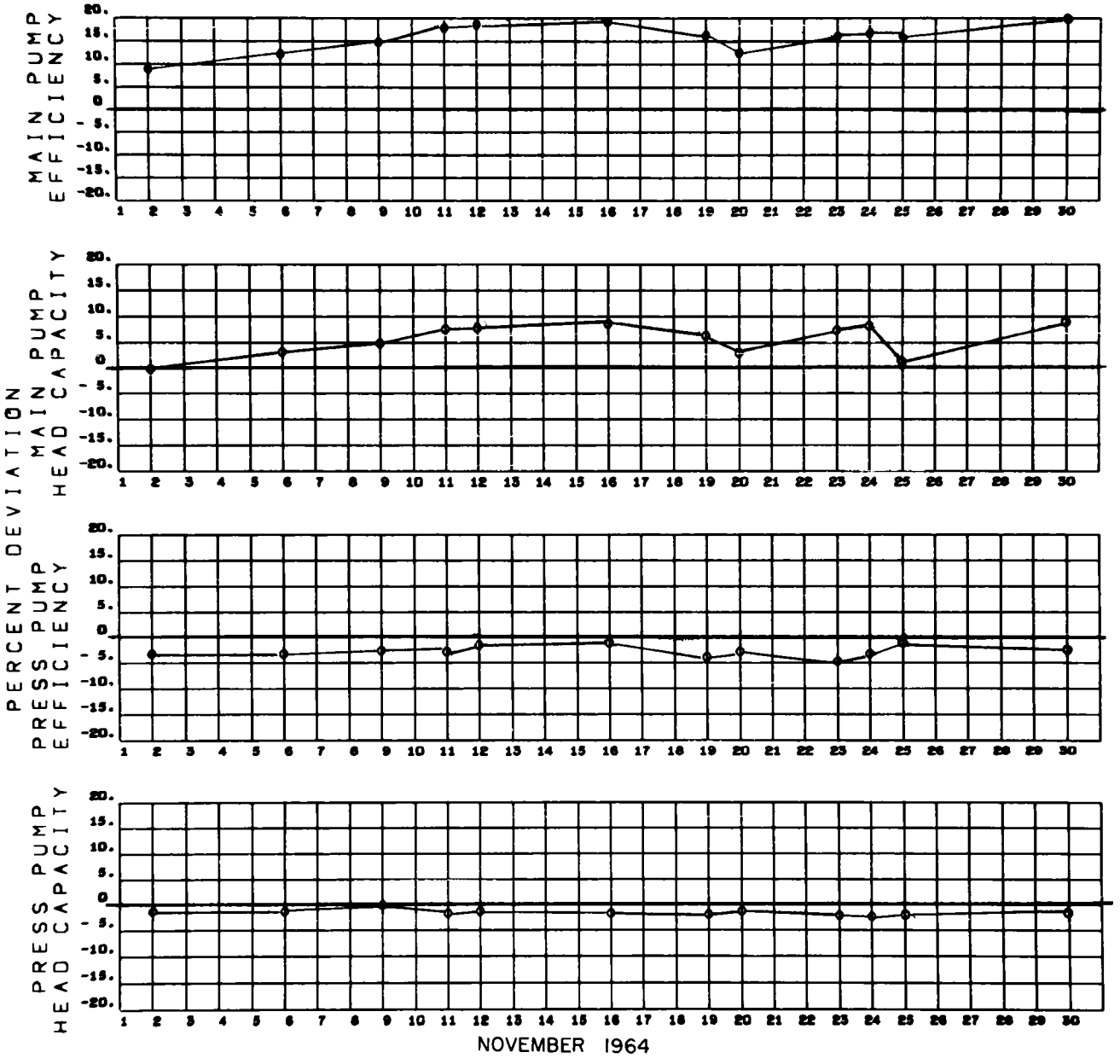

Figure 13. Main- and Pressurizing-Pump Performance

program. The trend noted on November 6 continued throughout December, due to the high in-vessel filter ΔP.

3. Pressurizing Pump Performance

Pressurizing pumps P-3A and P-3B were employed singly or in combination to provide flow through the core while the reactor was shutdown and to provide the necessary degasification flow rate during power operation. During August, considerable difficulty was experienced in controlling the seal temperature of P-3A, eventually causing the pump to be removed from service on two occasions (August 13 and August 30) for repair. Disassembly of the pump following the first shutdown revealed a piece of metal lodged in the impeller.* Performance data (for the combined pumps) following the August 13 shutdown showed no apparent loss in efficiency. However, with the existing instrumentation in the pressurizing loop it is not possible to evaluate the performance of only one pump when both pumps are operating. Hence, only the overall efficiency of the two pumps in parallel was evaluated. The calculated combined pump efficiencies were 38.2 and 37.0% for August 20 and 27, respectively, vs a predicted efficiency of 39% based on manufacturer's data. These efficiencies are also in good agreement with results obtained prior to reactor shutdown.

On August 31, pressurizing pump P-3A was removed from the system and disassembled to investigate the cause of the high seal-temperatures and vibration of the pump. It was determined that the shaft was worn at the bearing. The shaft was repaired, the bearing replaced, and the pump reassembled and installed in the system on September 3. During the time that P-3A was removed from the system, pressurizing loop flow was maintained by P-3B. This mode of operation provided an opportunity to check the performance of one-pump instead of the normally calculated two-pump performance parameters. The single-pump operating data and results are summarized in Table VI for September 1, 2, and 3. The close agreement between measured and predicted efficiency and head is indicative of satisfactory pump operation. The data shown in Table VI for September 8-28 are for parallel pump (P-3A and P-3B) operation. Again, good agreement between predicted and measured performance parameters is observed for this mode of operation. However, since it is not possible

*Piqua Nuclear Power Facility Monthly Operating Report No. 16, August 1964, issued by City of Piqua.

TABLE VI

TYPICAL PRESSURIZING PUMP PERFORMANCE

Date	Total Flow Rate (gpm)	Pump Head (ft)	Pump Head (psi)	Hydraulic Horsepower Per Pump (hp)	Brake Horsepower Per Pump (hp)	Calculated Pump Efficiency (%)	Predicted Efficiency (%)	Predicted Pump Head (ft)
9/1*	325	304	117.2	22.2	36.1	61.6	62.5	310
9/2*	325	304	117.4	22.3	36.4	61.2	62.5	310
9/3*	320	307	118.3	22.1	36.1	61.2	62.5	310
9/8	325	299	115.1	10.9	26.7	40.9	39.5	310
9/9	330	301	116.1	11.2	27.3	40.9	40.0	310
9/11	330	301	116.1	11.2	27.5	40.6	40.0	310
9/15	315	305	117.8	10.8	27.5	39.3	38.5	312
9/21	325	308	118.8	11.3	27.3	41.2	39.5	310
9/23	320	307	118.4	11.1	27.8	39.7	39.0	311
9/28	325	310	119.5	11.3	28.3	40.0	39.5	310

*P-3B only in operation - P-3A removed for repair of shaft

to evaluate the performance of P-3A separately, it is not known definitely if any change in the single-pump efficiency resulted from the shaft and bearing rework.

Additional performance data for the pressurizing pumps are shown in the lower two graphs of Figure 13 which present the deviation between measured and expected efficiency during the month of November. Similar results were obtained for operation during December. This excellent agreement between measured and predicted values, as well as the agreement with previous data, is indicative of satisfactory pump performance.

4. Steam Generator Performance

During preparations for power operation following the extended plant shutdown, a water or steam leak into the main coolant loop, evidenced by a sudden increase in the pressure of the purification and degasification systems, was observed on July 31. The pressure in the degasifier tank increased from a control setting of 5 to 17 psia, and the pressure on the steam side of the steam generator began to decrease, indicating the possibility of the leak being in the boiler or superheater. Prior to the incident, reactor coolant was being maintained at 450°F by pump heat and was being circulated with full flow through the superheater and a small flow through the boiler. The boiler had previously

been filled with feedwater. No off-normal operating conditions were noted prior to the sudden increase in purification column pressure.

Subsequent investigation showed the source of leakage to be a superheater tube failure in the third row from the vertical baffle on the steam inlet side (the fifth tube in the row from the north side). The point of failure was approximately 2 in. below the center line of the organic outlet nozzle. Due to interference caused by the bottom head of the superheater, it was not possible to examine the failed tube with a boroscope.

Repair of the tube leak by plugging at the tube sheet was completed during the first week of August and the system hydrostatic tested successfully at 900 psig. Steam generation was resumed on August 11.

The boiler heat transfer coefficients measured after startup were in good agreement with results obtained during April and May, prior to the reactor shutdown (see Figure 14). These results indicated no reduction in boiler heat transfer capability during the shutdown for fuel changing and superheater repair.

The superheater heat transfer coefficient following startup (59.1 Btu/hr-ft^2-°F at 62.5% of full load) was significantly below that of the previously calculated results of approximately 82 Btu/hr-ft^2-°F (expected coefficient) at 62.5% of full load, and continued to be lower than the previous one throughout subsequent operation. Review of plant operating data showed that the steam temperature at the superheater outlet (TR-437) is currently reading ~6 to 7F° lower than previously, while the superheated steam temperature measured at the Piqua Power Plant (TR-438) has remained essentially unchanged. During the shutdown period, the transmitter for TR-437 was changed to provide a more accurate temperature readout by introducing a 300F° zero offset in the transmitter and an expanded chart in the recorder. The calibration of TR-437 was rechecked and found to be accurate within 0.5F°. Thus, the lower superheated steam temperatures and lower heat transfer coefficients are correct. It is believed that the superheated steam temperatures reported previously (read on a 0 to 800°F scale) were high by ~5 to 6F°. Since the steam temperature read at the power plant remains essentially the same as before the shutdown, there has been no real decrease in superheating capacity of the plant, only an apparent decrease due to the erroneous temperature reading of TR-437 during the previous plant operating period.

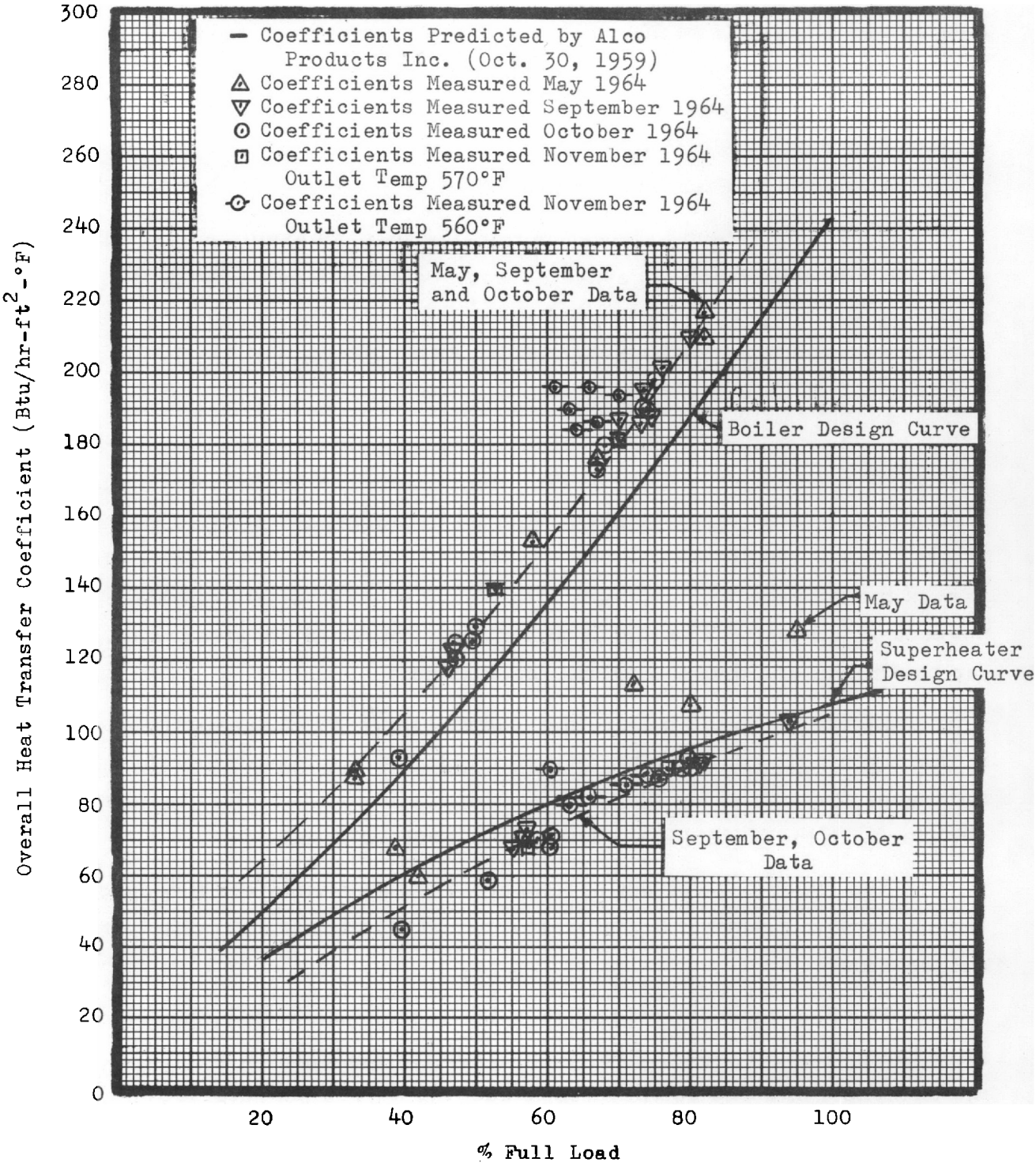

Figure 14. Steam Generator Heat Transfer Performance

On October 7, failure of another superheater tube allowed water inleakage to the organic coolant. As in previous cases, the leak was indicated by increasing degasifier pressure and high waste gas flow. The failed tube was

located and plugged, and the main heat transfer system filled by October 14. The superheater now contains four plugged U-tubes. There has been no noticeable derating in the superheated steam conditions as a result of plugging the tubes. (Approximately 35 tubes could be plugged before the outlet steam temperature would decrease from 560 to 550°F at a flow of 150,000 lb/hr.)

Following return to power in mid-October, overall heat transfer coefficients for the boiler and superheater were calculated by using the MHTS analysis computer program. Very good agreement between measured and predicted values were obtained for both the boiler and superheater through mid-November. These data are plotted in Figure 14.

On November 20, the reactor outlet temperature was reduced from 570°F to ~560°F to reduce the fuel cladding temperatures. In the superheater, the lower inlet organic temperatures resulted in a decrease of the superheated steam temperature from ~560 to ~552°F. As a result of the lower steam ΔT across the superheater, a larger steam flow was required to produce the same percent of full load. The higher steam flow improved the steam side heat transfer coefficient and thus the overall coefficient.

Likewise, in the boiler, the lower organic ΔT necessitated an increase in the organic flow through the boiler to obtain the same power. In this case, the higher flow improved the organic film coefficient (which is the controlling resistance in the boiler) and, thus, the overall coefficient.

The lower organic outlet temperature was maintained throughout December with resultant higher-than-normal heat transfer coefficients as discussed above.

The heat transfer capability of the superheater was reviewed to determine the maximum capacity of the unit. In the analysis, it was assumed that the superheater would be operated to superheat 425 psia saturated steam to a temperature of 550°F. Organic coolant conditions were: 575°F superheater inlet temperature and 14,000 gpm flow rate. Two cases were considered with coolant containing 10 and 30% HB, respectively. In both cases it was necessary to extrapolate measured heat transfer coefficient values beyond the region for which test data were available. The actual coefficients may, therefore, differ somewhat from those used in this study.

The analysis showed that with coolant containing 10% HB the superheater would be capable of superheating ~240,000 lb/hr of 425 psia steam to a temperature of 550°F. This is equivalent to a reactor power level of 73 Mwt.

With coolant containing 30% HB, the predicted heat transfer coefficients had to be reduced to take into account the increased coolant viscosity. Under these conditions, the capacity of the superheater was estimated at 200,000 lb/hr of steam at 550°F and 425 psia (equivalent to a reactor power level of 60 Mwt).

It must be pointed out that the above mentioned power levels represent actual limitations only under the present operating conditions of the reactor. It is anticipated that operation of the second core could be extended to higher power levels with a higher organic coolant reactor outlet temperature and flow rate. Under these conditions, the heat transfer capability of the superheater tube bundle would be increased even further. Actual limitations would have to be defined on the basis of projected operating conditions which have not yet been established. It must be noted that this evaluation has been based only on an analysis of the capability of the superheater tube bundle, and did not take into consideration any limitations imposed by the steam separation capacity of the boiler.

B. FLOW RATE AND PRESSURE DROP FOR MAIN HEAT TRANSFER AND DEGASIFICATION SYSTEMS

1. Main Heat Transfer System Filters

During the May-July 1964 shutdown period, the 67 glass-spool filter assemblies located above the fuel elements were removed from the reactor vessel and disassembled, new glass spools were installed, and the clean units were reinstalled in the reactor. Following system startup on July 21, the pressure drop across the filters was 4 psi at a main loop coolant flow of 14,000 gpm. These data are shown in Figure 15 and are in good agreement with data recorded during early operation with the old filter elements. Data from early January, when the main loop flow was 14,000 gpm, indicated a 5-psi ΔP for the old filters, which at that time had already accumulated some particulate matter during the precritical system cleanup and testing period.

The pressure drop remained between 4 and 4.5 psi throughout July and August. However, starting in early September, the pressure drop showed a

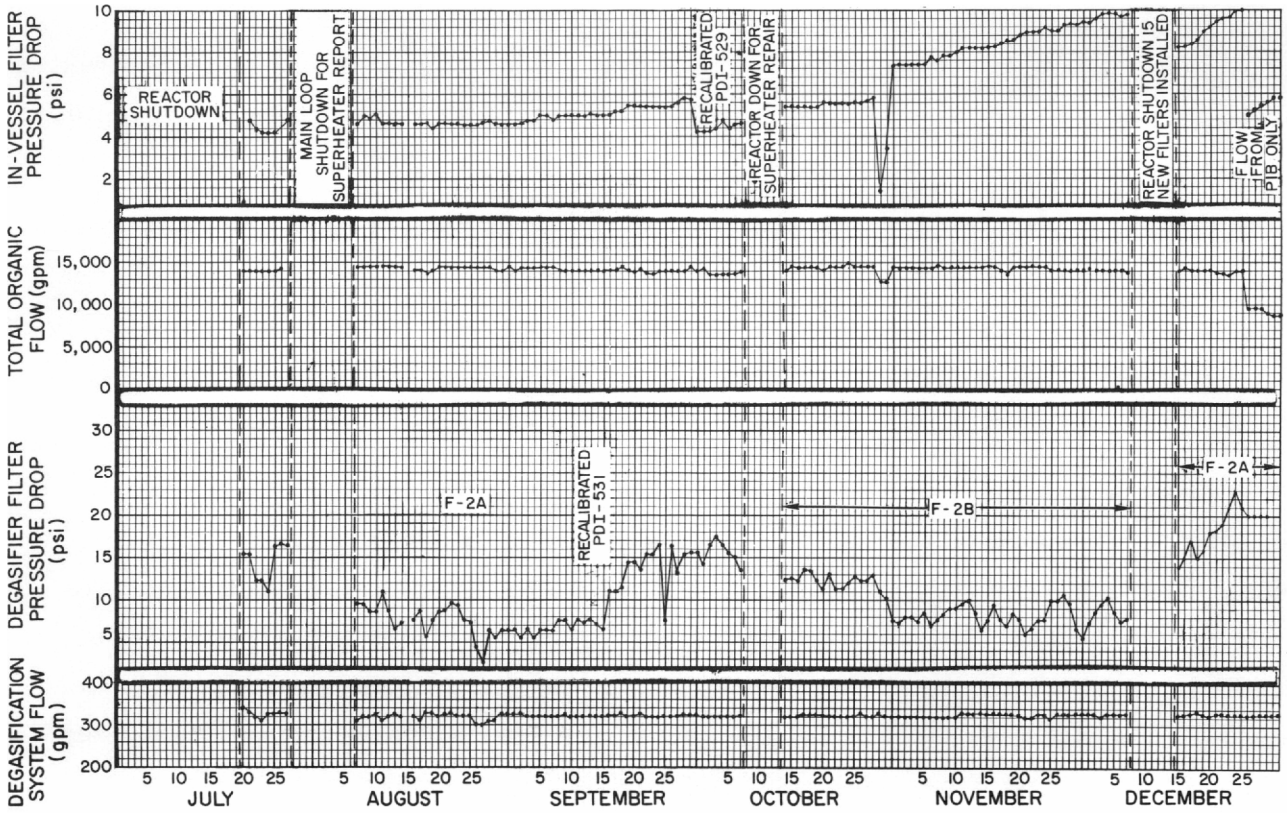

Figure 15. Flow and Pressure Drop for MHTS and Degasification System

gradual increase with time and reached the limiting value of 10 psi on December 8. The 10-psi limit is dictated by structural considerations of the upper guide grid which seals the filters within the vessel and is exposed to the same ΔP as the filters.

At that time, the reactor was shut down to remove the second examination fuel element and replace 15 of the in-vessel filters with spare units available at the site. Following return to power, the ΔP was ~8.1 psi which was in excellent agreement with a predicted value of ~8.2 psi calculated by using the electrical analogy of combining resistances in parallel and assuming the pressure drop varied as the square of the flow.

Between December 17 and December 22, the pressure drop increased from ~8.4 to ~9.6 psi (see Figure 15) at a flow rate of approximately 14,000 gpm. This rate of rise was greater than observed at any previous period of operation. On December 18, the filter ΔP showed a step increase of 0.3 psi and, concurrently, the waste gas flow increased to 40 scfh at a reactor

power of 40 Mwt; waste-gas activity was high, primarily from argon. As in the past, the high waste-gas flow rates and high argon activity were associated with air in-leakage to the system. It was determined that a valve bonnet in the line returning coolant from the FELS tank to the degasifier tank was loose, allowing air to enter the system. This line discharges below the liquid level in the degasifier; thus, the air was in good contact with high temperature coolant containing 6 to 7% HB. Previous experimental work had shown that organic coolant absorbs oxygen very rapidly at temperatures near the operating temperature of the degasifier, ~570°F. Thus, it appears feasible that polymerization of the coolant into oxygen containing compounds or increased corrosion product formation may be an indirect reason for the rapid in-vessel filter pressure drop increase.

Analysis of the material collected on the filter spools removed during the next reactor shutdown should provide additional valuable information on the type and nature of material responsible for the rapid filter plugging. The filters installed during August have plugged gradually during normal reactor operation. However, the 15 filters installed in December have seen the rapid pressure buildup and the system conditions during the known air inleakage. Any difference in material collected on the two sets of filters may show the effect of air contamination of the circulating coolant.

On December 25, the in-vessel filter pressure drop again reached 10 psi. Since replacement filters were not available at that time, and it was not desired to shutdown, it became necessary to reduce the total core flow. Of several methods available, operation with one main coolant pump rather than two was recommended as the best method of achieving the desired flow reduction. Operation with one main pump reduced the flow from ~14,000 to ~8800 gpm and the filter pressure drop from 10 to ~5 psi. It was recommended further that main coolant pump P-1A be maintained in service; this pump delivers coolant to the lower section of the superheater tube bundle. The coolant cross-sectional flow area outside the shroud as well as through the shroud is larger in the lower section of the superheater than it is in the upper section. Thus, coolant velocities, both outside the shroud and entering the tube bundle will be lower. At a flow rate of 8800 gpm, the velocities in the annular space were calculated to be 21.2 and 14.2 ft/sec in the top and bottom sections, respectively, and the velocities

through the shroud cutout 5.4 and 3.7 ft/sec at the top and bottom, respectively. Also, the tube sheet, located at the bottom of the exchanger will provide additional rigidity to the tubes at the higher-than-design flow rates.

Two alternate methods for reducing core flow were considered, but were rejected as being unsatisfactory. These methods were (1) throttling flow with the main pump discharge valves, and (2) adding system pressure drop by changing the setting of the boiler flow control valves. The first method was rejected due to possible damage to the gate valves on the pump discharge, and the second method was rejected due to possible plant control problem resulting from readjustment of the boiler bypass valve.

With the proposed mode of operation, the plant power is limited to ~28 Mwt as determined by the power-to-flow comparators. Also, the coolant velocity in the orificed fuel elements of the core would decrease from 10.8 ft/sec to 6.8 ft/sec.

2. Degasification System Filters

When the degasification system was returned to service on July 20, circulation was established initially through degasification filter F-2B. This unit had not been employed during the previous period of power operation and was believed to be clean. However, the indicated pressure drop varied between 11 and 13 psi, which was considerably higher than expected. On July 25, F-2A, the filter employed during the previous operating period was returned to service and F-2B valved out of the system. The indicated ΔP for F-2A was approximately 17 psi as opposed to values of 11 to 12 psi recorded just prior to the system shutdown in May. Since these units had not been in service during the shutdown period and the increased ΔP could not be explained on the basis of changing physical properties, it was proposed to site personnel that the anomaly was due to drift of the pressure transmitters and/or indicator. Subsequent instrument checks indicated need for recalibration which was completed on July 30. Following the recalibration, the ΔP returned to 8-10 psi which is similar to levels reported prior to plant shutdown in May. The pressure drop across the filter showed a continued increase throughout August and September, peaking at ~18 psi in early October (see Figure 15).

Following repair of the superheater tube leak in October, degasifier filter F-2B was placed on line, rather than F-2A. This change in filters was

made in conjunction with a program to determine the source of particulate contaminants found on occasion in the coolant. The pressure drop across the F-2B filter, which contains 2μ pore size glass spools, as opposed to the 3μ spools in F-2A, was extremely erratic. On several occasions, the ΔP decreased 2 to 3 psi over a 1 to 2 day period. The pressure drop across the degasifier filter, F-2B, has been extremely erratic throughout the month (see Figure 15). On several occasions, the ΔP decreased 2 to 3 psi over a 1 to 2 day period of operation. Also, the radiation levels at the surface of the filters have decreased steadily during the month. The erratic ΔP data and the decrease in surface activity are indicative of possible bypassing of the filter media within the housing, or possible structural damage to the filter cartridges.

Due to the erratic behavior of the pressure drop across F-2B, it was valved out of the system during the plant shutdown, and F-2A replaced in service. A sharp increase in F-2A ΔP is noted commencing on December 18, concurrent with the step increase in in-vessel filter ΔP and the detection of the air in-leakage into the degasification system and again demonstrates the detrimental effect of 0_2 on the organic coolant.

C. COOLANT DISTILLATION SYSTEM

During the period that the reactor was shutdown for fuel handling and filter replacement, the coolant distillation system was operated to maintain coolant purity. Average coolant feed rate to the column is shown in Figure 16. Through July 29, the column feed was supplied from either the main loop or the reactor building drain tank. As a result of the continuous purification, the HB level of the coolant was maintained below detectable limits. Due to the extremely low (essentially zero) HB content in the column feed material and the necessary method of operation, a considerable quantity of useful coolant was discharged from the bottom of the column to the HB decay tank T-9. During the period that the waste fired boiler was shutdown for filter replacement, July 30-31, material from decay tank T-9B was processed through the column to recover the useful terphenyl prior to reactor startup..

With the reactor operating at an average power level of approximately 20 Mwt and an average purification rate of 800 lb of irradiated coolant per hour, calculations indicated an equilibrium HB content of ~6%. These results are

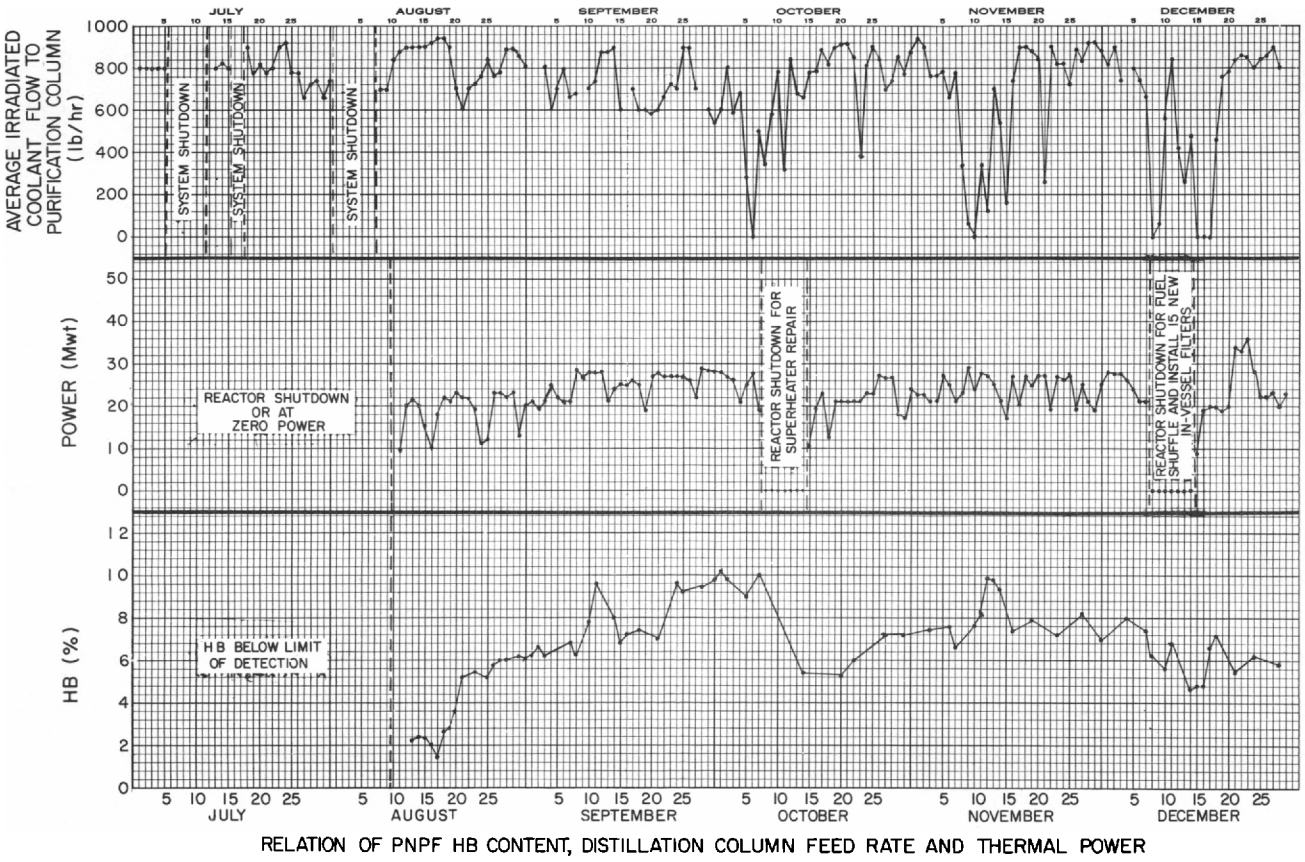

Figure 16. Relation of HB Content, Distillation Column Feed Rate, and Thermal Power

substantiated by data recorded following reactor startup near the end of August which showed an HB content of 6 to 6.3% (see Figure 16).

Throughout September, October, and November, operation of the system was sporadic due to frequent malfunctions of the HB transfer pumps and difficulties with steam tracing circuits on the HB lines, and plugging of lines in the vacuum system.

The frequent shutdowns during the early part of October resulted in the HB content of the coolant increasing to a maximum of ~10% on October 7 (see Figure 16). During these shutdowns, various portions of the steam tracing circuits leading from the bottom of the column to the bottoms transfer pumps were reworked and improved in an effort to ensure adequate heating of these lines. Following these improvements, the column operated satisfactorily during the time the reactor was shutdown for the superheater repair and the HB content of the coolant was reduced to ~5%.

As part of a special test conducted near the end of October to evaluate the performance of the cold traps in the off-gas system, the steam tracing on the vacuum lines around the cold traps was temporarily turned off. During the time the test was being run, it is believed that organic condensed in the cool line. When the steam tracing was subsequently turned back on, the collected organic was suddenly loosened from the hot pipe wall and carried downstream where it collected to plug the pipe and steam jet. It should be emphasized that this difficulty was caused by operation of the system in an off-normal condition for purposes of a special test and is not associated with normal operation of the system.

During the first two weeks of November, the distillation system operation was subject to frequent level and pressure control problems. On November 9, the system was shutdown, and the top of the column removed for visual inspection of the column internals. The demister in the flash chamber of the column was found to be loosened from its normal position in the column (See Figure 17 for schematic view of column) and was partially blocking the vapor outlet from the column. On November 12, the column condenser was removed and a large number of Raschig rings (used as packing in the stripping section of the column) were found in the vapor inlet line to the condenser.

Displacement of the demister pad and the presence of column packing in the condensers is evidence of periods of very unstable operation and sudden, extremely high vapor velocities through the column. During previous periods of operating difficulties with the column bottoms transfer pumps, the column level control was lost several times and the column pressure was increased to increase the suction head on the bottoms pumps. It is possible that during these periods actual physical flooding of the column with liquid may have occurred and considerable superheat was added to the HB in the bottom of the column as it circulated through the reboiler. When the vacuum in the column was subsequently restored, the superheated liquid

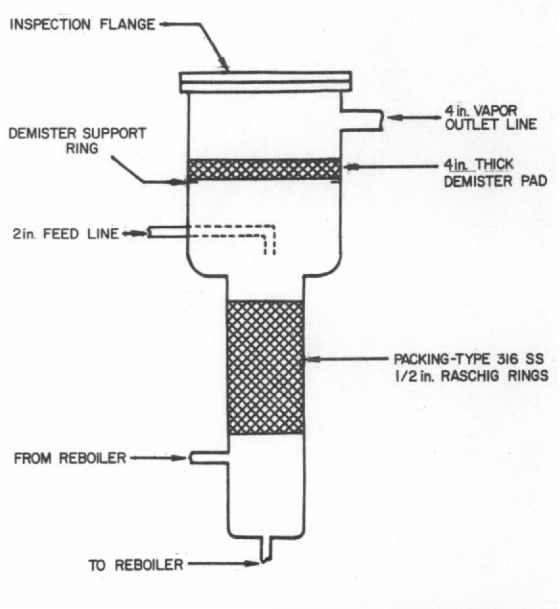

Figure 17. Distillation Column Sketch

in the column would vaporize resulting in a sudden surge of vapor through the packed section of the column with carryover of liquid and some packing into the vapor line to the condenser.

The carryover of liquid to the condenser was later verified by the finding of particulate matter in the distillate tank. During normal column operation, any particulate matter in the coolant stream or removed from the electric heater surfaces is concentrated in the HB in the bottom of the column. The only plausible mechanism for transport of these particles to the distillate system is physical flooding or high vapor velocities through the column.

In an effort to eliminate any further problems associated with plugging of the HB transfer lines, the system was shutdown on December 15 and a new bottoms transfer line installed between the bottom of the column and the pump suction. The new line is considerably shorter than the original line, being installed at floor level in a direct route between the column and pumps. The new installation makes adequate steam tracing and insulation possible to ensure elimination of possible cold spots and frozen HB in this transfer line. Following installation of the new piping, operation of the system has been trouble free with column feed rates averaging 800 to 900 lbs/hr (see Figure 18).

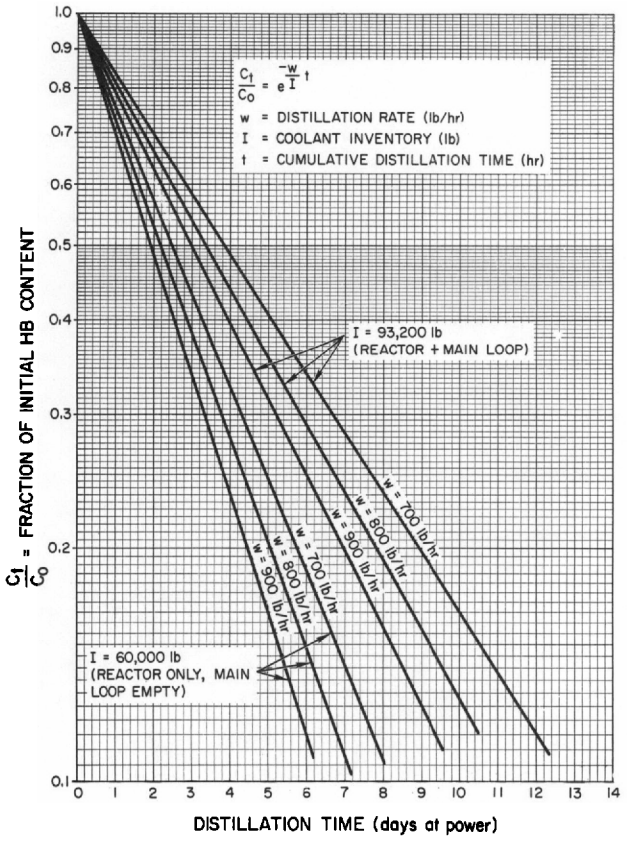

Figure 18. HB Content vs Distillation Time Following Shutdown

In conjunction with any extended reactor shutdown, it is desirable to reduce the HB content of the coolant prior to removing the reactor lid and potentially exposing the coolant to air. This can be achieved by continuous distillation of the coolant following reactor shutdown. The PNPF distillation system removes a side stream from the main coolant loop and returns the distillate via the degasification and pressurization system. Assuming that

all the HB is removed in the distillation column, the rate of change of HB content is given by the relation $WC = \frac{-d}{dt}(IC)$ where W is the distillation rate in lb/hr, C is the rate fraction of HB in the coolant, I is the coolant inventory lbs to be processed, and t the processing time. If it is assumed that the coolant inventory (I) is maintained constant by replenishing the system with fresh terphenyl, the relation is simplified to $WC = -I\frac{dC}{dt}$, which can be solved to yield $\frac{Ct}{Co} = e^{-\frac{W}{I}t}$ where $C_{t/Co}$ is the fraction of the initial HB content remaining after a processing time t, with the reactor at zero power. This equation is plotted in Figure 18 with distillation rate, and system inventory as parameters. Two system inventories were considered. One assumed the reactor and heat transfer system piping are filled with coolant (93,200 lbs), the second assumed that the heat transfer piping was either drained or valved out of the system and only the contents of the reactor vessel (60,000 lbs) are distilled. It can be seen from Figure 18, that with the reactor vessel and main loop piping filled, the system "half-time" is approximately 3 days with a distillation rate of 900 lbs/hr. Thus, regardless of the initial HB concentration, approximately 3 days of continuous distillation are required to reduce the concentration by a factor of 2, 6 days to reduce the level by a factor of 4, etc.

The time required to lower the HB level can be considerably reduced by draining the main loop piping to the reactor building drain tank where it can be maintained under an inert gas atmosphere, and distilling only the contents of the reactor vessel. It can be seen from Figure 18 that with this method of operation, the system half-time is reduced to slightly under 2 days.

D. DECAY HEAT SYSTEM

On July 28, the decay heat condenser X-6 failed due to waterside corrosion of the carbon steel tube bundle. This was a continuation of the trouble first noticed following plant shutdown in late May at which time the leaking tubes were plugged and the unit returned to service. At the time of the second failure however, the corrosion due to the untreated city water was general enough to render the carbon steel unit beyond repair and necessitated the installation of a new tube bundle. The tube bundle was purchased by site personnel, is fabricated of copper tubes brazed into a 285, Grade-C, carbon-steel tube-sheet, and contains

considerably more area than the initial exchanger. During initial operation, considerable water hammer was encountered. This difficulty was partially overcome by increasing the temperature of the cooling water to the condenser and improving the drainage from the tubes. These changes improved operation, but did not completely eliminate the problem. It was then noted that steam was leaking from the tube, tube-sheet joint indicating incomplete sealing of the tubes into the tube-sheet. Further investigation showed that several tubes had not been rolled into the tube-sheet at the manufacturer's plant; therefore, steam was bypassing the tube bundle and contacting the cold condensate which caused the water hammer. Following rerolling of all tubes into the tube-sheet no difficulties were experienced with system operation.

E. WASTE-FIRED BOILER OPERATION

During the report period, the waste-fired boiler was operated periodically, first on an experimental basis to evaluate various system parameters on the burning operation and later on a semicontinuous basis for the disposal of 200,000 lb of high boilers. A representative of the burner manufacturer, Thermal Research and Engineering Corporation, was at the site during the experimental portion of the burning operation. Based on observation of the flame, it was concluded that part of the difficulty was caused by moisture in the steam employed for atomization. Preheated air was later substituted for atomizing steam resulting in some improvement, but the flame still lacked stability at the HB flow rates required to maintain exhaust gas temperatures within the limitations of the flue gas cooler and dust collector.

Review of the viscosity data for the high boilers indicated that the viscosity of the HB from the PNPF system is approximately 15 cp, whereas the viscosity used in specifying the burner and piping system, based on OMRE HB from a 30% HB system, was significantly higher (58 cp). As a result of the low viscosity and low flow rate of the HB, it was believed that the fuel could be burned without any atomizing fluid being employed. By using this method of operation, the burner was operated periodically; several shutdowns were required for repair of mechanical components of the system and to remove the soot collected in the F-6 exhaust gas dust collector. It is still impossible to empty the soot from the dust collector hopper while the system is in operation.

The rotary air lock valve at the bottom of the collector hopper does not seal tightly. As a result, the air being drawn through the hopper and the high combustion-gas velocity through the collector is entraining the dust within the collector and not allowing it to settle in the hopper for removal. Methods of preventing air inleakage to the collector, and of isolating the collection hopper from the collector to facilitate removal of soot without the necessity of shutting down the system are being investigated.

Operation was interrupted on October 10 when it was discovered that the tube to tube-sheet joints at the rear of the pressure vessel were leaking and water was entering the combustion chamber. The system was shut down for a total of five days for cooldown, rerolling of the tube to tube-sheet joints, and drying of the refractory. Following these repairs, the system has operated extremely well, with only two shutdowns required to remove the soot from F-6 and changing of the absolute filter F-5. The improved operation following repair of the tube leaks suggests that the previous high dust-collector pressure drops may, in part, have been caused by steam leaking into the exhaust gas stream and caking dust on the filter medium.

The waste-fired boiler was operated in an essentially routine manner for 22 days during November. Several shutdowns of a few hours duration each were required to remove the accumulated soot from the exhaust system dust collector and repair of the HB feed pump. An 8-day shutdown (November 9 through 16 was required for routine State boiler inspection and minor maintenance to control valves and associated instrumentation. The results of the boiler inspection were very satisfactory, indicating adequate boiler feedwater chemistry control.

Additional investigation of this problem is in progress prior to making recommendations to eliminate the reoccurrence of the high pressure drop in the system.

F. AQUEOUS WASTE AND WASTE-GAS SYSTEM

1. Aqueous Waste System

Operational difficulties have been encountered in the aqueous-waste and waste-gas system resulting in a concentration of organic in the aqueous waste holdup tank (T-14) in excess of 7000 ppm. The problems encountered are:

1) The organic liquid reaching the API Basin with the water from the steam jets does not separate adequately from the waste layer. Batch decanting with the existing installation has not worked and there is insufficient organic for a continuous "skimming" operation.

2) An organic layer forms on top of the water in the aqueous waste holdup tank (T-14); this layer collects because the water entering T-14 from the API Basin contains organic or there may be an organic water emulsion. As the water cools the organic solubility decreases, causing an organic phase to appear. An organic layer is not detected in the pump discharge until the amount collected is greater than the heel left when the tank is pumped out.

Most of the organic material originates in the waste gas stream from the degasification and purification system and is continuously transferred to the aqueous waste system when the waste gas stream is contacted with steam in the steam jet ejectors; it subsequently condenses in the ejector condenser X-11. Additional organic is added from intermittent regeneration of the organic adsorbers. Analysis of the organic shows it to be benzene, zylene, biphenyl, o-terphenyl, and m-terphenyl that reaches the aqueous waste system.

The waste gas stream is passed through water cooled exchangers to remove as much as possible prior to entering the steam jets. The cooling water used in these exchangers has a temperature variation between 40°F in the winter and 80°F in the summer. During the winter months, the organic carryover is reduced to a low if not an acceptable level; however, the problem manifests itself during the summer when warm water must be used.

The investigation of different methods of obtaining an optically clean aqueous waste effluent has been completed. The laboratory testing of an oil adsorbent (Sorbo Cel) at PNPF confirmed earlier qualification results that Sorbo Cel does remove emulsified organic. Additional information indicates that between 0.2 or 0.3 wt % Sorbo Cel gives a clear filtrate with a filtering rate equal to that of distilled water. The oil layer was not completely removed by using this material.

The use of a refrigeration system to cool the waste gas stream directly upstream of the steam jet was found to be feasible but expensive and a potential

maintenance problem. Another possibilitv was considered and was recommended as a "fix" to the organic carryover problem.

Rather than using a mechanical refrigeration system for cold traps at the steam jet suction (0.5 psia), use of a water cooled cold-trap at the degasifier pressure (8 psia) would be as effective and much simpler. Since the flow of decomposition gas and light-ends is almost entirely from the degasifier with only a negligible amount of organic from the purification column, a cold-trap in the degasifier system "sees" essentially the same vapor as a cold-trap in the combined stream would see. Calculations based on a "best-guess gas-composition" show that a condensing temperature of 90°F at 8 psia is comparable to 14°F at 0.5 psia. Thus, the installation of a water-cooled cold-trap operating at the degasifier pressure would give performance equal to that of refrigeration. Also, since the degasifier pressure is fairly arbitrary, a higher pressure may be used without adversely affecting the plant.

2. Waste Gas System

The Waste gas delay train developed a high pressure drop on several occasions. During prepower operation, a high pressure drop occurred in September 1963. At that time, the pressure increase occurred after the cooling water to the steam jet condenser was accidently turned off and the waste gas flow meter was bypassed. This permitted steam and possibly organic material to reach the charcoal in the delay tanks. The high pressure-drop was reduced by blowing charcoal containing some organic material out of the inlet dip line in the first tank.

The waste-gas delay tanks remained in operation until August 1964, when a high pressure-drop again occurred. At that time, steam was introduced into the tanks in an attempt to remove the expected return of organic. Blowing charcoal from the inlet dip line alone did not reduce the pressure drop.

Water that had collected in the bottom of the tanks was frequently drained and an air purge was established through the charcoal beds to dry them and thereby reduce the pressure drop. This approach was successful in reducing the pressure drop through the waste-gas delay-tanks. It is believed that the undrained condensate from the steaming, mixed with the charcoal fines and the larger mesh material to form a mortar-like material at the bottom of the tanks. This mixture causes a high pressure-drop at low gas-flow rates.

Since the unplugging operation in August, water has been drained from the tanks when a high pressure drop has become apparent. Draining water usually reduced the pressure drop and enabled the system to perform satisfactorily. The water (believed to have been held by the charcoal since the steaming operation) was slowly running off the charcoal and was drained from the tank. Most of the drainings occurred before October 12, 1964.

In November, a high pressure-drop developed that could not be reduced by draining. After localizing the problem to the "B" tank in the series, the charcoal was removed, inspected, and found to be wet. This finding caused speculation that the water may have been from a source other than the August steaming operation.

Two mechanisms for the appearance of the water are suggested. (1) It is possible that only the outer surface of the charcoal was dried with the August air purge and that because the drying of charcoal pores is by diffusion, a slow process, a large amount of water could have been left in the charcoal. Subsequent diffusion of water vapor could then saturate the waste gas and temperature differences within the delay tanks could cause moisture to condense at the cold points. (2) The other possibility is that water is only adsorbed on the charcoal. In this case, the temperature of the carbon varies, the capacity of the charcoal for holding water would change; then, if the change produces water in amounts greater than that which the flowing waste gas can pick up, the water would drip off the charcoal. Adsorption data for this particular charcoal is not available.

G. PLANT RADIATION LEVELS

1. Plant Radiation Levels

At power levels up to ~34 Mwt, the radiation levels at the surface of the 20-inch main coolant piping remained very low. During periods of normal operation, these radiation levels were approximately 2 to 4 mr/hr. A peak value of 5 mr/hr was recorded during the period of December 19-23 when an air inleakage with possible increased system corrosion was known to exist (see Figure 19). Radiation survey data for the degasification tank, T-15, and the waste gas delay tanks, T-5, also reflect the air inleakage and subsequent high waste-gas activity. The high waste-gas activity is due to the activation of argon as it

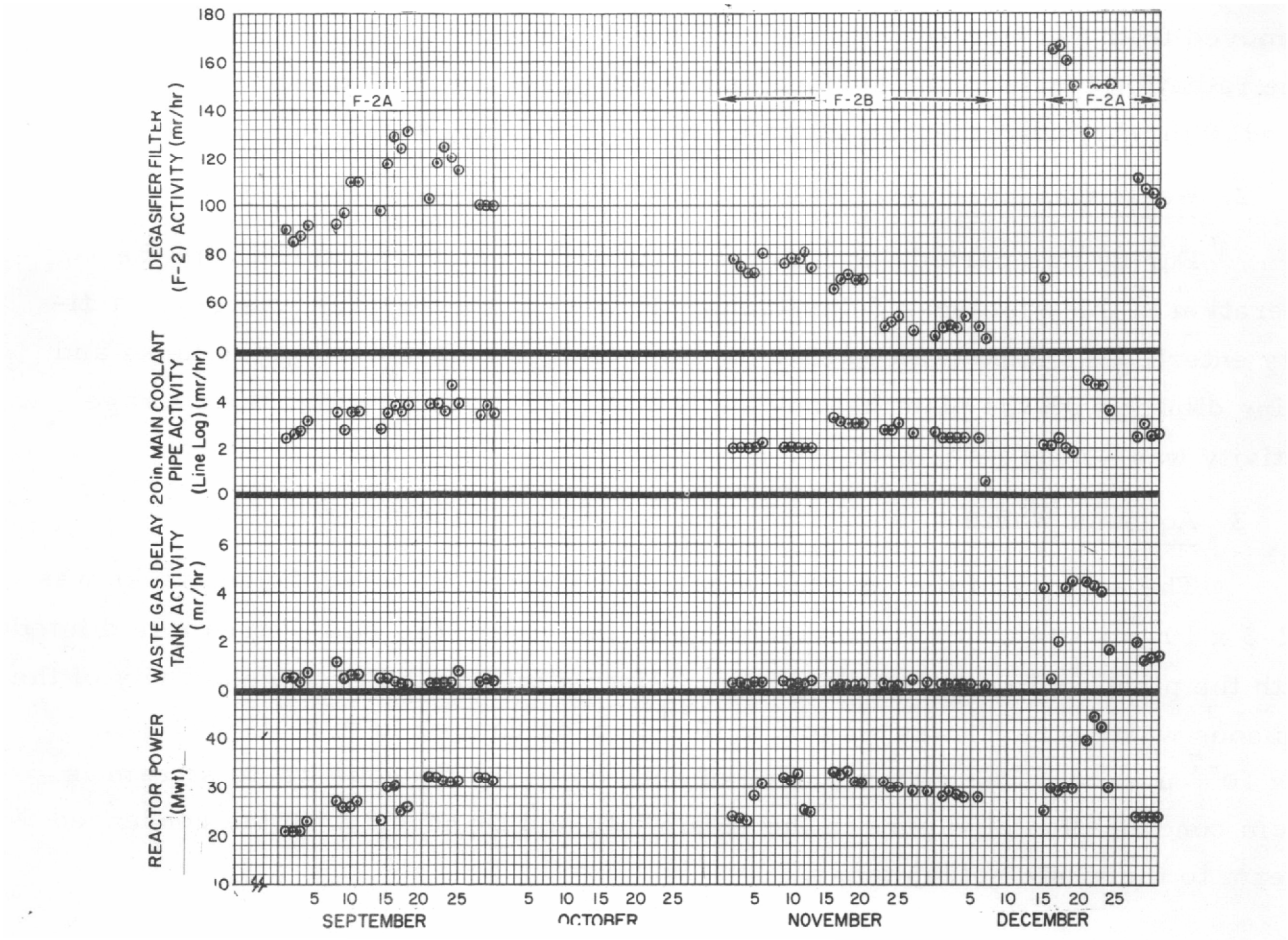

Figure 19. Plant Radiation Levels

passes through the core. The activity at the delay tank reached a maximum of ~30-35 mr/hr for a 3-day period during the air inleakage.

In general, the radiation levels throughout the plant have remained sufficiently low to permit operator access for maintenance without imposing any time limitations. The only exception is the area near the degasification filters where radiation levels of 40 to 140 mr/hr γ were recorded.

The radiation level at the degasifier filter F-2B which was placed in service in mid-October 1964 was significantly lower than that indicated by the data previously reported for F-2A at similar reactor power levels. The radiation level at the surface of F-2B was initially ~80 mr/hr but decreased to ~50 mr/hr by mid-December. This decrease in conjunction with the decrease in filter ΔP was indicative of possible failure of the filter or of significant coolant bypassing the filter. Because of this erratic behavior of F-2B it was

removed from service on December 15 and F-2A was valved into the system. The radiation levels at the surface of F-2A quickly reached an equilibrium value of ~100 mr/hr indicating improved filtration efficiency with this unit.

2. Waste Gas

During this period, considerable difficulty was encountered with the operation of the waste-gas delay-tanks. However, the average waste-gas activity entering the tanks was ~2-3 x 10^{-3} μ c/cc, and after leaving the tanks and being diluted with the plant heating and ventilating discharge air, the average activity was ~2 x 10^{-9} μ c/cc.

3. Aqueous Waste

The activity of the aqueous waste collected in the waste holdup tanks was ~2-3 x 10^{-6} μ c/cc. Prior to discharge to the river, the waste stream is diluted with the plant cooling water discharge. After dilution, the average activity of the aqueous waste stre was ~2 to 5 x 10^{-9} μ c/cc compared to a MPC of 1 x 10^{-7} μ c/cc. The major source of activity in the aqueous waste stream is from condensation of vapors in the steam jets and transport with the condensed steam to the waste holdup tanks.

H. FAILED ELEMENT LOCATION SYSTEM

During the reactor shutdown, the electronic circuits of the Failed Element Location System (FELS) were checked out, and all twelve BF_3 counters were made operable. On August 27, a complete FELS scan was obtained. This was the first FELS survey following the shuffling of the fuel elements. A summary of the shuffling and count rate data is shown in Table VII along with readings for the two mixed-mean coolant samples.

Comparison of readings for a given fuel element at two locations indicates the possibility of a cladding imperfections on elements P-1015 and P-1071. The normalized count rate for element P-1015 was 1326 and 1284 in old and new core-locations, respectively. However, the count rate for element P-1057 currently in the core location previously occupied by element P-1015 is only 555 cpm; this indicates that the activity was probably not associated with the sampling system, and subsequent data have shown sufficient scatter to invalidate any conclusion regarding malintegrity of this fuel element's cladding. Data

TABLE VII

FELS SURVEY DATA FOR SHUFFLED FUEL
(Element Number in Parenthesis)

Core Location	Normalized Count Rate Before Change (c/min)	Normalized Count Rate After Change (c/min)	Comments
B-11	(P-1015) 1326	(P-1057)* 555	Replaced irradiated fuel with new fuel. Apparently element P-1015 has cladding defect or surface contamination.†
F-7	(Dummy Element) 800	(P-1006) 780	Replaced special dummy element with irradiated fuel. Apparently irradiated fuel is sound.
D-5	(P-1006) 940	(P-1062) 490	Shuffle of irradiated elements. Both elements sound.
D-3	(P-1062) 470	(Dummy Element) 390	Replaced irradiated fuel with dummy. Old fuel apparently sound.
F-15	(Dummy Element) 900	(P-1055) 920	Replaced dummy element with irradiated fuel. Fuel cladding apparently sound.
H-17	(P-1055) 780	(P-1054) 690	Shuffle of irradiated fuel. Apparently both elements sound.
H-19	(P-1054) 445	(Dummy Element) 560	Replaced irradiated element with dummy. Element apparently sound.
D-9	(P-1071)§ 1280	(P-1015) 1284	Shuffle of irradiated elements. Elements P-1071 and P-1015 have apparent cladding imperfections.
MM-1	1240	1050	
MM-2	1140	900	

* New fuel element.
† Apparent cladding imperfection substantiated by high delayed neutron count of same element in core location D-9.
§ Element removed for destructive testing.

taken on October 27, December 19, and January 6 gave readings of 600, 1400, and 900 respectively.

The other element P-1071, associated with a high count rate, was removed from the core during the shutdown for destructive testing. Examination of the element did not reveal any noticeable cladding imperfection.

The other core locations involved in the fuel shuffle show no change in count rate data, indicating apparent integrity of fuel cladding. However, one significant change is noticed in the count rate reported for element P-1073 in core location C-12. Previous FELS surveys showed normalized count rates of ~12,000 cpm, whereas the survey of August 27 resulted in a normalized count rate of approximately 4000 cpm.

On October 27 a partial Failed Element Location System (FELS) survey was made using one of the two sample valves. In all, 45 of the 90 core locations were sampled. In general, the data show no significant change from data obtained from previous FELS surveys. Count rate data for the two mixed-mean coolant samples and for the five highest-activity channels are shown in Table VIII. These data show the only two significant changes from previous

TABLE VIII

FAILED ELEMENT LOCATION SYSTEM SURVEY ACTIVITY (CPM)*

Core Location	Date					
	2/2/64	4/12/64	5/9/64	8/27/64	10/27/64	12/19/64
Mixed Mean Outlet						
MM-1	1370	1200	1240	1050	1160	1200
MM-2	1390	1235	1142	880	990	1130
Fuel Channels with Maximum Activity						
C-12	12,000	11,200	12,200	4150	8800	11,400
D-7	6300	5550	4300	3500	5200	6600
B-7	4600	4820	4740	4230	4500	5300
D-13	3500	3250	4180	2970	3060	3200
D-11	4650	3400	4460	1830	1770	2200
D-5	960	650	950	490	515	690

*Data normalized to 45.5 Mwt, sample flow of 10 gpm, 12 BF_3 tubes in operation.

data; the activity from core locations C-12 and D-11 continued to show a significant decrease from the data taken on February 2, April 12, and May 9 but were in general agreement with the 8/27 data. Although the decrease in count rate could be indicative of some surface film deposit, this conclusion could not be substantiated by in-core temperature measurements.

Data taken during December indicated a large discrepancy from previous results. It was later discerned that the sample valve position indicator was in error, and that the data had been shifted by one sample position. Correction of this error resulted in excellent agreement with previous data. It is noted that the activity associated with core location C-12 has returned to its previous level.

I. FLUX AT CHARPY IMPACT SPECIMENS AND NEUTRON WINDOW

Two Charpy impact specimen assemblies are installed in the PNPF reactor vessel. These are located in the outermost ring of dummy fuel elements in core locations L-16 and A-6 (See Figure 20). Each assembly consists of 72 Charpy specimens mounted in 6 tiers of 12 specimens each. The specimens in one assembly are located in the active core, those in the other assembly are above the active core serving as control specimens. Each specimen is 2.165 in. long by 0.394 in. in height and width, and is fabricated of ASTM A-212 GrE carbon steel (See Figure 21) which is the same material as the reactor vessel. Previous calculations* have estimated the fast and thermal neutron flux at the edge of an 85 active element core. With the existing 61-element core, additional organic is present between the edge of the active elements and the Charpy impact specimens.

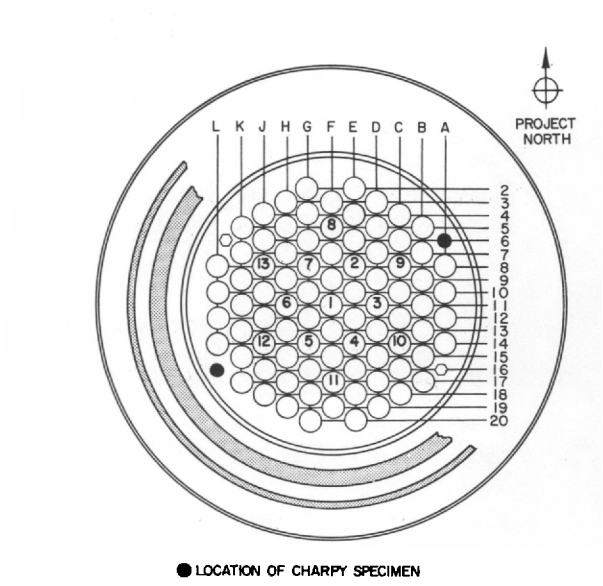

Figure 20. Charpy Specimen Locations in Core

Correcting the values reported in NAA-SR-TDR 3650 for the attenuation provided by the additional organic, the

*D. S. Duncan, "Reevaluation of Shield Requirements for OMR-Piqua Neutron Detectors," NAA-SR-TDR 3650, March 1959

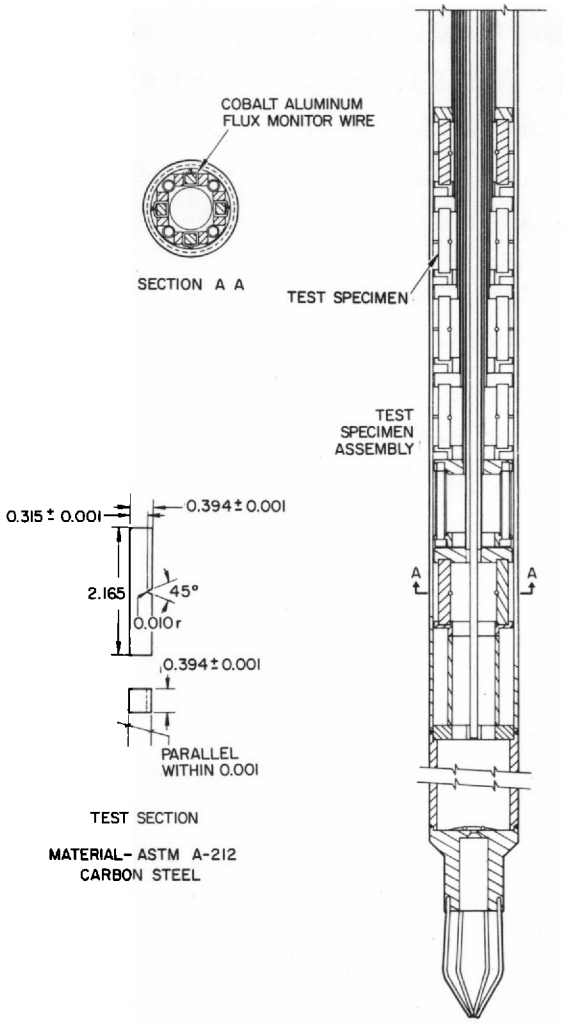

Figure 21. Charpy Impact Specimen and Assembly

neutron flux >1 Mev at the Charpy specimens is estimated to be ~4 x 10^{11} neutrons/ cm^2-sec at full power. The time integrated flux was calculated to be ~3 x 10^{18} nvt. Based on published data*, this exposure could correspond tc an increase of 100 to 150°F in the nil ductility transition temperature.

An 8-in. carbon steel pipe spool imbedded in the biological shield provides a potential experimental facility designated as the "neutron window". One end is capped at the point of contact with the outside of the thermal shield at the core midplane height. The other end of the pipe spool terminates in the fuel storage pool and is closed with a bolted flange. Based on data presented in NAA-SR-TDR 3650, the neutron flux >0.625 ev was estimated to be ~5 x 10^8 n/cm^2-sec, and the flux <0.625 ev to be ~5 x 10^9 n/cm^2-sec. Although it may be feasible to utilize this neutron window as an irradiation facility, no procedures have been prepared and the plant Technical Specimens (Section J) state that at the present time "No experiments shall be performed in this facility."

J. COOLANT DECOMPOSITION RATE

Coolant inventory and material balance data were routinely analyzed to determine approximate values of the terphenyl decomposition rate. The values of the decomposition rates are approximate due to inaccuracies in reading tank levels and lack of analysis of material held in the two organic drain tanks.

*Carpenter, et al., "Anomalous Embrittling Effects Observed During Irradiation Studies on Pressure Vessel Steels," Nuclear Science and Engineering, May 1964

Since the volume of material in the drain tanks changes by only a small amount during the period of time over which the material balances are made, its composition is assumed to be constant without introducing any significant error.

Throughout the past six months of operation, the HB content of the coolant was maintained at 6 to 10% during normal power operation. The average calculated decomposition rate for this period was 2.1 lb/Mwhrt. These results are in excellent agreement with the predicted value of 2.1 lb/Mwhrt at 6% HB.

IV. EXAMINATION OF INCORE FILTERS

A. INTRODUCTION

Essentially the entire PNPF organic coolant stream is filtered continuously through glass fiber cartridge filters located in the reactor vessel upper plenum above (and upstream of) the reactor core (Figure 22). These filters were first installed in August 1963 during PNPF Test Phase II, initial nuclear tests. The filters were removed and the original glass fiber cartridges were replaced with new cartridges in July 1964 during a scheduled reactor shutdown period for fuel rearrangement following the initial period of reactor power operation. Just prior to this shutdown, the pressure drop across the filters had reached (with two-pump operation) the established maximum allowable level of 10 psi. The original filter cartridges had been in use for a total of 3239 Mwdt of reactor operation.

In order to determine that this period of exposure of the filter cartridges to the hydraulic, thermal, and nuclear PNPF service conditions had not altered their properties such that continued use (had the filter pressure drop not reached the maximum allowable level) might have affected PNPF operations adversely, glass fibers were removed from one of the original filter cartridges and subjected to a series of analyses and tests.

B. SUMMARY OF RESULTS

Basically, three types of material properties were covered by the filter fiber examination program: chemical composition, crystalline or amorphous structure, and fiber strength.

Since changes in chemical composition of the filter fibers in service would be significant only to the extent that they impaired the physical properties of the material (and this would be evident in other tests), no attempt was made to detect small differences in composition between the new and used fibers. Also, tolerances in the concentrations of the constituents in the manufacturer's standard composition of the fibers did not permit the detection of small changes. Analysis of the new and used filter fibers by emission spectroscopy failed to indicate any gross differences in chemical composition.

Photomicrographs showed no crystalline structure in either the new or the used fibers. Analysis of the new and used filter fibers by x-ray diffraction revealed no crystalline components in the new fibers, but showed the presence of small amounts of magnetite (Fe_3O_4) and quartz (SiO_2) in the used fibers. Corrosion products and foreign material in the coolant stream were the probable sources of the magnetite and quartz, small amounts of which may have adhered to the filter fibers despite attempts to clean the fibers thoroughly before analysis. Manual examination of the new and used filter fibers failed to disclose any general or obvious differences in strength and ductility. However, machine tensile testing of individual fibers indicated a reduction in tensile strength from about 175,000 to 105,000 psi which created no operational problems.

In addition to the tests involving the above principal categories of material properties, several other examinations were performed and provided for the following general related information.

a) Both the new and used fibers appeared to have the same general texture, but the used material was gray and the new material was white. As concluded from a combustion analysis (ashing), at least some of the discoloration of the used fibers was probably due to residual coolant which had adhered to the fibers despite a prior thorough rinsing with xylene.

b) X-ray fluorescence and gamma-ray spectrography revealed the presence of small amounts of Fe, Zn, Co, Cr, and Mn on the used fibers. These had probably originated as corrosion products or other impurities in the coolant stream, and had become activated in the core before being removed from the coolant by the filters. Of the above listed elements, Fe was predominant.

c) Electron microscopic examination of one of the used fibers showed the presence of particles in the submicron range on the surface of the fiber. The absence of any particles was noted on the new fiber.

C. CONCLUSIONS

The results of the examination of the initial PNPF in-vessel filters indicate that the filter fibers did experience some physical damage while in service.

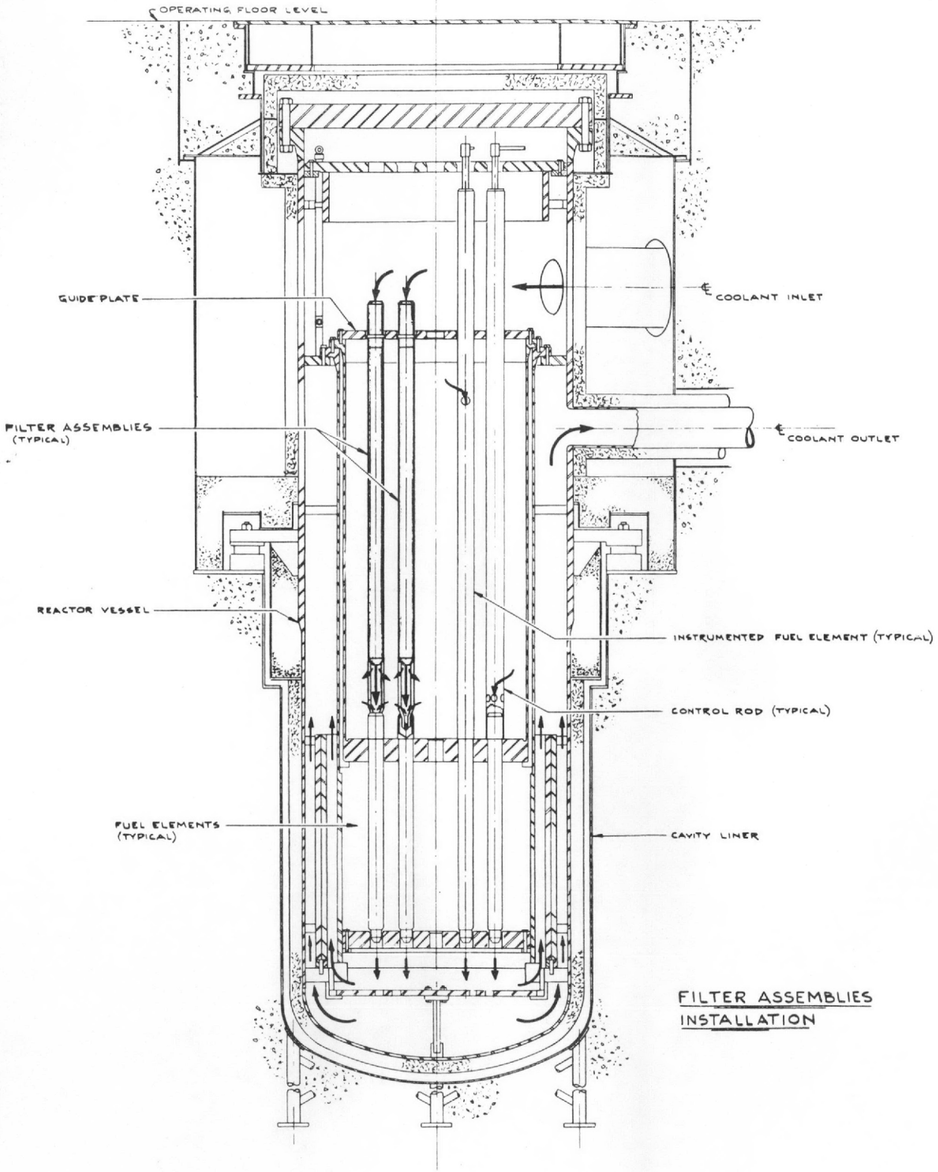

FILTER ASSEMBLIES INSTALLATION

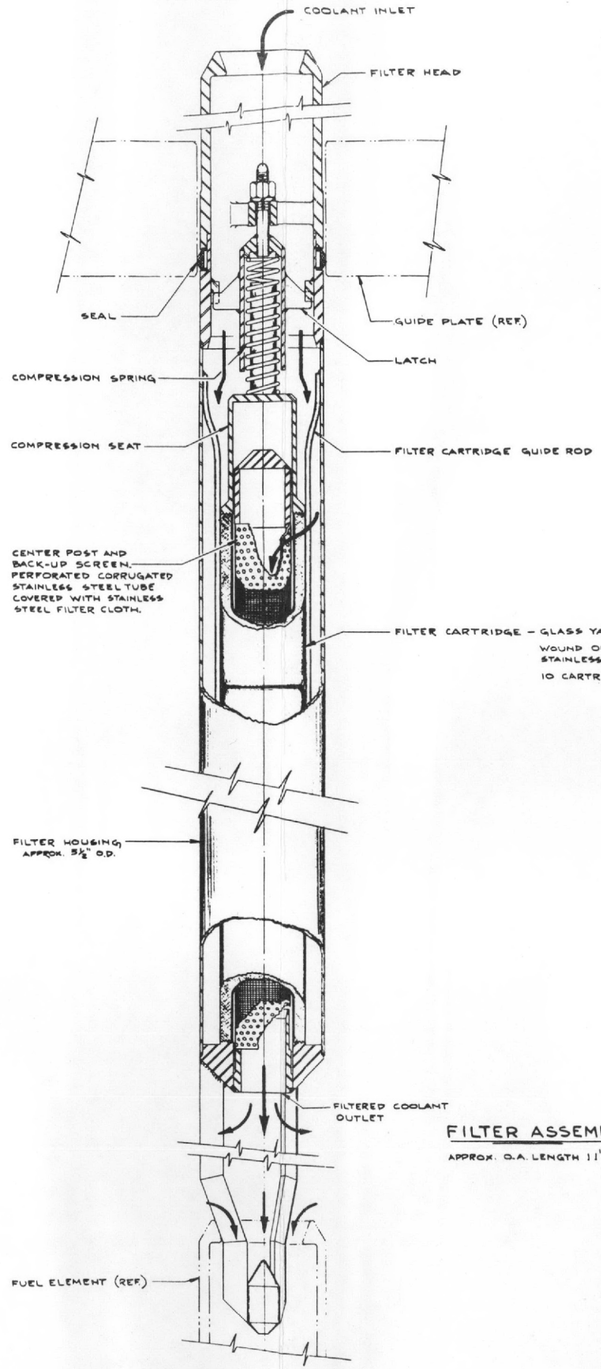

FILTER ASSEMBLY

APPROX. O.A. LENGTH 11'-7"

7537-79409

Figure 22. Reactor Vessel Filter Assembly Installation

However, the filters remained in good condition and suitable for continued use, had the filter pressure drop not reached the maximum allowable level of 10 psi. This limit was established as the maximum allowable pressure differential across the top guide grid plate.

D. FILTER SAMPLE SELECTION AND PREPARATION

1. Sample Selection

The used filter fibers subjected to the examination were taken from the lower end of the filter in core position D-9. Since the filters are disposed as a vertical parallel bank above the core (Figure 22), the lower ends are closest to the core; core position D-9 is near the center of the core. Thus, the fiber sample was selected from the high radiation region of the filter installation. From hydraulic and thermal aspects, all parts of all filters probably experienced essentially identical service conditions.

The new filter fibers, which were utilized to establish standards against which the used material was compared, were taken from one of the lots of glass fibers which was used in the original fabrication of the filters.

2. Sample Preparation

The used filter fibers were rinsed in hot xylene (90°C); the rinse xylene was then drained and replaced with clean xylene. This procedure was repeated several times until the rinse xylene drained clear. The filter fibers were then dried in a drying oven for one-half hour at 100°C.

Two samples of used fibers were ashed to determine the extent to which they had been washed free of coolant. The results obtained were 99.40 and 98.79% ash (glass)*.

E. EXAMINATION PROCEDURES AND RESULTS

1. Visual Appearance

The new filter fiber was white, the used material gray. Because of the small cross-section of the fibers (~3 microns), it could not be determined whether the discoloration of the used material was just a surface condition or existed in depth.

*A. I. Chemical Analysis Report; Request 9348: Laboratory No. 6459 (June 30, 1964)

Both the new and used samples appeared to have the same general texture. Figure 23 shows new and used glass fiber filter cartridges; both are 10 inches long but appear unequal because of the camera angle. Figure 24 shows individual new and used glass fiber yarns.

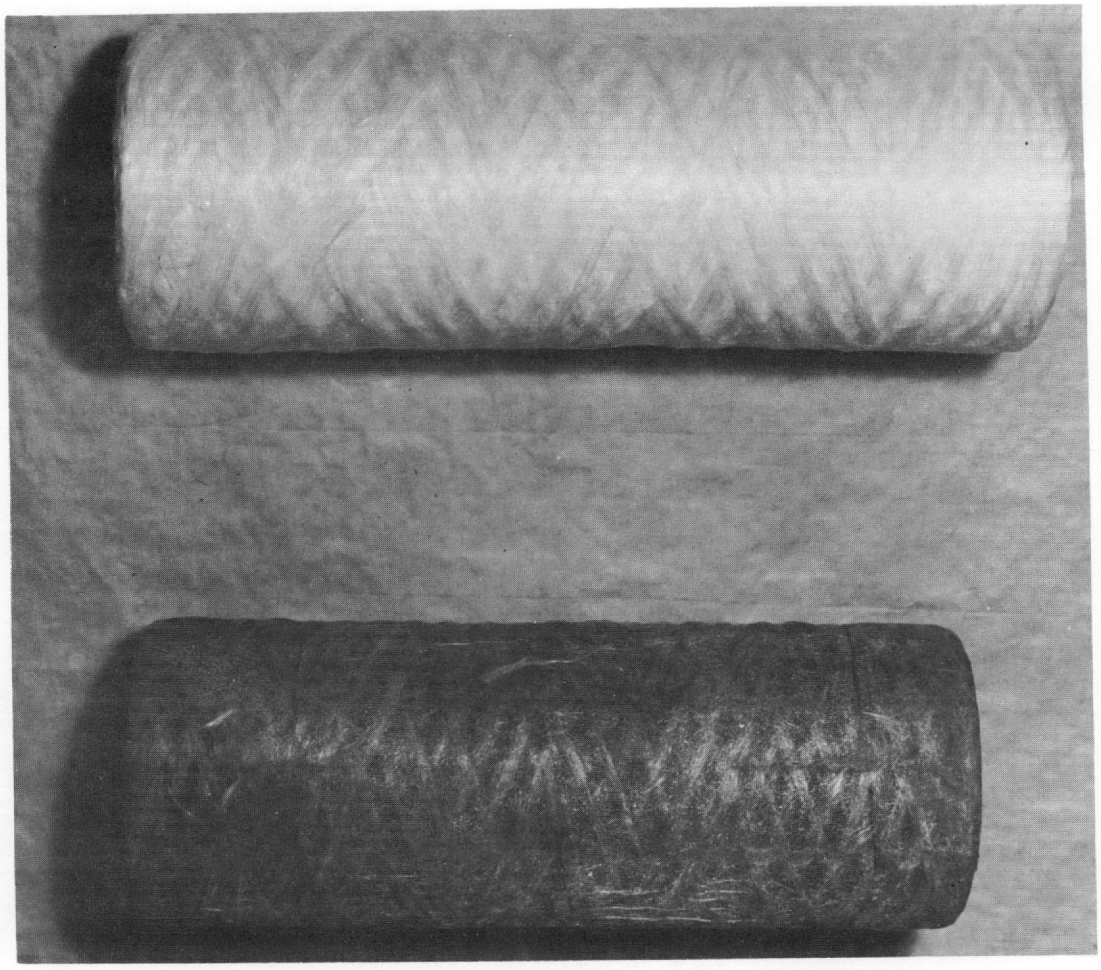

Figure 23. Glass Fiber Cartridges

Several epoxy encapsulations were made of the new and used fibers. These were then sectioned, both transverse and parallel to the fibers, and polished. Figures 25 and 26 are photomicrographs of the new fibers, and Figures 27 and 28 of the used fibers. All are magnified 750 times. None show any crystalline formation or structural damage to the fibers. Certain dark areas, particularly in Figure 26 are due to incomplete encapsulation of the fibers by the epoxy. A few dark spots may be attributed to small pieces of fiber flaking off during sectioning of the encapsulated sample.

Figure 24. Glass Fiber Yarns

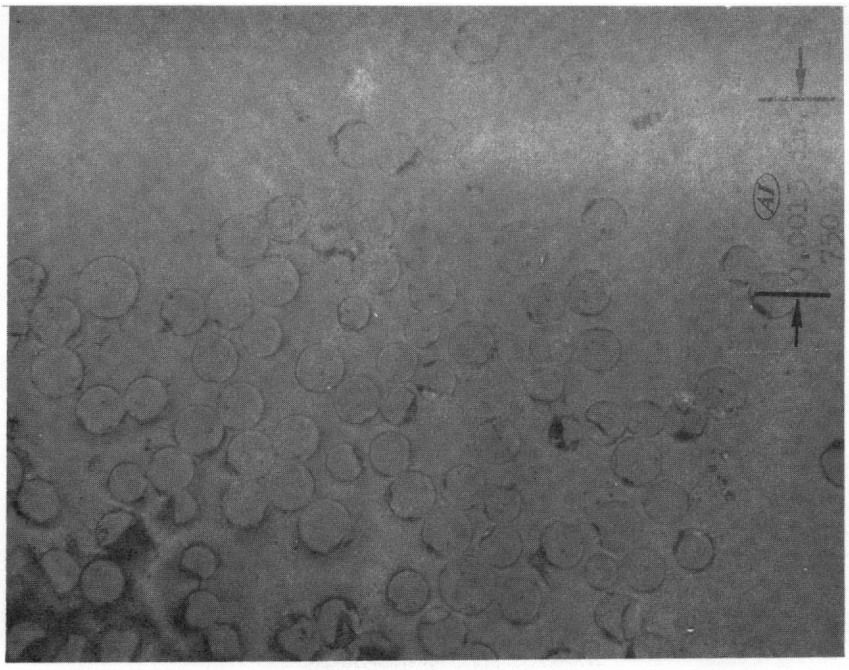

Figure 25. Transverse Section of New Glass Fibers

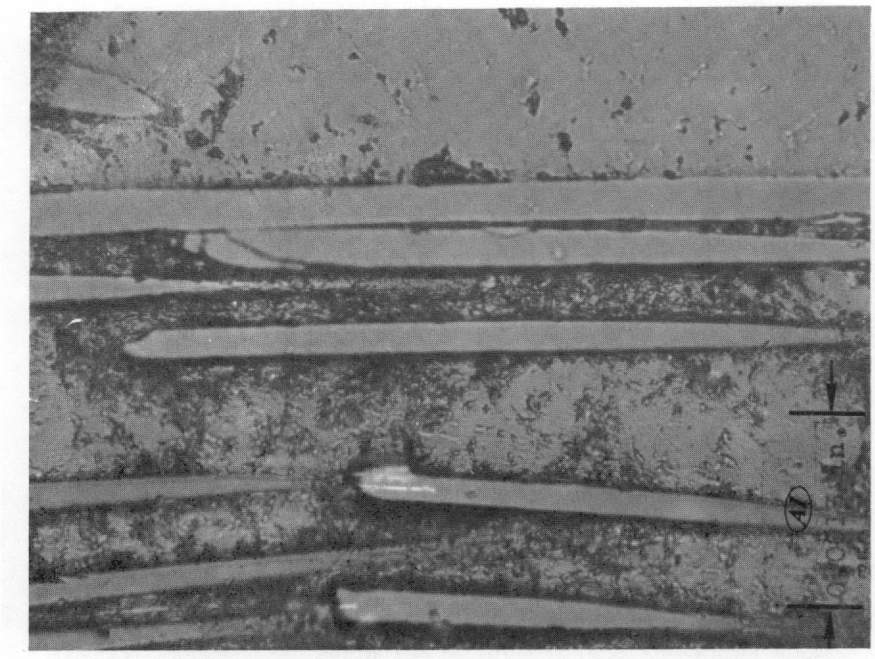

Figure 26. Longitudinal Section of New Glass Fibers

Electron microscopic examination of one of the used fibers after Soxhlet extraction with chloroform to remove coolant and loosely held particles shows the presence of particles in the submicron range on the surface of the fiber

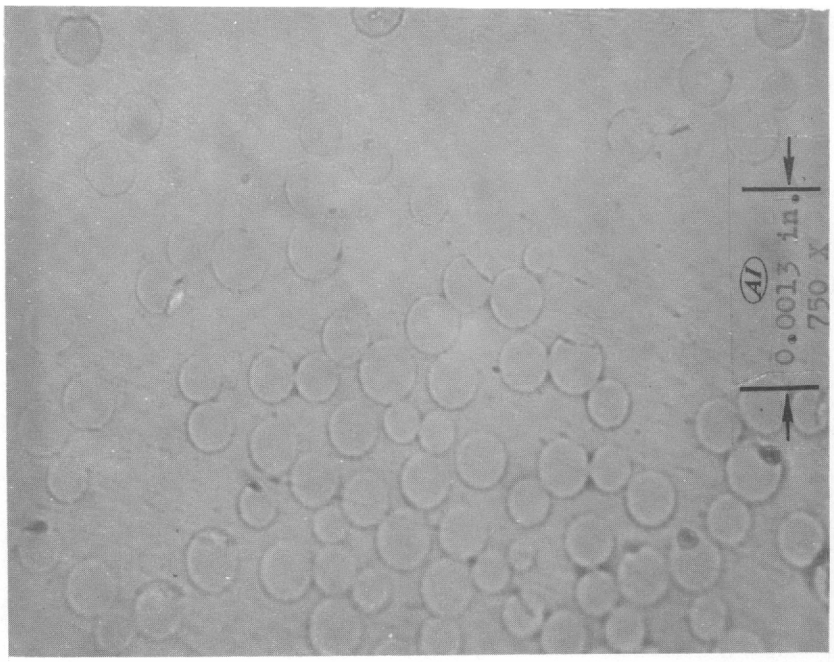

Figure 27. Transverse Section of Used Glass Fibers

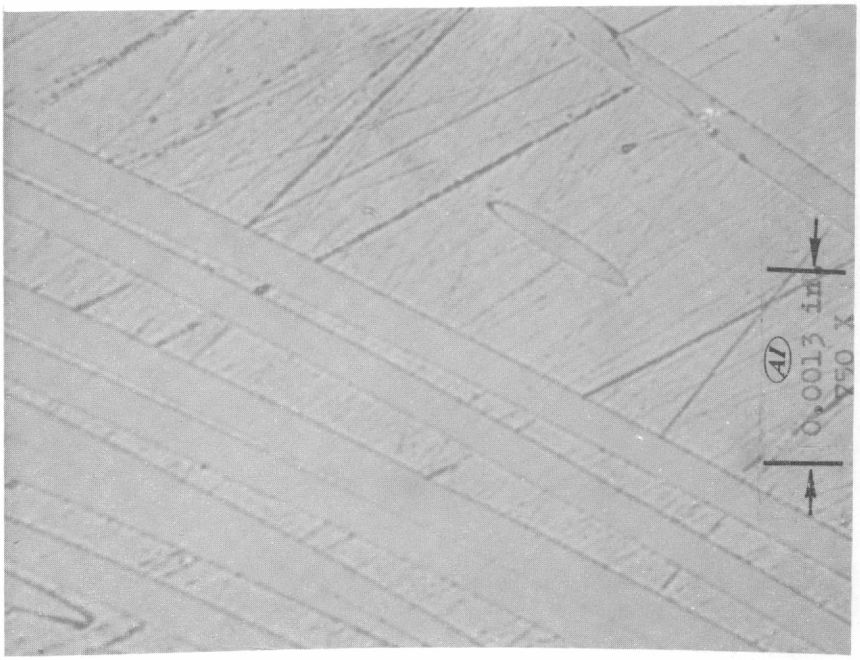

Figure 28. Longitudinal Section of Used Glass Fibers

(Figure 29). A photo of a new fiber is shown in Figure 30. Note the absence of any particles on the surface. A particle size determination of the particles separated from the fiber by solvent extraction did not appear fruitful for two reasons: (1) most of the smaller particles were retained in the Soxhlet Thimble

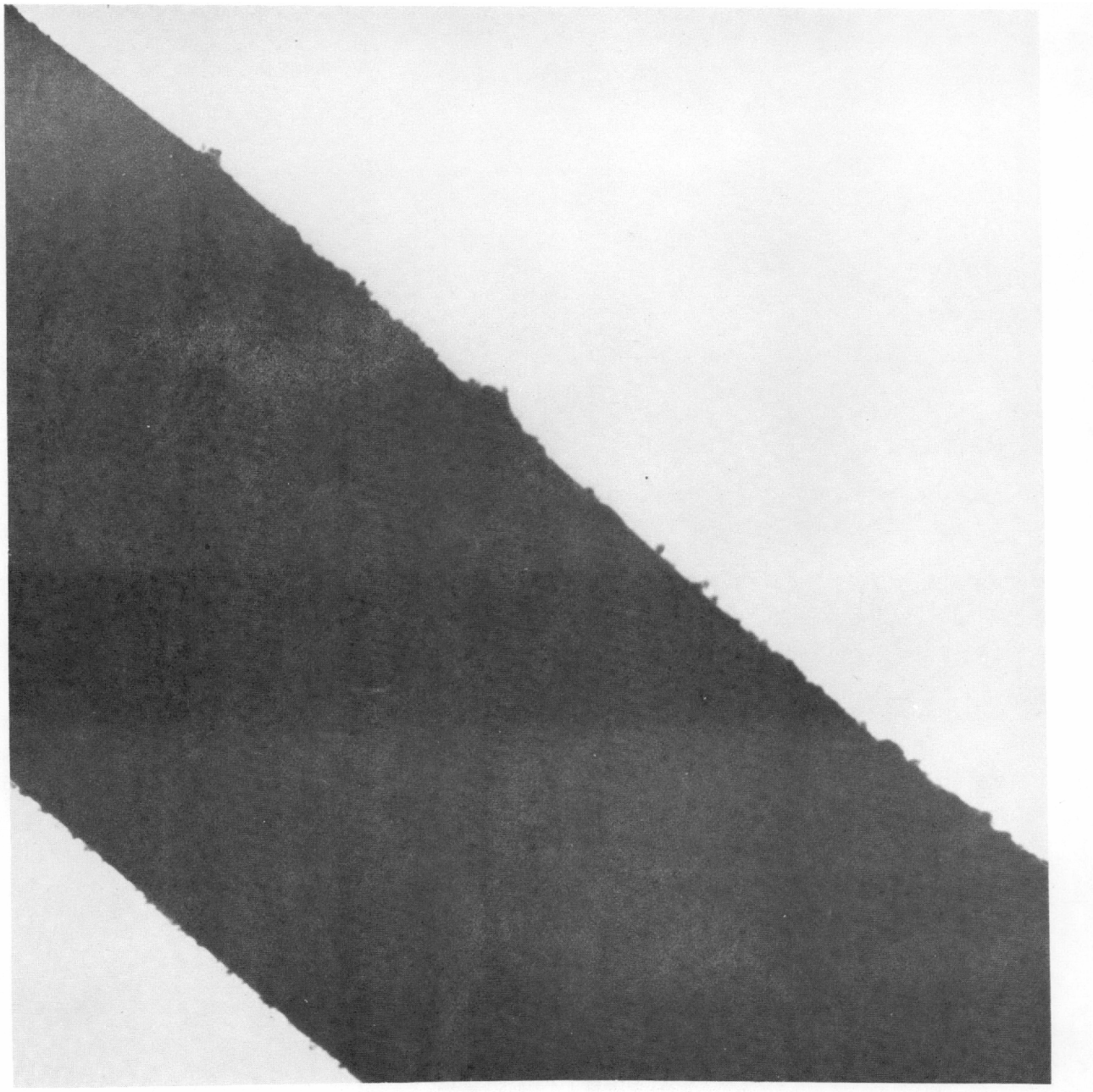

Figure 29. Electron Micrograph of Incore Filter Fiber After Solvent Extraction

and also were retained in the pores of the fine glass frit used for filtering the particle-chloroform mixture; and (2) large particles ($> 25\mu$) were apparent in the separated particles, some of which had probably agglomerated after solvent contact and drying. Some of the individual particles seen by the electron microscope in both the solvent treated and untreated in-core filter fibers were 25μ or more in diameter.

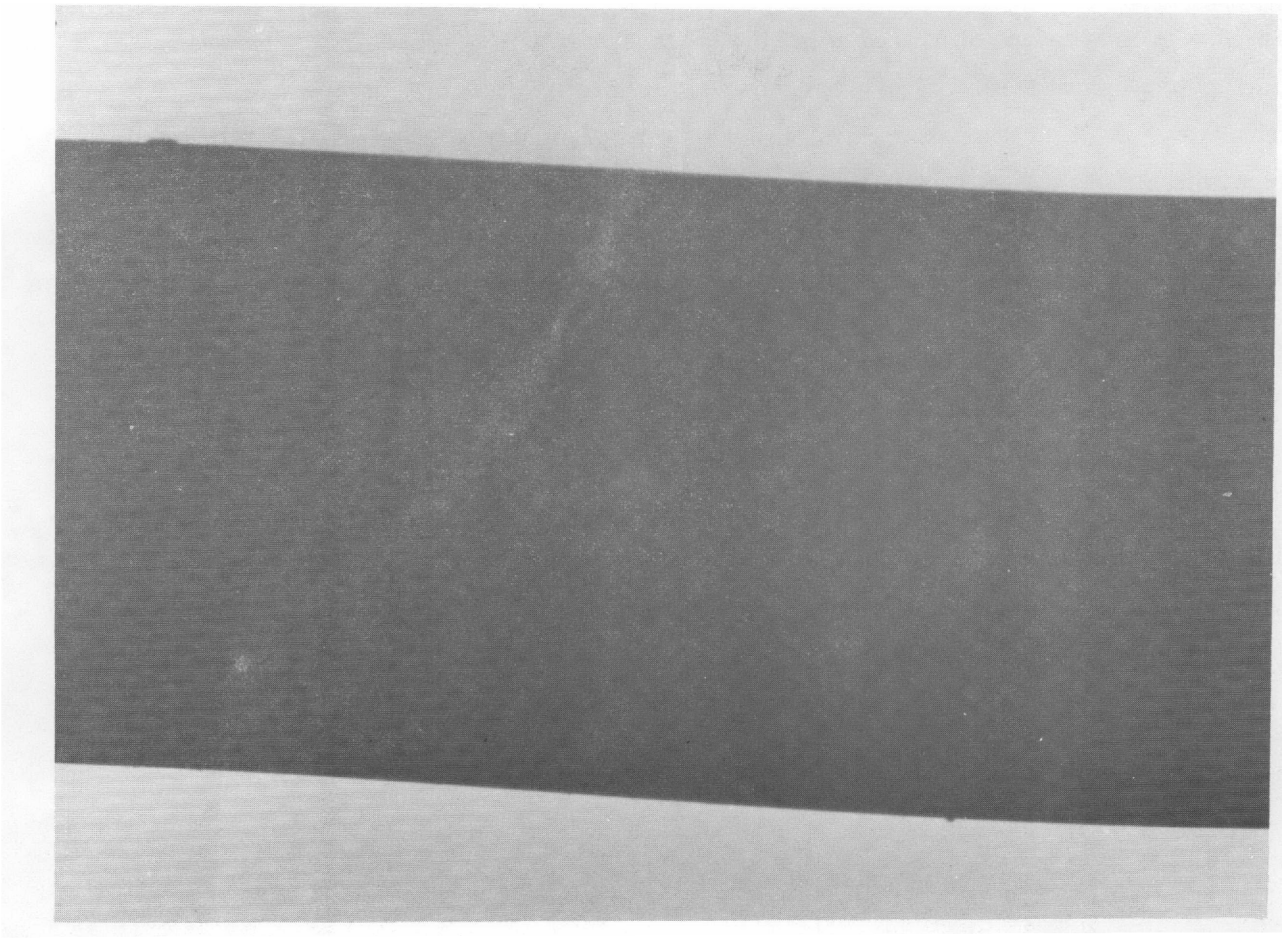

Figure 30. Electron Micrograph of Unused Glass Spool Filter Fiber

The small particles seen on the surface of the fiber in Figure 29 are apparently held to the glass surface by very strong forces since they were not removed by prolonged soaking in the hot chloroform. This information is significant since the glass fiber is known to have a highly adsorptive surface*, and a high surface area. Furthermore, as shown in previous studies, the particles in the coolant will deposit or absorb on any available surface in the system†. The total estimated surface area in the in-core filters (assuming a total of 670 in-core filter spools) is 3.8×10^8 cm^2. This is a significant particle scavenging surface when compared to the fuel element surface area, estimated at 3.1×10^6 cm^2. The available fiber surface area, and related

---

* W. A. Zisman, "Surface Chemistry of Glass-Fiber-Reinforced Plastics," " NRL Report 6083, June 9, 1964

† R. J. Sullivan and R. T. Keen, "Film Formation on Heat Transfer Surfaces," Organic Summary Report, In Press

surface chemical properties which affect spreading, wetting, adhesion, friction, adsorption, and desorption, can therefore be significant factors in the overall efficiency of the glass fiber matrix in removing coolant particles, in addition to the purely mechanical "trapping" of coolant particles. The fact that glass is by nature hydrophilic (prolonged heating above 350°C is required to dehydrate the surface) can also be a factor in the particle retention mechanism by adsorption, since the surface will adsorb polar organic molecules.

2. Spectrographic Analysis

Analysis by emission spectroscopy provided approximate chemical compositions of the new and used fibers. These results*, together with the standard range of certain of the constituents as listed in the manufacturer's catalog†, and a chemical analysis of the new fibers as performed by an independent laboratory§, are listed in Table IX.

The analyses listed in Table IX are sufficiently in agreement, within the precision of the methods utilized, to indicate the absence of any gross change in chemical composition of the filter fiber material.

Gamma-ray spectrography of the used fibers disclosed the presence of irradiated contaminants as follows**.

Isotope	Activity (μc/gm)
Co-58	0.021
Cr-51	0.021
Mn-54	0.037
Fe-59	0.006
Zn-65	0.046

*A. I. Spectrographic Analysis Report; Request 9348: Plate No. 1928, 1929 (July 7, 1964), and 1930 (July 8, 1964), Request 9386 (July 14, 1964)

†Owens-Corning Fiberglass Corp., (Toledo, Ohio); Publication No. 1-GT-1375-A (June 1961); Page 10

§W. B. Coleman & Co., (Phila., Pa.); Report of Analysis; Laboratory No. 846620 (October 31, 1962)

**A. I. Chemical Analysis Report; Request 9348: Laboratory No. 6459 (June 30, 1964)

TABLE IX

CHEMICAL ANALYSIS OF NEW FIBERS
(wt %)

Element	Used Fibers	New Fibers	Independent Lab Analysis	Mfrs. Analysis
Al	2.0	2.5	2.53	1.1 - 3.2
B	1.5	2.0	2.23	0.6 - 2.2
Ca	8	9	10.4	15 - 20
Mg	2.0	2.5	2.53	
Cr	0.01	0.005	0.0	
Cu	0.01	0.005	0.0	
Fe	1.0	0.3	0.0	
K	0.25	0.25	0.24	8 - 12
Na	4.0	4.5	4.24	
Li	0.003	0.001	N. D.	
Mn	0.2	0.3	0.0	
Mo	< 0.05	< 0.05	N. D.	
Ni	0.02	< 0.005	N. D.	
Si	20	25	29.5	28 - 31
Sn	0.01	< 0.005	N. D.	
Ti	0.2	0.05	0.0	
V	< 0.05	< 0.05	0.0	
Zn	0.05	< 0.05	N. D.	
Zr	0.08	0.08	0.0	

3. X-Ray Diffraction

No crystalline components were noted in the new fibers; however, small amounts of magnetite (Fe_3O_4) and quartz (SiO_2) were detected in the used fibers*. The presence of the magnetite was probably due to the filtration and adhesion of corrosion products to the fibers. The quartz probably originated as a contaminant in the coolant stream, or could have resulted from the crystallization of a small amount of the SiO_2 component of the glass fiber.

* A. I. Chemical Analysis Report; Request 9348: Laboratory No. 6459 (July 7, 1964)

4. Manual Examination

Samples of new and used filter fiber were examined manually for general differences in strength and ductility. No differences could be noted in this manner. Samples of each were also ground with mortar and pestle; they behaved similarly.

5. Tensile Strength

Attempts were made to obtain breaking strength comparisons between individual new and used fibers. However, much difficulty was encountered due to the extremely small size of the fibers (~8 to 10 microns diameter), which taxed the sensitivity of the testing equipment. Exhaustive efforts finally produced four successful tests, two each on new and used fibers. The tests were performed on an Instron tensile testing machine equipped with special fiber jaws attached to a 10-gram load cell. The following results were obtained*:

Fiber Tested	Breaking Load (gm)	Unit Tensile Strength (psi)
New Fiber No. 1	5.9	172,000
No. 2	6.1	177,000
Used Fiber No. 1	3.3	96,300
No. 2	3.8	111,000

For the unit tensile strength calculation, a diameter of 0.00031 inches was used for all four fibers. This value was selected from microscopic examinations of the fibers. Slight variations in cross-section were noted along the lengths of each fiber, but no significant differences were noted between fibers. The 0.00031-inch diameter represented a judgment approximation rather than a precise value.

The tensile strength of the type of glass fiber used in the filters is listed in the manufacturer's catalog† as 200,000 to 220,000 psi§. In view of the

* Materials Testing Laboratories (Los Angeles, Calif.); Laboratory No. 24559-6-1 (August 31, 1964)

† Owens-Corning Fiberglas Corp. (Toledo, Ohio); Publication No. 1-GT-1375-A (June, 1961); Page 11

§ This range of values is based on tests on continuous glass filaments, rather than staple filaments. The PNPF in-vessel filters utilize staple glass filaments. By virtue of their greater cross-sectional uniformity, greater length, and larger diameter, tensile strength measurements on continuous filament fibers are more easily made and are more reliable.

difficulty of performing this type of measurement, the tensile strength values obtained for the new fibers may be considered in reasonable agreement with the manufacturer's values. A possible partial explanation for the lower values of the staple filter fiber (as against the manufacturer's listed values) is the probable formation of extremely fine scratches on these fibers during the yarn and filter fabrication operations.

The reasonable agreement between the tensile strength of the two new fibers and between the two used fibers tends to lend confidence to the test data. Assuming the reduction in tensile strength of the fibers (due to use as in-vessel filters) to be real, the extent of such reduction, though ~40%, is not judged to be significant. The tensile strength of the used fiber is still, in an absolute sense, appreciable. Further, the design of the filters utilizes the glass fibers in the form of a yarn which is wound helically around a perforated metal tube. During filter fabrication and service no great demands are placed on the strength of the fibers. The absence of any evidence of filter fiber invasion of the coolant stream during operation tends to indicate that the reduction in filter strength, if real, did not result in any filter disintegration.

6. X-Ray Fluorescence

The purpose of this test was to detect and identify metallic particles adhering to the used fibers. Iron was readily noted, although a small amount of zinc was detected also*, with perhaps 20 to 30 times as much iron as zinc. No particular significance is attached to these findings nor are they surprising, since a slight amount of residual contamination of filtered material on the fibers was not unexpected despite the fact that the fibers had been thoroughly rinsed.

*A. I. Chemical Analysis Report; Request 9348: Laboratory No. 6459 (July 7, 1964)

A. REVIEW OF COOLANT QUALITY

A summary of coolant analyses performed at the site over the six month reporting period is shown in Figure 31. The ash data, with a few exceptions,

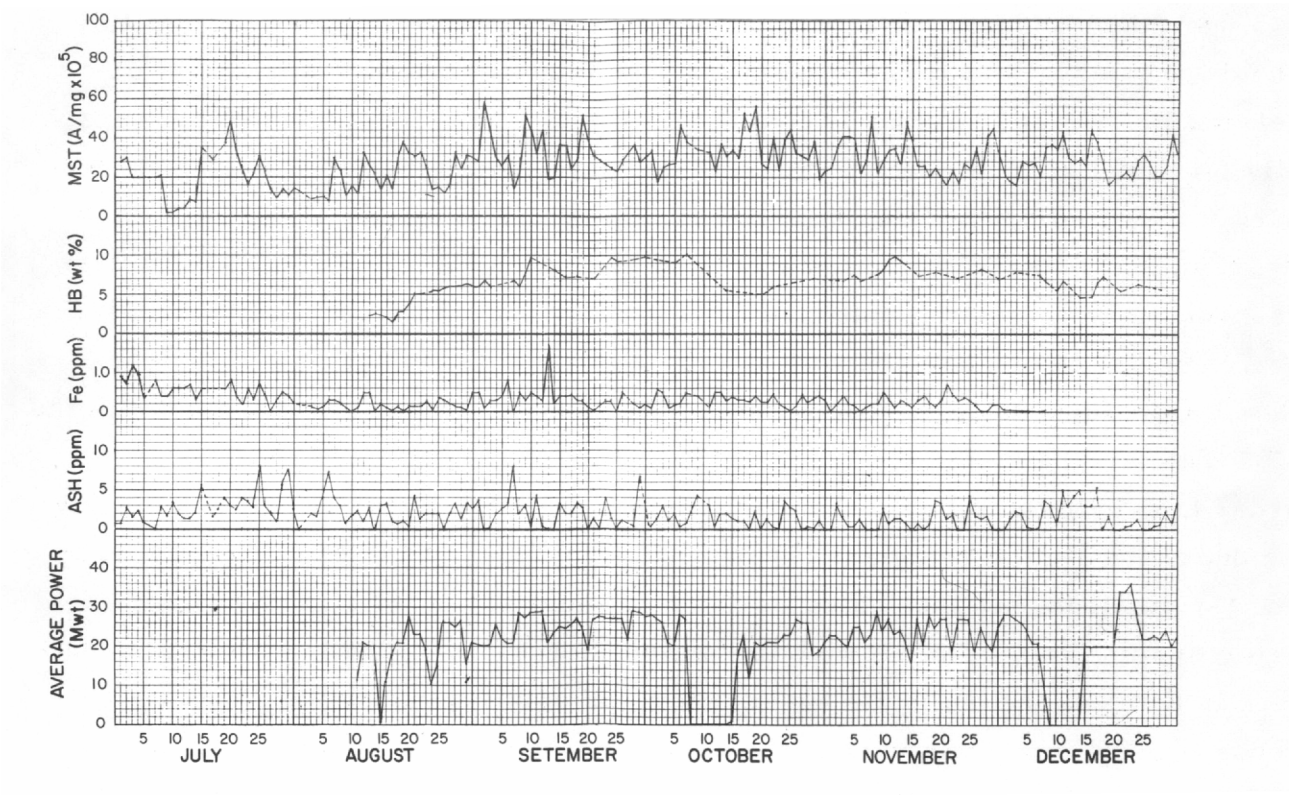

Figure 31. Coolant Analysis History for Core 1-B

show variation in the range of 1 to 5.0 ppm. There is a trend towards higher ash values during shutdown periods; i.e., July 1 to August 11, October 7 to October 14, and December 7 to December 14. This is explainable on the basis of a much lower coolant flow through the in-core filters when the reactor is down (300 gpm flow rate) compared to full flow through the filters (14,000 gpm) when the reactor is producing power. Another significant factor is that of moist air - coolant contact during shutdown, some of which occurs despite the fact that a nitrogen purge is used. It is interesting to note, in this respect, that after the air-inleakage incident of December 18 through December 21 when the reactor was producing power at full flow, there was no apparent increase in

ash content of the coolant. The fairly random variations in ash content over the entire period are attributable in great part to the relative accuracy (±2.0 ppm) of this analytical procedure. During the December operations which included a shutdown, the standard deviations of triplicate sets of ash analyses were calculated. It will be seen that even during intervals when the ash values were at the 5.0 ppm level, the standard deviation was as high as 3.0. The iron determinations (by x-ray fluorescence) with few exceptions show values at the 0.5 ppm level or less. A somewhat higher trend is observed during the July shutdown interval for reasons discussed previously for ash content. In observing the ash and iron analytical data, it becomes evident, due to the generally low level of impurities in the coolant, that some other technique is necessary for evaluating the possibility of sampling anomalies as a perturbation in the resultant data. The membrane stain test, or MST, is very useful in this respect. The calculated standard deviation for triplicate sets of MST analyses performed in December show most values to be in the range of 1.0 or less. Despite the inherently good precision of this test, some cyclical patterns in the MST data and some fairly significant day-to-day variations were noted. In order to determine the possible reasons for the latter, tests were made using: (1) duplicate beaker samples, (2) duplicate analyses of the same beaker sample, and (3) duplicate breaker samples after an increase of the flushing volume prior to sampling. The results are shown in Table X. The high-low MST pattern is noted in the duplicate beaker samples with normal flush, as is its absence in a duplicate analysis of the same beaker sample, and the smaller difference in the duplicate beaker samples taken with extended flushing of the line. Note, also, that overall, the differences being considered are of 4 to 10 MST units ($A/mg \times 10^5$) in the duplicate beaker samples. The problem of sampling variation was also investigated further from the point of view of the maximum flushing volume required before sampling in order to obtain good agreement in MST values of duplicate beaker samples. The results as summarized in a previous report* indicated good agreement between duplicate sets of samples, in most cases, when a flushing volume of 4 and 5 times normal was used.

*Piqua Nuclear Power Facility Reactor Operations Analysis Program, Monthly Report No. 27, November 1964

TABLE X

EFFECT OF SAMPLING VARIATIONS ON MST DATA

MST ($A/mg \times 10^5$)											
Duplicate Beaker Sample with Normal Flush of Line (2 qts.)								Single Beaker Normal Flush		Duplicate Beaker with Extended Flush (6 qts.)	
OC-829 Oct. 27		OC-833 Oct. 28		OC-836 Oct. 29		OC-838 Oct. 30		OC-846 Nov. 5		Nov. 11	
37	31	35	29	39	28	28	18	40	40	34	30
40	32	37	28	38	30	28	19	40	40	34	30
41	31	37	29	37	30	28	19	41	40	34	29

Although the available data are somewhat inconclusive, it appears that there were two types of perturbations which could bias the MST results: (1) sampling variance, caused by material hanging up on the sampling pipe and not being removed by adequate flushing prior to sampling, and (2) air exposure effects which may vary from sample to sample. The solution recommended for the first problem was to continue using larger flush volumes (4X to 5X) until some changes could be made in the sampling piping at sample station No. 1. In late December of 1964, a modification was made at sampling station No. 1 which could be a significant improvement. The 6-in.-long by 1/2-in.-ID length of the pipe below the sample discharge valve, used heretofore, was replaced by a needlevalve and a piece of tubing 1-in. long by 1/4-in. ID. The open end of the tube is capped when not used. Further studies will indicate whether this will be adequate in eliminating or minimizing the observed anomalies in the MST data, or whether further modification of the sample station will be necessary.

As a first approach to minimizing the coolant oxidation problem, it was recommended that the time and temperature required for reheating of samples in the laboratory in air be reduced as much as possible. This is particularly important for coolant samples taken on weekends and run the following Monday. It has been noted in a number of cases that weekend MST values were somewhat higher, and also that the standard deviations for weekend analyses are also in the higher range of values.

The HB data in Figure 31 show a maximum of 10 wt % over the entire operating period. It should be noted that during the December shutdown, when the reactor was opened and a nitrogen purge used to minimize air contamination, the HB level reached a minimum of 4.5 wt %. While this is significantly higher than the HB level in the coolant before Core 1-A was opened (approx. 1.0 wt % HB), the December shutdown interval was shorter and the actual time the reactor was open and the nitrogen purge was used was three days (see discussion on air-inleakage effects).

B. PHA ANALYSIS OF COOLANT

The analysis of the gamma emitting radioisotopes in the coolant continued on a routine basis over the report period when the reactor was operating and producing power. The data for the six isotopes (N^{13}, Mg^{27}, Cl^{38}, Mn^{56}, Na^{24}, and As^{76}) are plotted (Figure 32) to ascertain if any significant trends occurred. In evaluating these data (through October 31, 1964) it was noted that there were some inconsistencies in the calculation of specific activities at the site and that the basic procedures used required improvement and/or standardization. In order to improve the reliability of the PHA data and make it more useful in observing daily coolant trends, suggestions have recently been made* regarding PHA procedures used at the site. These are as follows.

a) The equation for calculation of the specific activities of three of the isotopes routinely reported (N^{13}, Mg^{27}, Mn^{56}) using the subtracted spectrum technique requires a baseline correction for the integrated counts under the photopeak. The correction (which is subtracted from the total counts in the difference spectrum) is made by dividing the sum of the counts in the first and last channel of the photopeak by two, and multiplying by the total number of channels.

b) The number of channels counted in the photopeak for a particular isotope on a day-to-day basis should be the same. Since the number of channels in the photopeak will generally increase with gamma energy (as was shown by a plot of energy in Mev vs the number of channels at 20 kev per channel in the TDR), a method is available for

*H. Mandel, "Recommendations for Standardization and Improvement of PHA Procedures at PNPF," NAA-SR-TDR-10888, Jan 7, 1965

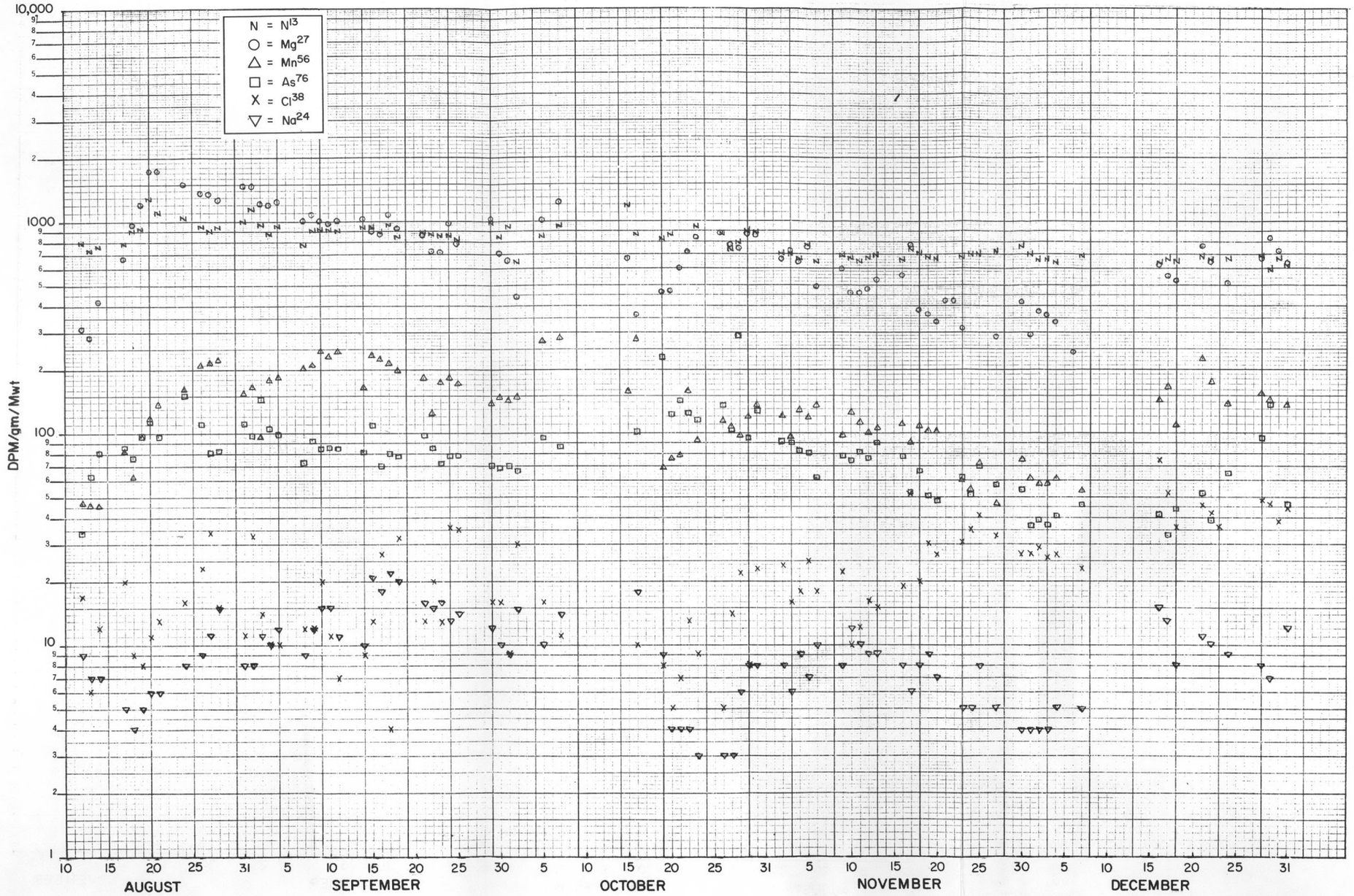

Figure 32. Specific Activities of Radioisotopes in Core 1-B Coolant

choosing the correct number of channels; this should be used to eliminate inconsistencies and errors in judgement.

c) Total counts in the photopeaks for Na^{24} and Cl^{38} had been found to be too low to be statistically reliable (<1000 counts per photopeak) and it was suggested that this be improved by using a 20-min count for Na^{24}, and two 4-min counts for Cl^{38}.

d) A new and improved procedure utilizing relatively simple equations was recommended for calculating effective power levels for various isotopes of interest (in dpm/gm-Mwt).

e) The gross counting of daily coolant samples in units of CPM/gm-Mwt was recommended as a useful index of coolant trends. The determination is easily obtained with the PHA unit after a 30-min decay and a 2-min count (which measures mostly N^{13} and Mg^{27}) or after a 3-hr decay and a 20-min count (which focuses attention on Mn^{56}, As^{76}, and Na^{24} as the more significant trend indicators).

The fact that baseline corrections were not applied for the N^{13}, Mg^{27}, and Mn^{56} PHA data through October 31, 1964, means that the values to that date are high by about 20%. A decreasing trend in Mg^{27}, Mn^{56}, As^{76}, and Na^{24} activity is apparent from November through the shutdown of December 7, 1964. A decreasing trend in gamma activity was also observed in the bypass filter F-2B in November along with a lower trend in gamma activity of the coolant. Since the F-2B filter was operating at a relatively low efficiency at that time (see later discussion on F-2B filter efficiency), the coolant activity decrease observed must be attributed to other possible causes; namely, a higher distillation efficiency and a lower degree of coolant air contact.

C. PHA ANALYSIS OF GASEOUS FISSION PRODUCTS

During the time both cores 1-A and 1-B were used, fission products were observed in the waste gas stream, as determined by PHA at the site. A comparison of the specific activities (dpm/cc-Mwt) of fission product isotopes detected during both operating periods is shown in Table XI. The trends for both operating periods are similar, and it is significant that the activities are of a low order and that there is no apparent increasing trend in the activities of

TABLE XI

GASEOUS FISSION PRODUCT ACTIVITIES
DURING CORE 1-A AND 1-B OPERATION

Date	Specific Activity (dpm/cc-Mwt)					Power	Remarks
	Kr^{85M}	Kr^{87}	Kr^{88}	Xe^{133}	Xe^{135}	Mwt	
Core 1-A							
1/25/64	2.2	ND	ND	-	0.1	39	
2/27/54	6.8	13.2	11.4	0.7	22.3	22	Air-leak
3/20/64	4.0	11.7	9.0	0.5	31	30	
4/1/64	4.9	11.8	10.6	0.4	13.0	33	
4/11/64	4.1	12.0	8.5	0.2	11.5	39	
4/28/64	4.2	12.2	6.5	0.2	10.4	38.5	
5/6/64	3.8	11.0	8.0	0.2	10.0	30	
Core 1-B							
8/11/64	-	-	14.7	0.1	1.7	5.0	Start-up
8/21/64	4.8	7.9	7.4	0.4	11.5	32.2	
8/25/64	3.6	9.0	10.0	2.9	12.0	17.3	
9/3/64	3.1	9.5	8.7	1.0	9.3	21.6	
9/11/64	1.9	9.4	8.4	0.6	7.0	33.5	
9/23/64	2.3	12.1	8.5	0.7	7.1	31.7	
9/29/64	2.0	11.0	8.3	0.7	7.7	32.7	
10/5/65	2.0	10.6	6.9	0.4	4.9	32.3	
10/15/64	-	-	-	-	-	2	Start-up after SH-1 repair
10/22/64	2.7	10.5	9.3	0.2	5.4	23.8	
10/29/64	1.9	11.2	5.3	0.5	8.4	23.9	
11/13/64	2.1	8.2	6.8	0.8	12.2	21.5	
11/18/64	-	8.4	7.9	-	-	25.4	
11/30/64	1.5	9.9	7.7	0.4	4.2	33.6	
12/15/64	1.7	9.2	7.5	0.5	6.4	28.2	
12/21/64	-	-	-	-	-	2	Rx Start-up
12/22/64	-	-	-	1.9	5.8	41.4	After air-leak

fission products in the waste gas when the reactor is at power for prolonged periods, (which would be the case if there were a serious fuel element failure).

D. EVALUATION OF AIR INLEAKAGE TO COOLANT

An evaluation was made of the extent of air inleakage during use of Cores 1A (January to May 1, 1964 power operation) and 1B (August to December 1964 Power operation) in which all of the available analytical data for both coolant and waste gas were used.

The waste gas activity (μc/cc) during the low-power operations in November 1963, and also the high Ar^{41} activity, definitely indicated that air inleakage was occurring. High waste-gas activities were observed at the start of full-power operations on January 9, 1964 (10^{-2} μc/cc), and, in fact, some high gas activities (10^{-2} to 10^{-3} μc) were observed periodically during January and February 1964 power operation, concurrent with high Ar^{41} values (see Figure 33). During the remainder of Core 1-A operation, through May 21st, the waste gas activities (10^{-4} to 10^{-5} μc/cc) and Ar^{41} values (3-4 dpm/cc-Mwt) were low. During Core 1-A operation, also, Ar^{41} values were counted in the coolant by PHA. There was an apparent downward trend in these values from 100 dpm/cc-Mwt in January to approximately 5 dpm/gm-Mwt in May, 1964. For Core 1-B operation, high Ar^{41} values in the gas were observed at startup on August 11, 1964, which leveled off to the 200 to 300 dpm level in September, 1964 (See Figures 33 and 34). High Ar^{41} values in the coolant were also observed at startup (approx. 200 dpm/gm-Mwt) which leveled off to about the 4 to 8 dpm/gm-Mwt by the end of August. Through December 1, 1964 of Core 1-B operation, Ar^{41} values in the coolant were not reported. During this period, the Ar^{41} values in the coolant were not obtained by counting but were checked qualitatively by looking for the photopeak in the X-Y plots of the gamma spectra. In other words, some Ar^{41} may have been present at low levels during most of Core 1-B operation, similar to that during Core 1-A operation, when Ar^{41} was counted routinely. A recent recheck of tapes for coolant gamma spectra obtained in December, indicated a value of 2.0 dpm/gm-Mwt of Ar^{41} in the coolant on December 1, 1964. After the December 7, 1964 shutdown and the startup on December 15, 1964 (and removal of fuel element F-13), an air leak was detected on December 18, 1964 based on significantly higher activities observed in the offgas and in process systems (degasifier, P-1A and the 106 coolant line). Offgas flow also increased significantly during the air leak, to a maximum of ~40 scfh (normally, offgas flow even at full power does not much exceed 25 scfh). Ar^{41} values in the coolant for the period of December 16, 1964 through December 22, 1964 are shown in Table XII.

The highest Ar^{41} value obtained on December 21, 1964 probably <u>does not</u> represent the <u>maximum</u> Ar^{41} concentration in the coolant during the air leak (the Ar^{41} in the offgas was about 3000 dpm/cc-Mwt at about the same time these

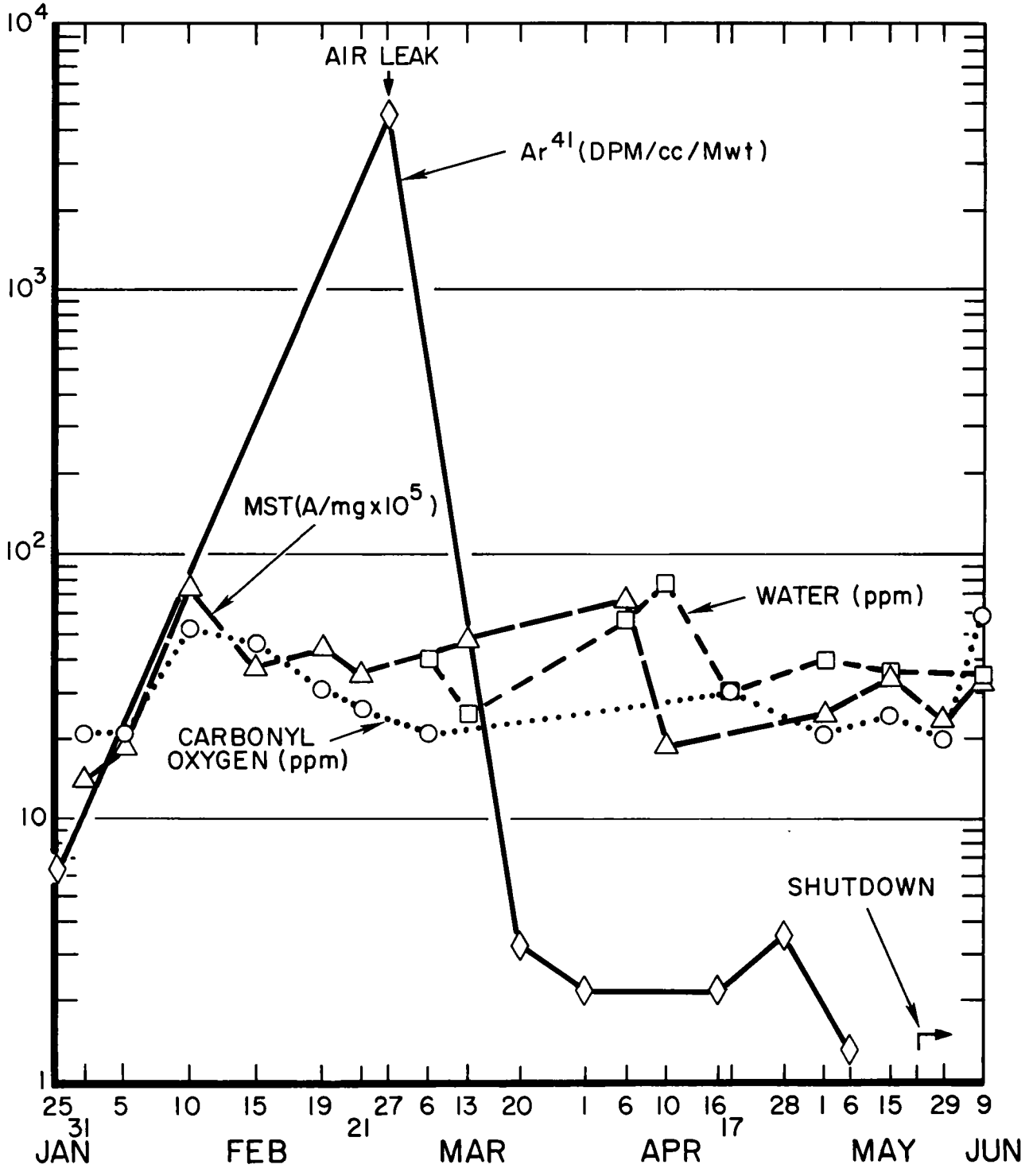

Figure 33. Ar^{41} Activity and MST Carbonyl and Water Values for Core 1-A

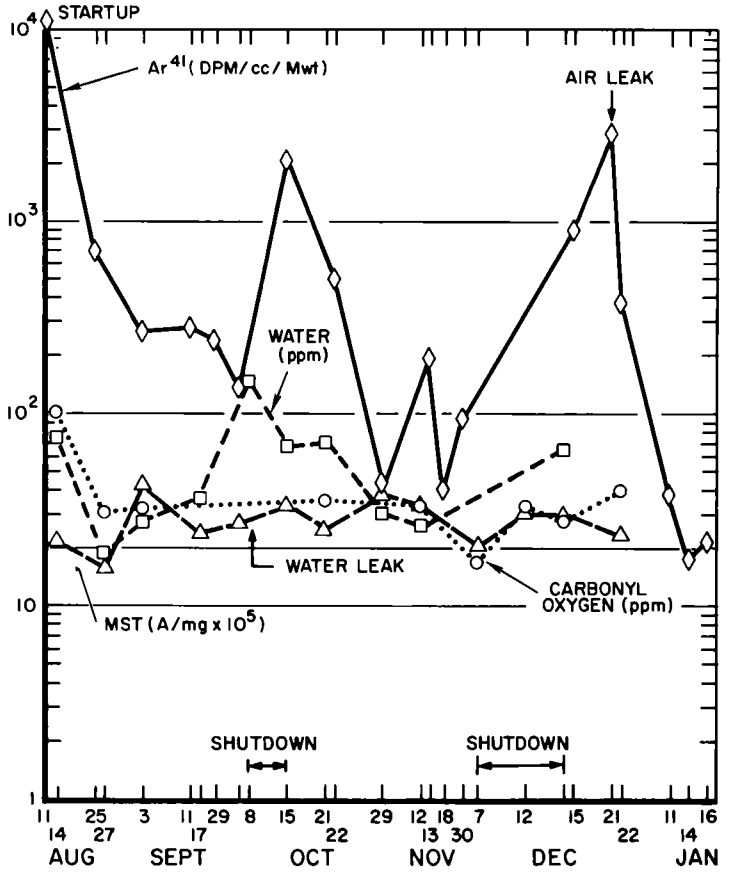

Figure 34. Ar^{41} Activity and MST Carbonyl and Water Values for Core 1-B

TABLE XII

Ar^{41} VALUES IN PNPF COOLANT BEFORE AND AFTER AIR LEAK

Date	Ar^{41} Activity in Coolant dpm/gm-Mwt
Dec. 16, 1964	1.3
Dec. 17, 1964	4.2
Dec. 18, 1964	7.3
Dec. 21, 1964	30.0
Dec. 22, 1964	4.8

coolant samples were counted) and therefore is not very useful for estimating total oxygen in the coolant during the air leak. Although there is a similar problem as regards timing and frequency of sampling and the Ar^{41} activity found in

the offgas during reactor operation, an attempt was made to evaluate relative air content of the coolant during the year's operation based on the Ar^{41} activity in the offgas. Since the Ar^{41} activity is generally considerably higher than that which may be in the coolant, the counting statistics are also better.

To make this evaluation, a simple model was used: the irradiation of 1 cc of air by a flux per Mwt of 4.27×10^{11} neutrons/cm^2-sec (the average thermal neutron flux in the coolant at 45.5 Mwt was taken to be 1.94×10^{13} n/cm^2-sec). The concentration of radioargon may be computed by using the following data and the formula below.

σ = 0.53 barns

$N = (\rho/M)\, A$ atom/cc

ρ = 0.94% x density of air

= 0.94×0.00120 gm/cc $\times 10^{-2}$ at 20°C, 1 atm

= 1.13×10^{-5}/gm/cc

$N = 1.13 \times 10^{-5} / 40 \times 0.6 \times 10^{24} = 1.69 \times 10^{17}$ atom/cc

$N\sigma = 0.9 \times 10^{-7}$ 1/cm

ϕ (per Mwt) = 4.37×10^{11} n/cm^2sec

$N\sigma\phi = 3.84 \times 10^{4}$ atoms of Ar^{41} formed/cc-sec

M_{Ar} = 40 gm/mole

$A = 0.6 \times 10^{24}$ atoms/mole

production rate

$R = N\sigma\phi \times V$; $\quad V$ = 1 cc of air

$R = 3.84 \times 10^{4}$/cc-sec X 1cc

= 3.84×10^{4} atoms of Ar^{41} produced per second

At steady state, as many Ar^{41} atoms go into the offgas as are produced.

$\therefore$ Let C be concentration of Ar^{41} in offgas,

and

let F be offgas flow rate = 1 scfh = 7.87 cc/sec;

then,

$$R = CF,$$

and

$$C = R/F = \frac{3.84 \times 10^{4} \text{ atoms/sec}}{7.87 \text{ cc/sec}} = 4.88 \times 10^{3} \text{ atoms/cc in offgas.}$$

Activity is λC, where $\lambda = 1.05 \times 10^{-4}$ 1/sec; half-life = 110 min.

$$\text{Activity} = 1.05 \times 4.88 \times 10^{3} \times 10^{-4} \text{ dis/sec-0.1/cc}$$

$$= \frac{0.512}{3.7 \times 10^{4}} \mu c/cc$$

$$= 1.4 \times 10^{-5} \mu c/cc .$$

This activity (1.4×10^{-5} μc/cc in the offgas) is equivalent to 1 cc of air (at 20°C, 1 atm) activated in the reactor at an offgas flow rate of 1 scfh. This value was used to calculate the equivalent moles (at STP) of air activated in the reactor based on the available Ar^{41} and offgas flow data. From this, the equivalent moles of oxygen were calculated.

The results for the January through December, 1964 operating periods are shown in Table XIII. It should be emphasized that the absolute comparisons of air in the coolant during the operating periods; i. e., Core 1-A and 1-B operation, are not really valid, since we do not have Ar^{41} data for a sufficient number of days, especially during Core 1-A operation. On a relative basis, it does appear that the oxygen equivalent values (using the parameter defined here) were higher during most of Core 1-B operation than during Core 1-A operation. What effect if any this may have had on acceleration of fouling during Core 1-B operation in uncertain. It should be recalled that air inleakage was a problem during January and February operations with Core 1-A, and also prior to that during low-power operation in November and December of 1963. Activity levels on the F-2B filters were also quite high in January, 1964 (~40 mr/hr-Mwt maximum) indicating that corrosion product concentrations during early operations were high also. Nevertheless, the fouling observed on the fuel element removed in May of 1964 was negligible. Evaluation of fouling on fuel element F-13 removed in December, 1964 is still in progress. We have good reason to believe that oxidation of the circulating irradiated coolant has

TABLE XIII

ESTIMATED EQUIVALENT MOLES OF OXYGEN ACTIVATED IN THE PNPF REACTOR BASED ON Ar^{41} ACTIVITY AND OFFGAS FLOW

Core	Date	Offgas Ar^{41} Activity (dpm/cc-Mwt)	Offgas Flow (scfh)	Equivalent* Moles of Oxygen per second at STP
1-A	1/25/64	65	10	0.0002
	2/29/64	4,100	20	0.0230
	3/20/64	3.3	15	<0.0001
	4/1/64	2.2	19	<0.0001
	4/16/64	2.2	25	<0.0001
	4/28/64	3.6	25	<0.0001
	5/6/64	1.3	20	<0.0001
1-B	8/11/64	11,000	10	0.0312
	8/21/64	240	19	0.0013
	8/25/64	700	10	0.0020
	9/3/64	265	20	0.0015
	9/11/64	278	22	0.0014
	9/23/64	32	25	0.0002
	9/29/64	245	20	0.0014
	10/5/64	139	10	0.0004
	10/15/64	2,090	15	0.0089
	10/16/64	234	15	0.0010
	10/22/64	500	15	0.0021
	10/29/64	44	15	0.0002
	11/13/64	196	23	0.0013
	11/18/64	40	23	0.0003
	11/30/64	95	17	0.0004
1-C	12/15/64	895	12	0.0031
	12/21/64	2,850	43	0.0348
	12/22/64	375	36	0.0038

*Based on model used in discussion

deleterious effects on fouling based on OMRE operating experience* and on recent Canadian experience with the U-3 loop.†

An attempt was also made to correlate the gas activity (as Ar^{41}) during Core 1-A and 1-B operation, with carbonyl-oxygen and water content, and MST.

*Organic Summary Report, Chapter 7, "Film Formation on Heat Transfer
†Surfaces," IDO-11401, Dec. 1964.
Report on Organic Liquid-Cooled Reactor Development, PR-Org-4, Oct-Dec 1964.

These data are shown in Figures 33 and 34. Actually, the data points for carbonyl-oxygen and water are insufficient to establish a connection between air inleakage and combined oxygen. Carbonyl-oxygen compounds formed may decompose rapidly due to combined temperature and irradiation effects. The available data do not indicate a significant difference between the two operating periods. Carbonyl-oxygen values show some increase after a shutdown when air is introduced into the system. It would appear from the trend shown for Ar^{41} during Core 1-B operation, that the expulsion of the gas from the system occurs gradually, and it is possible that the gas is removed at an increased rate after the decomposition gases (especially hydrogen) are present in high enough concentration to act as a sparge gas.

E. EVALUATION OF FILTER EFFICIENCY

Radioisotopic data were obtained by PHA on October 26, 27, and 28 on coolant samples taken upstream and downstream of the 2-micron glass spool filters (F-2B). The upstream samples were taken at the normal sampling location; i.e., from line 201 at sampling station No. 1, and the downstream samples from line 208 at pressure indicator No. 530 which is located downstream of the degasifier tank (T-15) and downstream of the degasifier pump (P-3A). The fact that the line 208 samples are downstream of the degasifier introduces some perturbations in the data in the case of the N^{13} and Cl^{38} activities, since some removal of these isotopes probably occurs (very likely as volatile organic compounds) by degasification. The major conclusions drawn from the data are as follows.

1) The N^{13} decay shows a variable coolant residence time through the filter-degasifier system of 5, 6 and 10 minutes, on each of the three days that the samples were taken. Unless it is assumed that some nitrogen (as N^{13}) is removed by degasification, there may be a problem of sampling variance on the 208 line, similar to that suspected on the 201 line (see PNPF-ROAP Monthly Report for October 1964).

2) Using the observed N^{13} decay times, the calculated removal efficiency of a number of isotopes is summarized in Table XIV.

TABLE XIV

ISOTOPE REMOVAL EFFICIENCIES* BY FILTRATION AND DEGASIFICATION

Radioisotope	Removal (%)
Mg^{27}	0 to 12
Cl^{38}	3 to 58
Mn^{56}	0 to 13
As^{76}	3 to 6
Na^{24}	48 to 59
Co^{58}	0 to 3

*Based on a single pass

3) The isotopes for which the removal ratios are the highest (Na^{24} and Cl^{38}) are also the least reliable due to their low count rates. (The counting statistics for Na^{24} have been improved since these tests were made, by using a 20-min counting period instead of the 2-min used previously.)

4) Removal rates for isotopes little affected by the varying residence times given, and which should not be affected by degasification (Mn^{56}, As^{76}, Co^{58}), show removal efficiencies of 13% maximum.

Another fact of interest in this connection is the slightly decreasing trend in gross counts of the coolant obtained by PHA during November. The average for the first half of November was 59 cpm/gm-Mwt; the average for the latter half was 49.2 cpm/gm-Mwt. (See Figure 35.)

All of the available data may now be summarized as follows:

1) An increase in ΔP in the in-core filters;

2) A decrease in gamma activity on the bypass filters and a slight decrease in total coolant gamma activity; and

3) The generally poor removal efficiency for long-lived isotopes by the bypass filters.

A possibility which must be considered is that of some malfunction in the F-2B filter assembly itself. Gamma activities measured on both the F-2A and

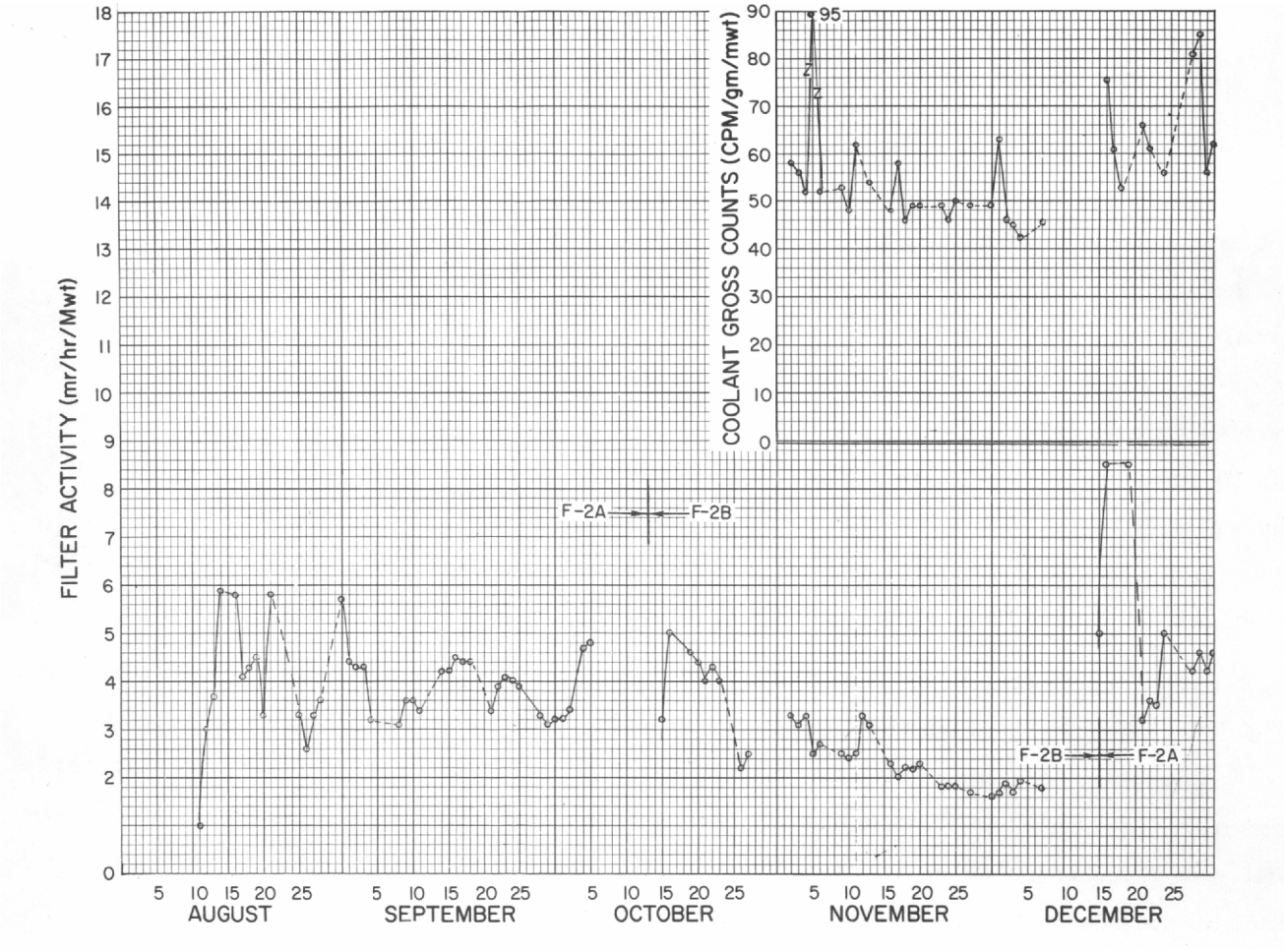

Figure 35. Radioactivity on Bypass Filters

F-2B filter housings during August through December operations show generally higher activities on the F-2A relative to the F-2B filter system. An examination of the internal F-2B filter internals is scheduled for the near future.

F. COOLANT PARTICLE ANALYSIS

Discrete black particles in the bottom of solidified beaker coolant samples were first observed in April of 1964. They were observed on an intermittent basis through the remainder of Core 1-A operation, and on a less frequent basis during Core 1-B operation (August to December 7, 1964). In tracing the problem of the high pressure drop across the purification column in November 1964, it was established that unstable still conditions had caused the column to flood, pushing the demister out of position, and carrying Raschig rings from the still column over into the column condenser. This flooding would have carried particles from the still pot over into product receiver tank, T-6, whence they could

be pumped back into the reactor system. A sample from the product receiver tank return pump discharge live (P-4A) contained black particles. The still pot is a natural collecting point for all corrosion products or other foreign matter. When flooded, it would serve to mass-inject these particles into the receiver tank; from here, the particles and coolant would go through the degasifier tank (T-15) and mix with the coolant stream returning to the reactor by way of the pressurizing pumps P-3A and P-3B. This coolant exits the reactor to the pressurizing loop via the 201 line, a portion of which is bypassed to the sample point at SS No. 1, ahead of the degasification filters. The 201 exit line in the reactor vessel is well below the upper guide grid plate on the surface of which particles had been observed previously.

There are two likely sources of these particles. The first is particles which were observed on the upper guide grid of the reactor vessel as far back as August of 1962, when the reactor vessel was flushed with hot organic coolant, and more recently in December of 1964 during the shutdown. The second possibility is the particles generated by coking of the column feed heaters where the coolant is preheated to ~700°F before being fed to the distillation column.

During the December 1964 shutdown, when the coolant level in the reactor vessel was lowered and the vessel opened, the surface of the upper guide grid was seen to be covered with a thin layer of black particles. The zone just above the upper guide grid plate is a low-velocity region (almost stagnant) of the reactor vessel. All the particles were removed before the reactor resumed power operation, and a sample sent to Canoga Park for analysis. Also during December samples of the incore filter removed with fuel element F-13 were obtained as well as a sample coke removed from one of the preheaters (H-1). The analytical data for these three samples (grid plate, H-1 heater, and in-core filter particles) are of considerable importance in tracing the possible source of the particles.

Data obtained by PHA of gamma emitting isotopes are summarized in Table XV.

It should be noted first, that here is a similarity of isotope distribution and isotope ratios (except for Cr^{51} which probably was present in these particles also) in the in-core filter and upper guide grid particles. There is reason to believe, therefore, that these are similar particles and from the same source,

TABLE XV

GAMMA EMITTERS IN UPPER GUIDE GRID, IN-CORE FILTERS, AND H-1 HEATER PARTICLES

Isotope	Specific Activity (dpm/gm)			
	H-1 Heater Sample (Dec. 1964)	In-Core Filter Particles (May 1964)	In-Core Filter Particles (Dec. 1964)	Upper Guide Grid (Dec. 1964)
Zn^{65}	3×10^3	8.3×10^5	2.3×10^6	2.6×10^6
Mn^{54}	-	4.2×10^5	3.9×10^6	2.2×10^6
Co^{60}	2.3×10^4	8.9×10^4	7.5×10^5	7.3×10^5
Fe^{59}	-	7.5×10^4	8.5×10^5	6.3×10^5
Cr^{51}	-	-	-	5.2×10^4
Co^{58}	1.8×10^4	-	-	-

i.e., corrosion products. The H-1 heater coke particles showed a lower order of activity; they did not contain Mn^{54} and Cr^{51}; Co^{58} was one of the prominent isotopes. Co^{58} is also the only isotope of significance which has been detected in coolant samples after the short-lived isotopes have decayed off; it was also the only isotope detected in a nondistillable high boiler sample analyzed in our laboratory. One may conclude then, that the material coking on the preheater originates mainly from coolant organic components rather than from the corrosion type particles. This is further corroborated by the ash and emission spectroscopy data shown in Table XVI.

There is a definite similarity in the elemental composition of the in-core filter and upper guide grid particles; note for example, that the Fe/Si ratios are similar. Differences in relative ratios of other elements present at lower concentrations in these two samples are probably not very significant due to the relative accuracy of the method. In observing the difference in ash content (23 vs 40 wt %) of these two samples, it should be noted first, that the in-core filter particles were separated from a small random filter sample by extraction with THF in a Soxhlet apparatus (the weight of particles actually obtained was 0.053 gm). Second, while it is being assumed that the upper guide grid particles are primarily the result of corrosion or erosion of the mild steel system, it is possible that a significant portion of this material originates from film

TABLE XVI

ASH AND EMISSION SPECTROSCOPY DATA FOR H-1 HEATER, UPPER GUIDE GRID, AND IN-CORE FILTER PARTICLES

Element	Relative Concentration of Elements in Original Sample (wt %)		
	H-1 Heater (Dec. 1964)	In-Core Filter Particles (Dec. 1964)	Upper Guide Grid Plate Particles (Dec. 1964)
Fe	1.0	12.0	8.0
Si	0.02	1.8	1.2
Al	<0.01	0.2	0.8
Ca	-	0.02	0.8
Zn	-	0.1	0.8
Ti	-	0.02	0.4
Mg	0.03	0.07	0.3
Cr	<0.01	0.02	0.2
Mn	0.01	0.2	0.2
Ni	<0.01	0.2	0.2
Na	-	0.1	0.08
Cu	<<0.01	0.2	0.02
Mo	<<0.01	0.02	0.01
Sn	-	0.02	0.02
Zr	<<0.01	0.01	0.02
Wt % Ash	2.6	23	40

which has flaked off of fuel element heat transfer surfaces. Since the active portion of the core is downstream of the full flow filters and since the major portion of this flow returns to the core without any subsequent treatment, these particles could collect in the semistagnant zone just above the upper guide grid of the reactor vessel.

Based on the analytical data available at this time it appears that the coke deposits found in the still preheaters and originating from coolant decomposition products, are the major source of the "black particles" found in the past in beaker samples taken at sample station No. 1. The upper-guide grid and in-core filter particles have inorganic compositions which would indicate a

similar origin. The relationship of these latter particles to material deposited and removed from fuel element surfaces is still uncertain until the results of analyses of fuel element film are available.

G. ANALYSIS OF RAW COOLANT

Analyses obtained from the vendor (Monsanto Chemical Company) for raw coolant purchased during Core 1-B operation are shown in Table XVII. New major points of interest are the water and chlorine data. The water values reported for the raw coolant by Monsanto (Karl Fischer titration using benzene-methanol as the solvent) average 71 ppm. We have not compared this with similar coolant samples seen by our azeotropic distillation procedure; but assuming these water concentrations to be reasonable, at makeup coolant addition rates of 50 to 100 lbs/hr and with distillation and degasification prior to mixing with the system inventory, the effect on the water content of the system should be negligible. This means, in effect, that when significant water increases are found in coolant bomb samples, they are due to water leakage into the system.

The chlorine* data reported by Monsanto indicates that the average of all lots submitted was within specifications (2.0 ppm). The average of the activation data indicate a somewhat higher value or approximately 3.0 ppm. Some discrepancies between wet chemical and activation analytical data for chlorine have been known to exist for some time, and for this reason an attempt was made to develop an x-ray fluorescence method for determining chlorine in PNPF coolant. Standards were prepared by dissolving Santowax OMP and triphenyl tin chloride in the THF (tetrahydrofuran) and drying before pelletizing. Optimum instrumental conditions were determined using a chromium target x-ray tube and a silicon analyzing crystal. Under these conditions, the limit of detectability appeared to be approximately 3.0 ppm, which was felt was not quite good enough. Due to the limited funding of the project and the marginal sensitivity, additional work with this method was not attempted.

---

*Chlorine analyses of raw and circulating coolant were not made at our laboratories during this report period, since the Shield Test Reactor facility normally used for activation analysis was shutdown for major modification. Chlorine analysis of circulating PNPF coolant in July, 1964, made by activation analysis at B.M.I., indicated <1.0 ppm.

TABLE XVII

RAW COOLANT DATA FOR CORE 1-B

Lot No.	No. of* Bags	H_2O (ppm)	Solution Point (°C)	1st Crystals (°C)	Biphenyl (%)	HB (%)	Chlorine (ppm)	
							Wet Chemical	Activation†
AD-35	100	61	157	153	0.42	0.16	1	-
AD-36	80	67	158	155	0.64	0.1	1	-
AD-37	67	61	158	156	0.51	0.1	2	-
AD-38	60	68	152	147	0.82	0.1	1	-
AD-39	80	85	153	149	1.10	0.1	1	-
AD-40	80	95	156	152	0.1	0.1	1	-
AD-41	57	84	157	156	0.1	0.14	1	2.7
AD-42	49	88	157	153	0.1	0.1	1	3.3
AD-43	60	68	155	152	0.1	0.1	1	1.0
AD-44	95	68	156	152	0.1	0.1	1	0.1
AD-45	68	78	157	153	0.16	0.1	1	1.4
AD-46	73	84	156	151	0.18	0.1	1	1.2
AD-47	67	66	154	151	0.40	0.1	1	0.9
AD-48	73	90	156	151	0.40	0.1	1	1.4
AD-49	57	90	158	156	0.1	0.1	1	1.8
AD-50	55	38	150	143	0.75	0.11	1	1.8
AD-51	75	58	153	146	0.63	0.10	3	8.0
AD-52	17	68	156	153	0.12	0.14	4	5.7
AD-53	80	61	150	142	0.23	0.48	3	4.8
AD-54	114	63	155	153	0.36	0.18	1	5.7
AD-55	58	62	153	151	0.12	0.20	2	3.9
AD-56	65	49	156	152	0.1	0.44	2	4.0
Average		71	-	-	-	-	1.45	3.03

*75 lbs per bag

†Obtained by activation analysis at Battelle Memorial Institute, Columbus, Ohio. The other data shown were submitted by the vendor (Monsanto Chemical Company)

VI. EFFECT OF OXYGEN ON IRRADIATED PNPF COOLANT

A. INTRODUCTION

During this fiscal year, it has been demonstrated as part of this project that irradiated coolant reacts with oxygen to form both organic oxygen compounds and gaseous oxygen compounds; e.g., CO, CO_2, and H_2O. Furthermore, operation of the OMRE and recent operation of the U-3 loop at Chalk River have shown that exposure of the coolant to oxygen increases the fouling rate. Moreover, the operating experience of the PNPF has shown that exposure of the coolant to air during maintenance and by air inleakage into low pressure systems; e.g., the degasifier and distillation system, is a frequent occurence. Therefore, this study was initiated to determine the mechanism of oxidation of the organic coolant under exposure to the atmosphere and relates this knowledge to its irradiation and processing history. In addition, it was expected from this work that recommendations could be made for processing irradiated coolant prior to a shutdown for refueling or maintenance operations. However, this project was terminated prematurely and the objectives were only partially attained.

B. OXYGEN UPTAKE BY IRRADIATED COOLANT

Two methods were developed to study the oxygen uptake by irradiated coolant. In the first method an air-helium mixture was bubbled through the hot coolant and the amount of oxygen which reacted was determined by analyzing the gas for oxygen and nitrogen before and after it passed through the coolant. In the second method, the coolant was heated under nitrogen to the desired temperature in a fixed volume. The nitrogen was then flushed out with oxygen and the disappearance of oxygen in the vapor phase was determined by gas chromatography. In both methods, the nitrogen concentration was observed to remain constant and, therefore, the nitrogen served as an excellent internal standard. In addition, CO, CO_2, and H_2O were determined by gas chromatography. Infrared spectroscopy was used to confirm the identification of these compounds. It was interesting to note that CO is produced, because it was found to be one of the necessary precursors to the formation of $Fe_{20}C_9$ which was found to be the main inorganic compound in OMRE Core-I and -II fouling films.

1. Experiments in Which Air was Bubbled Through PNPF Coolant

Oxidation of a PNPF coolant sample (October 21, 1964, 5.1% HB) for 333 hr, by bubbling of an air-helium mixture through the coolant at 236°C, showed that the oxidation rate increased after the initial 27 hr and passed through two maxima (See Table XVIII). The reaction rate at the second maximum was approximately double the initial rate. As the test progressed, it became increasingly difficult to maintain flow through the apparatus because low boiling compounds, produced during the oxidation, collected on the exit

TABLE XVIII

OXIDATION OF A PNPF COOLANT SAMPLE* (OCTOBER 21, 1964) BY BUBBLING AN AIR-HELIUM MIXTURE† THROUGH COOLANT AT 236°C.

Oxidation Time (hr)	Oxygen § Reacted (vol %)	Oxidation Time (hr)	Oxygen § Reacted (vol %)
0.5	8.2	99	11.5
1.0	8.2	126	15.9
24.0	8.2	147	17.8
26.5	8.2	171	13.9
29.5	12.9	193	10.6
48.0	14.9	213	6.7
50.0	12.9	260	7.7
55.5	12.9	281	8.2
56.5	10.6	313	11.5
80.0	10.6	333	8.6

*The sample contained 5.1% HB, 72 ppm H_2O, 30 ppm carbonyl-oxygen at the start of test. A 100 gm sample was oxidized.

† The He contained 0.66% O_2 for the first 80 minutes, then 0.38% for the remainder of the test. The flow rate was 95 ml/min.

§ These percentages are determined as the difference of influent oxygen $^{(A)}$ minus the effluent oxygen $^{(B)}$ divided by influent oxygen (A).

$$\left(\frac{A-B}{A}\right) 100 = \text{percent oxygen reacted.}$$

tube until the tube became plugged. For this reason, the test was terminated before the oxidation rate had decreased to the initial rate. Enough oxygen was passed through the coolant to have yielded 0.9 wt % oxygen in the sample. However, H_2O, CO, and CO_2 were detected in the exit gas indicating that oxygen was reacting to produce gaseous products as well as organic oxygen compounds. The carbonyl-oxygen content increased from 30 to 754 ppm. After the oxidation, it was observed that the coolant which had been initially a brown waxy solid had changed to a black sticky solid. The initial oxidation rate was measured at various flow rates and temperatures. The results are shown in Table XIX. The temperature dependence corresponds to an activation energy of 6 kcal at the highest flow rate, and 11 kcal at the other flow rates. This temperature effect no doubt includes the effect of viscosity and surface tension as well as chemical activation. The percentage of oxygen reacted decreased with increasing flow rate, while the total amount absorbed (given by the product of flow rate and percent oxygen reacted) increased.

TABLE XIX

EFFECT OF FLOW RATE AND TEMPERATURE ON OXIDATION OF PNPF COOLANT* BY BUBBLING AN AIR-HELIUM MIXTURE THROUGH LIQUID COOLANT

Air-Helium Flow Rate (ml/min)	Percent Oxygen Reacted †		
	230°C	196°C	165°C
95	14.2	9.4	5.8
38	-	17.7	8.2
25	-	20.7	9.4
10	-	33.3	16.0

*The coolant was taken October 21, 1964 in an inline sample bomb and transferred in vacuo.

† The experiments were carried out during ~2 hr. At the end of the test, checks were made at the same temperature and flow rate used at the beginning of the test and the results showed that the oxidation rate had not changed during this test.

2. Experiments Where Air Was Exposed to Coolant in a Closed System

Oxidation of irradiated PNPF Coolants in closed systems at various temperatures showed that the rate of disappearance of oxygen was first order with respect to the oxygen concentration. Therefore, to compare the results obtained at various temperatures on various coolants, the rate constant λ is expressed as the half-life, $t1/2 = 0.693/\lambda$, of oxygen in vapor space above the coolant. The results of these tests are given in Table XX. In addition to the disappearance rate of oxygen, the formation of CO, CO_2, and H_2O was also followed. The data from two runs are given in Tables XXI and XXII; these are typical of all runs.

TABLE XX

OXIDATION OF IRRADIATED PNPF COOLANT

Sample	Oxidation Temp (°C)	Oxidation Rate Half-Life (min)	HB (Wt%) Before/After		Carbonyl Oxygen (ppm) Before/After		MST (A/mgX10^5) Before/After		Oxidation Time (a) (hr)
DC-12-1-64	160	440	<1	<1	-	204	~4	10	8
DC-12-22-64	160	330	<1	-	-	-	~4	6	8
LD-10-15-64	160	1740	<1	<1	-	283	~4	67	240
LD-10-15-64 + OC-11-19-64	160	1035	0.31	~1	-	422	-	118	240
LD-10-15-64 + OC-11-19-64	160	520	0.68	~4	-	615	-	202	240
OC-11-19-64	160	~168[b]	7.9	-	-	1226	-	1005	240
OC-11-12-64	160	1430[b]	9.9	10.4	32	447	-	-	8[c]
OC-11-12-64	300	16.2	9.9	28	32	325	-	-	4[c]
OC-9-24-64	160	1970	9.7	-	-	-	-	-	-
OC-9-24-64	200	330	9.7	-	-	-	-	-	-
OC-9-24-64	260	110	9.7	-	-	-	-	-	-
OC-9-24-64	190	85[d]	9.7	-	-	-	-	-	-
OC-12-3-64	160	151	7.9	-	-	-	-	-	8

(a) Oxidation time indicates time before samples were taken for analyses.

(b) Note: There is some indication of a decay effect due to heating the sample before oxidation.

(c) Samples were heated over the weekend under N_2 before oxidation.

(d) This sample was sitrred; all others were stagnant.

LD - Laboratory distilled PNPF coolant.
DC - PNPF distilled coolant (from purification loop).
OC - PNPF operating coolant.

TABLE XXI

OXIDATION OF PNPF COOLANT SAMPLE* (NOVEMBER 12, 1964) AT 160°C BY EXPOSING QUIESCENT COOLANT TO AN ATMOSPHERE OF OXYGEN IN A CLOSED SYSTEM

Oxidation Time (min)	Oxygen in Vapor†		CO in Vapor (ml)	CO_2 in Vapor (ml)	Estimated H_2O in Vapor (mg) §
	(vol %)	(ml)			
0	99.2	444	0.0	0.0	
2	99.2	444			
5	99.3	445			
14	99.2	444		2.1	2.6
17	98.6	442			
22	98.7	442			
25	99.1	444			
28	98.6	442			
31	98.8	443			
109	87.3	391			
137	96.1	404		4.9	3.2
172	93.2	418			
178	93.9	421			
190	93.3	418	3.2	7.2	5.3
201	85.0	381	5.0		
284	87.4	392	4.3		
325	84.1	377	11.5		6.8
346	83.1	372	8.9		
386	79.1	354	12.1		
448	78.0	349	13.4		
478	76.0	340	6.2		

*Sample weight was 107.4 gm.

† Total vapor space was 448 ml and contained 99.2% and 0.8% N_2.

§ Water values are only given to indicate trend. Sampling problems precludes the use of these data as absolute number. The high initial water content is probably due to water in the coolant prior to oxidation.

TABLE XXII

OXICATION OF PNPF COOLANT SAMPLES* (NOVEMBER 12, 1964) AT 300°C BY EXPOSING QUIESCENT COOLANT TO AN ATMOSPHERE OF OXYGEN IN A CLOSED SYSTEM

Oxidation Time (min)	Oxygen in Vapor†		CO in Vapor (ml)	CO_2 in Vapor (ml)	Estimated H_2O in Vapor (mg)§
	(vol %)	(ml)			
0	79.0	350	0.0	0.0	31
2	78.0	346			
5	64.3	284			
7	58.1	258			
9	55.8	248			
11	48.7	216			
12				14.6	23.8
14	45.0	199			
17	45.4	202			
19	35.9	159			
20				24.7	31.8
22	34.0	151			
24	28.0	124			
26	24.3	108			
29	22.3	99			
30				35.2	28.8
34	8.0	36	34.0		
38				39.8	41.8
46	10.0	44			
47				43.9	44.4
49	9.3	41			
52	8.4	37			
55	8.8	39		44.2	28.4
57	7.4	33			
64	5.0	22			
70	4.3	19	34.7		
74				53.4	30.0
80	3.2	14			
82	3.1	14			
93	2.0	9			
98	1.6	7			
108				55.1	31.8
110	1.4	6			
122				69.1	27.4
207				68.4	29.5
240	<1.0	<5	36.3		
254	<1.0	<5		56.8	14.1
257	<1.0	<5	38.4		
287	<1.0	<5	46.8		
312	<1.0	<5		42.2	7.6
321	<1.0	<5	35.5		
362	<1.0	<5	47.0		

*Sample weight was 93.5 gm.

†Total vapor space was 444 ml and contained 79.0% O_2 and 21.0% N_2.

§Water values are only given to indicate trend. Sampling problems precludes the use of these data as absolute numbers. The high initial water value is probably due to water in the coolant prior to oxidation.

Analyses for H_2O were not meaningful because some water was observed on the cooler portions of the glass apparatus. However, the water content of the gas was observed to increase by a factor of 10 during the test at 300°C.

Determination of the CO and CO_2 shows that approximately equal volumes of both gases are produced. Insufficient data have been obtained to resolve the kinetics of the production of these gases. However, these preliminary results indicate that the rates of formation of CO and CO_2 are proportional to the oxygen concentration. It was also observed that organic compounds such as ethane, benzene, toluene, etc., increased in concentration in the vapor as the oxidation progressed. Hydrogen and acetylene were not detected, indicating <0.1% in the vapor. In addition to the gases and low boilers produced during the oxidation, the HB, MST, and carbonyl-oxygen content were observed to increase as shown in Table XX.

During the oxidation at 300°C, the HB content was observed to increase from 9.9 to 28%. This increased decomposition rate needs verification by additional experiments. After the distillation for the determination of the HB content, two of the distillates from oxidized coolant (LD-10-15-64 and LD-10-15-64 + OC-11-19-64) were analyzed for carbonyl-oxygen. The distillates contained 208 and 488 ppm carbonyl as compared to 283 and 422 ppm in the unoxidized coolant, respectively. These results show that most of the carbonyl compounds were distilled over during the HB determination. However, comparison of the carbonyl content of the sample oxidized at 300°C with the carbonyl content of the sample oxidized at 160°C shows that the carbonyl compounds decompose at the higher temperature. This decomposition has been observed previously in this laboratory. In addition, the results show that:

1) Distilled PNPF coolant oxidizes more slowly than the PNPF operating coolant. However, the oxidation rate is relatively rapid. It was expected that distillation would reduce the oxidation to a negligible rate.

2) As the HB increases, the oxidation rate increases for the same coolant.

3) Laboratory distilled PNPF coolant reacts more slowly without oxygen than PNPF-purification distillate.

4) The oxidation rate increases with an increase in the temperature from 160 to 300°C.

5) There is a possible reduction of the oxidizing rate due to storage time of the sample. Such an effect could be due to the decay of free radicals.

6) Stirring the sample to give more intimate contact between the coolant and oxygen gas increased the oxidation rate by approximately a factor of 4.

C. TOTAL OXYGEN IN IRRADIATED COOLANT

The modified Schütze-Unterzaucher method presently being developed to measure total oxygen in PNPF coolant was sucessfully applied to small quantities (~5 mg) of oxygen-containing organic compounds. This method is based on the pyrolytic decomposition of a coolant sample at 950°C in a helium atmosphere, to form primarily carbon and methane with the small amounts of oxygen being converted to carbon monoxide in the presence of a platinum catalyst. The carbon monoxide and methane are collected in a molecular sieve cold trap at liquid nitrogen temperature. When a run is complete, the trap is warmed and the gases are passed through a gas chromatograph* where the quantity of carbon monoxide is determined, from which the total oxygen content can be calculated.

Because of the very low oxygen levels in the PNPF coolant, it is necessary to pyrolyze ~200 mg of coolant in order to obtain accurate results. Pyrolysis of these larger samples created several problems that were not apparent with the smaller samples of known compounds. The pyrolysis of the 200-mg sample produced approximately 70 ml of methane. This large quantity of methane was found to plug the molecular sieve trap as well as mask the small amount (~50 μl) of carbon monoxide obtained during the pyrolysis. This problem was solved by placing a liquid nitrogen trap upstream of the molecular sieve trap. The trap was tested by injecting 10-ml samples of natural gas. The trap became more efficient after each such injection, presumably because of the deposition of hydrocarbons which sorb methane. After this treatment, the trap removed all but about 1 ml of methane without removing any CO.

*A Beckman GC-2 with a 6-ft molecular sieve column (Linde 5A 30/60 mesh) was used at 40°C with a flow rate of 125 ml/min.

Initially, the sample was introduced in small platinum crucibles which were dropped into the hot pyrolysis chamber. The rapid decomposition of the large sample caused part of it to be blown out of the pyrolysis chamber, therefore, it was necessary to insert the sample into a cold chamber and to heat the sample slowly. Too rapid heating caused some of the unpyrolyzed vapors to back stream out of the pyrolysis tube and condense on the cold surfaces.

Air entrained in the sample or adsorbed on the surface of the sample caused serious errors in the analysis unless adequate time was allowed for helium to remove the air. Blank determinations before heating the sample were high because of the eluted air. If the samples are volatile this procedure is not advisable.

The formation of carbon monoxide by the reaction of hot gases and carbon with the silica combustion tube has long been known to increase the blank. To reduce this problem, the combustion tube was coated with platinum. However, the platinum was observed to separate from the quartz (probably due to repeated thermal cycling) and the blank values were not as reproducible as desired. For this reason, it is recommended that a platinum tube be used rather than a quartz tube. Furthermore, obtaining low blanks is somewhat of an art because very small leaks or foreign material introduced into the system cause appreciable blank values.

Sampling of the coolant is a problem which is not easily solved. For example, a PNPF coolant sample taken September 10, 1964 in air at 575°F had an average oxygen content of 378 ppm which is an average of four analyses (408, 375, 380, and 350 ppm). A sample taken from the reactor in an in-line sample bomb gave ~80ppm oxygen. However, water and carbonyl-oxygen adds up to ~95 ppm on the same sample. Therefore, it is suspected that perhaps some of the water was lost before analysis by elution from the sample by helium. Attempts to inject liquid samples with a hypodermic syringe failed because of the high liquidus point of the coolant >300°F. Further development is necessary to resolve this problem.

The blank values of oxygen have been reduced to less than 10 μl CO. This indicates that the lower practical limit of the determination is about 30 ppm oxygen.

D. CONCLUSIONS

1. Oxidation by Bubbling Air Through Hot PNPF Coolant

1) In a 333-hr experiment at 236°C, the oxidation rate remained constant for 26-hr, then increased and passed through two maxima. The rate never became less than the initial rate.

2) The initial oxidation rate increased with temperature and with flow rate.

3) CO, CO_2, and H_2O were formed, and carbonyl content increased.

2. Oxidation of PNPF Coolant in Fixed Volume Experiments

During FY 1964, the experimental observations indicated the following preliminary conclusions. These conclusions are based on single experiments and need verification.

1) Samples of irradiated PNPF coolant containing 5 to 10% HB have been found to react rapidly with oxygen to produce organic oxygen compounds, CO, CO_2, and H_2O.

2) The formation rate of carbonyl compounds, low-boiling compounds, and HB has been observed to be acclerated by the presence of oxygen.

3) The oxidation rate increases with temperature.

4) The oxidation rate is proportional to the oxygen concentration in contact with the liquid.

5) The oxidation rate increases with HB content.

6) Removal of the high boiler fraction from PNPF coolant lowers the oxidation rate.

7) A laboratory distilled PNPF coolant oxidized slower than PNPF distillate. This observation requires further study. The samples had not been stored comparable periods of time after distillation and thus it is not conclusive that entrainment of HB in the plant distillation process is the cause of the effect noted.

8) Both MST and carbonyl-oxygen were found to increase with increasing oxidation rate.

9) Carbonyl examinations on the distillate obtained from the HB determinations after the test showed that most of the carbonyl compounds are distilled over.

10) Stirring the coolant increases the oxidation rate. This indicates that the oxidation rate is dependent on the rate of diffusion of oxygen into the coolant and the surface area of the coolant being exposed.

3. Total Oxygen Determination

At present, the lower practical limit of the determination appears to be about 30 ppm oxygen. This limit is set by the blank value of the procedure; i.e., CO is produced by reaction of carbon with the quartz tube. It was necessary to platinize the combustion tube to attain this sensitivity. However, the reproducibility of the blank is only fair and must be improved if measurements are to be reasonably accurate. A platinum combustion tube appears to be the most economic approach to reducing the blank to low and reproducible levels and thus provide an increase in the useable sensitivity of the method. In addition, sampling problems and the apparent mystery of what makes the glass cold trap work must be resolved.


ATOMICS INTERNATIONAL
A DIVISION OF NORTH AMERICAN AVIATION, INC.